*Zoological Journal of the Linnean Society*, 2025, 204, zlaf073
https://doi.org/10.1093/zoolinnean/zlaf073
Advance access publication 2 July 2025
**Original Article**

OXFORD

# Original Article

# An arboreal rhynchocephalian from the Late Jurassic of Germany, and the importance of the appendicular skeleton for ecomorphology in lepidosaurs

Victor Beccari[1,2,*], Alexandre R.D. Guillaume[3], Marc E.H. Jones[4,5], Andrea Villa[6], Natalie Cooper[4], Sophie Regnault[7] and Oliver W.M. Rauhut[1,2,8]

[1]Bayerische Staatssammlung für Paläontologie und Geologie, Munich, Germany
[2]Department of Earth and Environmental Sciences, Ludwig-Maximilians-Universität, Munich, Germany
[3]GEOBIOTEC, Department of Earth Sciences, NOVA School of Science and Technology, Universidade Nova de Lisboa, Campus de Caparica, P-2829 516 Caparica, Portugal
[4]Science Group, Natural History Museum, Cromwell Road, London SW7 5BD, UK
[5]Research Department of Cell and Developmental Biology, Anatomy Building, University College London, Gower Street, London WCIE 6BT, UK
[6]Institut Català de Paleontologia Miquel Crusafont (ICP-CERCA), Edifici ICTA-ICP, c/ Columnes s/n, Campus de la UAB, 08193 Cerdanyola del Vallès, Barcelona, Spain
[7]Aberystwyth School of Veterinary Science, Penglais, Aberystwyth SY23 3FL, UK
[8]GeoBioCenter, Ludwig-Maximilians-Universität, Munich, Germany

*Corresponding author. Bayerische Staatssammlung für Paläontologie und Geologie, Richard-Wagner-Strasse 10, 80333, Munich, Germany. E-mail: victor.beccari@gmail.com

## ABSTRACT

Here, we describe a new species of Jurassic rhynchocephalian from the Solnhofen Archipelago, *Sphenodraco scandentis* gen. et sp. nov., and highlight the importance of the postcranial anatomy for ecomorphological studies in the rhynchocephalian clade. The holotype of *Sphenodraco scandentis* is divided into a main slab, which has been mentioned in the literature and previously assigned to *Homoeosaurus maximiliani*, and a counterslab containing most of its skeletal remains. This new taxon shows an exclusive combination of osteological features that differs from previously described rhynchocephalians. *Sphenodraco* was recovered in our phylogenetic analysis as a component of a clade including *Homoeosaurus* and *Kallimodon*. To evaluate the ecomorphology of the new taxon, we compare fossil rhynchocephalians with the extant tuatara and squamates. We quantify the diversity of body proportions in lepidosaurs systematically, inferring lifestyle for extinct rhynchocephalians. Our analysis suggests that fossil rhynchocephalians had a diverse array of substrate uses, with some categorized as good climbers, and with *Sphenodraco* showing the extreme condition of limb elongation found in strictly arboreal lizards. This new taxon is here regarded as the first predominantly or even strictly arboreal rhynchocephalian. Furthermore, our analysis shows that the diversity of fossil rhynchocephalians might still be underestimated.

**Keywords:** ecomorphology; Germany; Jurassic; Rhynchocephalia; sphenodontian; taxonomy; tuatara

## INTRODUCTION

Rhynchocephalia is the sister group of squamates (lizards, snakes, and amphisbaenians), and it is currently represented by a single extant taxon, *Sphenodon punctatus* (Gray, 1842). During the Mesozoic, however, rhynchocephalians were diverse and major components of the global small vertebrate fauna (e.g. Evans *et al.* 2001, Jones 2008, 2009, Rauhut *et al.* 2012, Apesteguía 2016, Herrera-Flores *et al.* 2017, Hsiou *et al.* 2019, Chambi-Trowell *et al.* 2021, DeMar *et al.* 2022, Simões *et al.* 2022). The diversity of rhynchocephalians has received new interest in the past decade (e.g. Rauhut and López-Arbarello 2016, Herrera-Flores *et al.* 2017, 2018, Rauhut *et al.* 2017, O'Brien *et al.* 2018, Chambi-Trowell *et al.* 2019, 2020, 2021, Gentil *et al.* 2019, Hsiou *et al.* 2019, Romo de Vivar *et al.* 2020, Simões *et al.* 2020, 2022, Sues and Schoch 2021, 2023, Villa *et al.* 2021, Anantharaman *et al.* 2022, DeMar *et al.* 2022, Beccari *et al.* 2025), especially regarding taxonomy and phylogeny.

A significant number of fossil rhynchocephalian specimens were found in localities that are part of the Late Jurassic Solnhofen

Received 7 February 2025; revised 23 April 2025; accepted 16 May 2025
[Version of Record, first published online 2 July 2025, with fixed content and layout in compliance with Art. 8.1.3.2 ICZN. http://zoobank.org/urn:lsid:zoobank.org:pub:3DD80139-4BB3-411A-8380-9AE0C1A26D00]

Archipelago, in southern Germany (see Tischlinger and Rauhut 2015). This epoch represents a crucial time in lepidosaur evolution: Rhynchocephalia remain diverse, while the crown group of Squamata diversify (e.g. Evans *et al.* 2001, Rauhut *et al.* 2012, Jones *et al.* 2013, Bolet *et al.* 2022). Interest in Solnhofen fossils has a long history (e.g. von Meyer 1854, Cocude-Michel 1963) and has been rekindled by new descriptions (Rauhut *et al.* 2012, Villa *et al.* 2021, Beccari *et al.* 2025). However, several specimens from the Solnhofen Archipelago remain undescribed (e.g. Rauhut and López-Arbarello 2016, Rauhut *et al.* 2017, Beccari *et al.* 2023). To date, 13 rhynchocephalian species have been named from this setting: *Acrosaurus frischmanni* Meyer, 1854, *Homoeosaurus maximiliani* Meyer, 1847, *Homoeosaurus parvipes* Cocude-Michel, 1963, *Homoeosaurus solnhofensis* Cocude-Michel, 1963, , *Kallimodon pulchellus* (Zittel, 1887–1890), *Leptosaurus neptunius* (Goldfuss, 1831), *Oenosaurus muehlheimensis* Rauhut *et al.*, 2012, *Piocormus laticeps* Wagner, 1852, *Pleurosaurus ginsburgi* Fabre, 1974, *Pleurosaurus goldfussi* Meyer, 1831, *Sapheosaurus thiollierei* Meyer, 1850, *Sphenofontis velserae* Villa *et al.*, 2021, and *Vadasaurus herzogi* Bever & Norell, 2017.

Many of the Solnhofen taxa are based on complete skeletons, but their preservation is not always good, and many taxonomical issues are known to be present owing to the lack of proper descriptions and diagnoses (see e.g. Rauhut and López-Arbarello 2016, Rauhut *et al.* 2017, Simões *et al.* 2020, Villa *et al.* 2021, Beccari *et al.* 2025). Hence, the validity of some of these taxa has been questioned previously (e.g. Fabre 1981, Jones 2008), and their contribution to phylogenetic analyses has been limited (e.g. Evans *et al.* 2001, Rauhut *et al.* 2012, DeMar *et al.* 2022). One case involves *H. maximiliani* (von Meyer 1847), the holotype of which was destroyed in the Second World War. Therefore, a neotype was proposed (SNSB-BSPG 1887 VI 502), with a redescription and a new diagnosis for the species (Cocude-Michel 1963). This diagnosis, however, is based mainly on general anatomical features rather than concrete apomorphic characters or an apomorphic character combination that would differentiate it from other rhynchocephalians: the rounded skull and the elongated limbs in comparison to body size. Many specimens were assigned to this species (Cocude-Michel 1963), but the vague diagnosis makes this assignment tentative, at best. Notably, specimen *SMF R414*, housed in the Senckenberg Naturmuseum Frankfurt, shows significant differences from the neotype of *H. maximiliani*. Only the main slab of this individual was previously reported and tentatively referred to *Homoeosaurus* (Drevermann 1931, Cocude-Michel 1963), but not described. The counterslab of this specimen, which has not been reported previously, was recently found in the Natural History Museum of London (specimen *NHMUK PV R 2741*) by one of us (V.B., 2022). This specimen contains most of the bones not preserved in *SMF R414*, and thus both specimens together provide a complete skeleton for comparison with other rhynchocephalians and for an evaluation of its ecomorphology.

To date, only a few studies have evaluated ecomorphology in Rhynchocephalia, focusing on their diet, through their cranial anatomy and tooth morphology (e.g. Fraser and Walkden 1983, Reynoso 2005, Jones 2008, 2009, Meloro and Jones 2012, Rauhut *et al.* 2012, Romo de Vivar Martínez and Soares 2015, Lee *et al.* 2016, Romo-de-Vivar-Martínez *et al.* 2017, Vaux *et al.* 2019, Chambi-Trowell *et al.* 2020, Scheyer *et al.* 2020, Herrera-Flores *et al.* 2022). There has been some interest in the postcranial variation within the group and its implication for ecological variation, but no extensive systematic comparisons with other taxonomic groups (e.g. Fabre 1974, Carroll and Wild 1994, Reynoso 2000, Dupret 2004, Rauhut *et al.* 2012, Lee *et al.* 2016, Bever and Norell 2017, Gutarra *et al.* 2023, Beccari *et al.* 2025). The main exception concerns aquatic (and possibly aquatic or semi-aquatic) taxa, such as *Acrosaurus* von Meyer, 1854, *Ankylosphenodon pachyostosus* Reynoso, 2000, *Kallimodon* Cocude-Michel, 1963, *Palaeopleurosaurus posidoniae* Carroll, 1985, *Pleurosaurus* von Meyer, 1831, *Sapheosaurus* von Meyer, 1850, and *Vadasaurus* Bever and Norell, 2017 (Carroll and Wild 1994, Gutarra *et al.* 2023, Beccari *et al.* 2025). The traits usually used to infer an aquatic lifestyle include: elongation of the axial skeleton, short appendicular bones (at least in pleurosaurs), late ossification of appendicular bones, robust first metacarpal, pachyostosis, and specific histological features (Carroll and Wild 1994, Reynoso 2000, Dupret 2004, Houssaye 2009, Bardet *et al.* 2014, Lee *et al.* 2016, Bever and Norell 2017, Klein and Scheyer 2017, Gutarra *et al.* 2023, Beccari *et al.* 2025). Furthermore, only Lee *et al.* (2016) and Gutarra *et al.* (2023) included a systematic evaluation of the importance of limb morphology for an evaluation of locomotion in fossil rhynchocephalians, but again only for aquatic or semi-aquatic taxa. Owing to the lack of extant rhynchocephalians other than *Sphenodon* Gray, 1831, an alternative way to understand the ecomorphological importance of their appendicular skeleton is to look at the diverse group of their closest extant relatives, limbed squamates (i.e. lizards).

In contrast to rhynchocephalians, many studies have been conducted to infer ecomorphology in lizards, using their appendicular skeleton (e.g. Goodman *et al.* 2008, Goodman 2009, Tulli *et al.* 2009, 2011, Pelegrin *et al.* 2017, Foster *et al.* 2018, Cordero *et al.* 2021, Huie *et al.* 2021, Howell *et al.* 2022). Most of these studies focus on specific clades, e.g. iguanians (Velasco and Herrel 2007, Tulli *et al.* 2009, 2011, Grizante *et al.* 2010, Paparella *et al.* 2018, Feiner *et al.* 2020, 2021, Huie *et al.* 2021, Edwards *et al.* 2022, Howell *et al.* 2022), gekkotans (Zaaf and Van Damme 2001), and scincids (Goodman *et al.* 2008, Goodman 2009, Foster *et al.* 2018, Camaiti *et al.* 2023). Studies of the ecomorphology of fossil lizards are also available, and although most focus on their cranial anatomy (e.g. Watanabe *et al.* 2019, Herrera-Flores *et al.* 2021, Bolet *et al.* 2022), there are some that have compared the postcranial morphology of fossil and extant squamates for ecomorphological inferences (e.g. Sherratt *et al.* 2015, Lee *et al.* 2016, Dickson *et al.* 2017, Paparella *et al.* 2018, Caldwell *et al.* 2021, Villaseñor-Amador *et al.* 2021, Gutarra *et al.* 2023).

Many previous studies have compared limb morphology and size, body size, and substrate preferences in lizards (e.g. Hagey *et al.* 2017, Foster *et al.* 2018, Camaiti *et al.* 2021, Feiner *et al.* 2021, Riedel *et al.* 2024). Although some studies found no statistical significance between these traits and substrate use (see the discussion by Foster *et al.* 2018), more recent analyses using extensive datasets and different approaches have shown significant correlation between morphology and substrate use in some

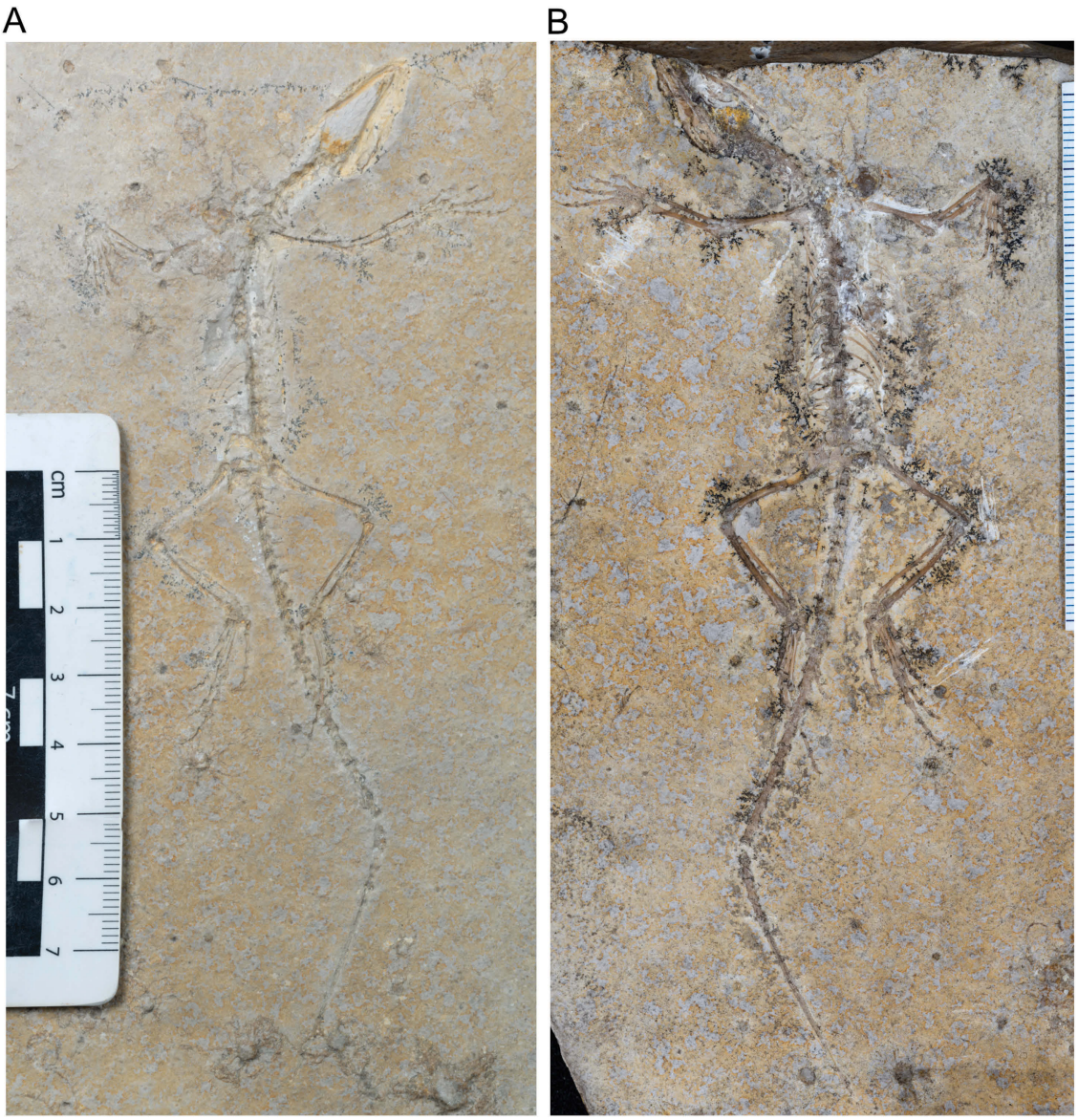


**Figure 1.** Photograph of the holotype of ***Sphenodraco scandentis***. A, *SMF R414*, the main slab, containing some bone remains and the imprint of the skeleton. B, *NHMUK PV R 2741*, the counterslab, containing most of the skeletal remains

lizard groups (e.g. Hagey *et al.* 2017, Foster *et al.* 2018, Riedel *et al.* 2024). These studies demonstrated that limb length and proportions may indicate habitat use and climbing performance. Terrestrial lizards show lower forelimb/hindlimb proportions and shorter limbs in comparison to body size than climbing lizards, i.e. saxicolous (rock-dwelling) and arboreal forms (Foster *et al.* 2018).

In this study, we describe a new genus and species of extinct rhynchocephalian with proportions that suggest arboreality, based on specimens *SMF R414* and *NHMUK PV R 2741*. Furthermore, we test this lifestyle using principal component analysis (PCA) and linear discriminant analysis (LDA) of postcranial measurements from a comprehensive sample of tuatara specimens of different ontogenetic stages and extant limbed squamates from different clades. We also evaluate substrate use among Jurassic rhynchocephalians. The goals of this study are to clarify the taxonomy of the two mentioned specimens and to establish a framework for evaluating ecomorphology among extinct lepidosaurs.

## MATERIALS AND METHODS

### Specimens in this study

This study focuses on the specimens *SMF R414* and *NHMUK PV R 2741* (Fig. 1), the main slab and counter slab of the same individual, containing most of the skeletal remains of a small rhynchocephalian, previously assigned to the species *Homoeosaurus maximiliani* (Cocude-Michel 1963, Fabre 1981). These specimens are respectively deposited in the public collections of the Senckenberg Museum, Frankfurt, Germany (SMF) and the Natural History Museum London, UK (NHMUK). The fossil comes from outcrops of the Altmühltal Formation (Early Tithonian) near Eichstätt, part of the Solnhofen Archipelago locality complex. *SMF R414* was previously also reported

as *Homoeosaurus* von Meyer, 1847, but not described, by Drevermann (1931). Interestingly, Drevermann (1931: 111) was obviously not aware at the time that a counterslab existed; how the fossil was divided and ended up in two different collections remains unclear.

The osteological description of the new taxon follows the terminology of Evans (2008) and Jones *et al.* (2011) for the skull, Hoffstetter and Gasc (1969) for the axial skeleton, and Evans (1981b) and Russell and Bauer (2008) for the appendicular skeleton. The new taxon was compared mainly with other fossil rhynchocephalians from the Solnhofen Archipelago, especially *H. maximiliani* and *Kallimodon pulchellus*, and the extant tuatara.

The specimens were photographed using a mirrorless camera (Nikon Z5; Nikon Corporation, Minato City, Tokyo, Japan), equipped with a LAOWA 100 mm macro lens (Venus Optics, Hefei, China). The counterslab *NHMUK PV R 2741* was photographed under ultraviolet (UV) light using the Alonefire SV003 10 W UV lamp, 365 nm (Shenzhen Shiwang Technology Co., Guangdong, China) and no filters.

### Sampling for ecomorphological analysis

A total of 150 specimens were used for this study: 85 extant limbed squamates from different major clades (Acrodonta Cope, 1864, Anguimorpha Fürbringer, 1900, Gekkota Cuvier, 1817, Lacertoidea Oppel, 1811, Pleurodonta Cope, 1864, and Scincoidea Oppel, 1811; for a complete list and repositories, see Supporting Information, Supplementary Data 1) and 65 rhynchocephalians. The latter include 43 specimens from the Jurassic of Europe (Germany and France), the holotype (*MNA.V.12442*) of *Navajosphenodon sani* Simões *et al.*, 2022 from the Jurassic of USA, and 21 extant tuatara specimens housed in different institutions (Supporting Information, Supplementary Data 1). Among the fossil rhynchocephalian specimens, some are yet unpublished and do not have precise taxonomic allocations; these are as follows: SNSB-BSPG XVIII P12 (a juvenile specimen from Brunn, Solnhofen Archipelago, Germany; Rauhut *et al.* 2017); SNSB-BSPG XVIII P3 and SNSB-BSPG XVIII P11 (two adult specimens from Brunn, Solnhofen Archipelago, Germany, with affinities to *Kallimodon*; Rauhut *et al.* 2017); and two *Oenosaurus* aff. *muehlheimensis* specimens (possibly pertaining to a new species; Beccari *et al.* 2023), SNSB-BSPG 2009 I 69 and SNSB-BSPG 2020 I 48, the latter being the cast of a privately owned specimen, HT 85/9.

All squamate specimens and a single tuatara specimen (UF. Herp 14110) were acquired through the online repository MorphoSource (https://www.morphosource.org/). These specimens were made available through the oVert project (Blackburn *et al.* 2024) or specific public institutions in the online repository (see the complete list of specimens in Supporting Information, Supplementary Data 1). Scans of some tuatara specimens in this study are publicly available online as part of a previous project on the sesamoid bones of tuatara (https://osf.io/bds35; Regnault *et al.* 2017), and some specimens (i.e. NHMUK Zoo 1935.5.14.3, MZH MS 1853, SAMA Herpetology 70524, SNSB-ZSM 1318-2006, SNSB-ZSM 20/1959, ZMB 9804, ZMB 10607, ZMB 13837, and ZMB 14023) are available in MorphoSource Supporting Information, Supplementary Data 1). The fossil rhynchocephalian specimens in this study are deposited in public collections (except for one *Oenosaurus* aff. *muehlheimensis* specimen, HT 85/9, of which a high-fidelity cast is available at SNSB-BSPG) and were photographed and measured by the authors of this study. Specimens available as CT scan-derived data (image stacks) were segmented for the creation of three-dimensional models using the software Avizo v.9.2 (Thermo Fisher Scientific, MA, USA).

### Phylogenetic analysis

To understand the phylogenetic affinities of our new taxon and yet undescribed rhynchocephalian specimens (i.e. SNSB-BSPG 1993 XVIII 3, SNSB-BSPG 1993 XVIII P12, and SNSB-BSPG 2009 I 69), we scored them into a modified version of the character matrix from the study by Simões *et al.* (2022) [a derivation from the original matrix published by Simões *et al.* (2020)] using the free online platform MorphoBank (https://morphobank.org/; O'Leary and Kaufman 2012). Additionally, the following taxa were added into the character matrix: *Acrosaurus frischmanni* (based on specimen SNSB-BSPG AS I 564), *Ankylosphenodon pachyostosus* (based on the description by Reynoso 2000 ), *Homoeosaurus solnhofensis* (based on the holotype *SMF R4073*), *Kallimodon cerinensis* Cocude-Michel, 1963 (based on the main slab MNHN CRN 77 and counterslab SNSB-BSPG 1908 I 76), *Opisthiamimus gregori* DeMar *et al.*, 2022 (*USNM PAL 722041*), and *Vadasaurus herzogi* (*AMNH FARB 32768*). We revised the scoring of many operational taxonomic units (OTUs), i.e. *Clevosaurus brasiliensis* Bonaparte and Sues, 2006, *Clevosaurus hudsoni* Swinton, 1939, *Derasmosaurus* Barbera and Macuglia, 1988, *H. maximiliani*, *H. parvipes*, *Kallimodon pulchellus*, *Leptosaurus* Fitzinger, 1840 (MNHN CNJ 72), *Oenosaurus muehlheimensis*, *Pleurosaurus ginsburgi*, *Pleurosaurus goldfussi*, *Piocormus* Wagner, 1852, *Priosphenodon avelasi* Apesteguía and Novas, 2003, and *Sapheosaurus* von Meyer, 1850.

A total of 20 new characters (4 cranial and 16 axial characters) were added to the data matrix (for a complete list of new characters, see Supporting Information, Supplementary Data 2). Character 70 (fusion of palatine dentition into a single longitudinal element, with character state 0 being absent and 1 being present) was removed from the dataset. In our personal observations, we found that this character was problematic, because we observed no longitudinal palatine tooth plate in any of the scored OTUs. In the original dataset by Simões *et al.* (2022), character 70 was scored as 1 in *Kallimodon pulchellus*, *Oenosaurus muehlheimensis*, and *Sapheosaurus thiollierei*. In *Kallimodon pulchellus*, the palatine dentition is made of discrete teeth, as can be observed in SNSB-BSPG 1922 I 15 (character state 0). The holotype of *Oenosaurus muehlheimensis*, *SNSB-BSPG 2009 I 23*, shows a poorly preserved dental ridge in the palatine, and no information can be gained on the presence and morphology of palatine dentition (unknown character state). Likewise, the palatine dentition of *Sapheosaurus thiollierei* is poorly preserved and cannot be scored confidently (unknown character state). Given that these three taxa are the only ones having previously been scored with character state 1, their change makes character 70 uninformative in the present analysis.

The final data matrix consists of 149 characters and 46 OTUs (Supporting Information, Supplementary Data 2 and 3). The maximum parsimony phylogenetic analysis was run in the

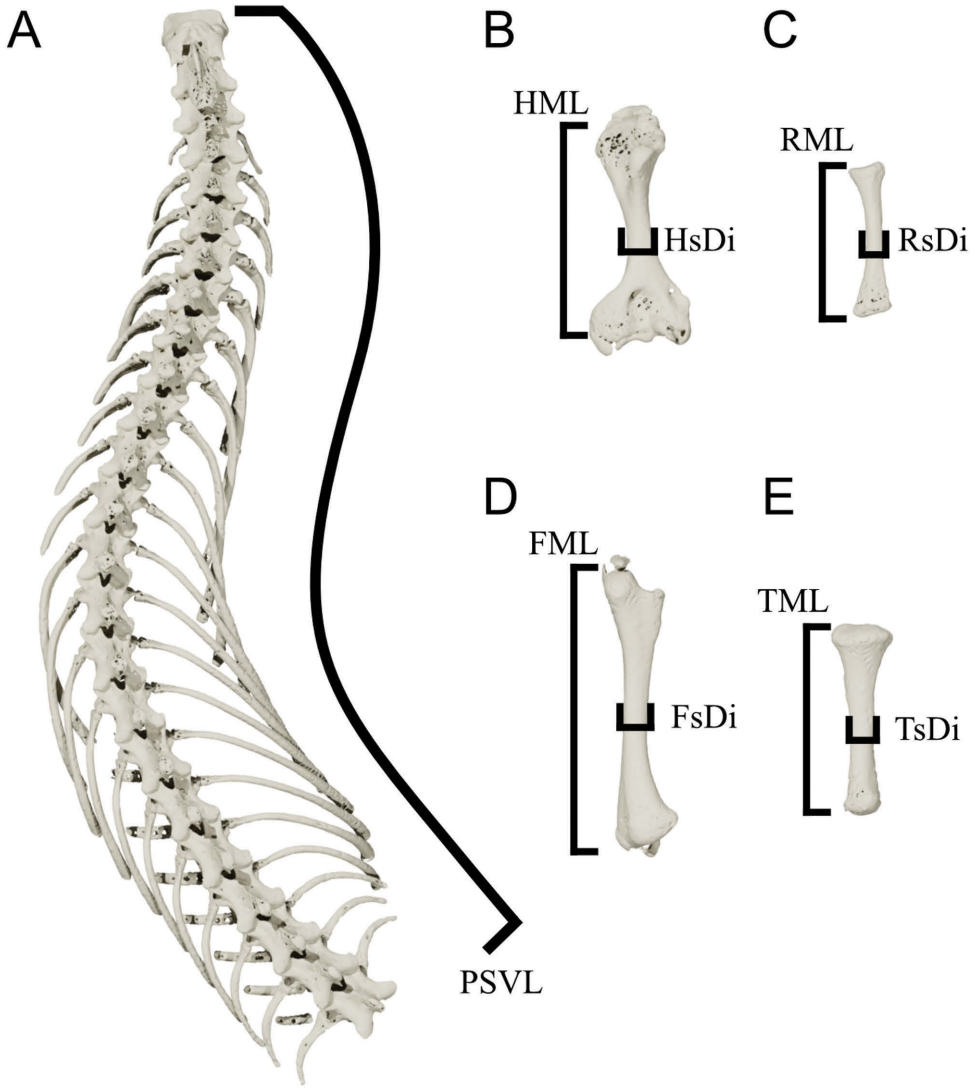


**Figure 2.** Measurements for the ecomorphological analysis. Measurements showcased on the three-dimensional model of a subadult *Sphenodon punctatus* specimen (ZMB 9804). A, presacral series. B, left humerus. C, left radius. D, right femur. E, right tibia. Abbreviations: FML, femur, length between metaphyses; FsDi, femur, shaft diameter; HML, humerus, length between metaphyses; HsDi, humerus, shaft diameter; PSVL, presacral vertebrae length; RML, radius, length between metaphyses; RsDi, radius, shaft diameter; TML, tibia, length between metaphyses; TsDi, tibia, shaft diameter.

software TNT v.1.6 (Goloboff and Morales 2023) using New Technology Search, finding the minimal length 50 times, using Ratchet, Drift, and Tree Fusion. The analysis was with implied weighting for the characters ($k = 8$) following the protocol of Ezcurra (2024). The reduced consensus trees, which removes rogue OTUs from the analyses, was recovered using the command 'pcr.>0;nel//{0}' in TNT. Rogue taxa were removed from the final parsimony analysis.

An unrooted Bayesian phylogenetic analysis was conducted in RevBayes v.1.2.6 (Höhna *et al.* 2016) using the Mk model (Lewis 2001) for discrete characters. The model incorporated gamma-distributed rate variation among characters (Yang 1994, Capobianco and Höhna 2025), and characters were partitioned by their number of states (Khakurel *et al.* 2024). Four independent Markov chain Monte Carlo chains were executed for 100 000 generations. The script and trees of the Bayesian analysis can be found in Supporting Information, Supplementary Data 4. Suprageneric taxonomy in this study follows Simões *et al.* (2020) for rhynchocephalians and Simões and Pyron (2021) for squamates.

### Linear measurements

Nine linear measurements across the axial and appendicular skeleton were taken for each specimen in this study (Fig. 2; Supporting Information, Supplementary Data 1). These measurements were chosen because they have been correlated with substrate use in previous studies, and to include the highest number of fossil specimens in our analysis (the sample limitations is discussed in the section 'Defining habitat use in rhynchocephalians and sampling limitations' below). Most rhynchocephalian specimens from the Solnhofen Archipelago show a high degree of taphonomic deformation and some degree of breakage; the matrix, in addition to incomplete preparation, complicates access to measurable variables. The preservation of

these specimens hampers a consistent acquisition of measurements available throughout our sample. For body size, the total presacral vertebrae length (PSVL, measured from the anterior tip of the axis to the posterior margin of the last presacral vertebra; in millimetres) was used instead of snout–vent length, because some specimens in this study lacked either a complete skull or a complete sacral region. Eight further measurements (all in millimetres) were taken for the appendicular skeleton: humerus length between metaphyses (HML); humerus mid-shaft diameter (HsDi); radius length between metaphyses (RML); radius mid-shaft diameter (RsDi); femur length between metaphyses (FML); femur mid-shaft diameter (FsDi); tibia length between metaphyses (TML); and tibia mid-shaft diameter (TsDi). The length between proximal and distal metaphyses (measured between proximal and distal ends of the appendicular bone, excluding the epiphyses) was preferred to the complete limb bone length (measured between both proximal and distal epiphyses) because hatchlings and juveniles, in addition to some fossil rhynchocephalians (e.g. pleurosaurids, *Kallimodon*, and *Leptosaurus*), have poorly ossified or unossified epiphyses (Cocude-Michel 1963, Fabre 1974, 1981, Dupret 2004, Russell and Bauer 2008). The mid-shaft diameter of the limb bones was measured as a proxy of limb bone robustness, because the cross-section in these bones is usually subcircular (Russell and Bauer 2008). All fossil specimens in this study were selected on the basis of preserving at least one complete humerus, radius, femur, and tibia.

The three-dimensional models of CT scan-derived data were measured digitally for all squamate and tuatara specimens and for some fossil rhynchocephalians (see Supporting Information, Supplementary Data 1). These specimens were imported into the open source, free software Blender v.4.1 (Blender Foundation, Amsterdam, The Netherlands), and measurements were acquired using its Measuring tool. Most of the fossil rhynchocephalian specimens were measured using a digital calliper (resolution, 0.01 mm; accuracy, 0.04 mm), or with the free software ImageJ v.1.54g (Schneider *et al.* 2012) when only pictures were available. All the specimens have been photographed or measured physically by the authors of this study, except for the holotype of *Leptosaurus neptunius* (*StIPB 1305*). This specimen has been misplaced or lost (Rauhut and López-Arbarello 2016), and only published pictures of it are currently available (e.g. Cocude-Michel 1963). Nevertheless, Cocude-Michel (1963) provided most measurements of interest.

All linear measurements were transformed using a log-shape ratio approach (Mosimann 1970), i.e. for each specimen we divided each of the nine measurements by its geometric size, that is, the geometric mean of the nine measurements. This method separates size and shape but retains the allometric consequences of variation in size (Klingenberg 2016).

These measurements were used to perform linear morphometrics by using PCA and LDA. Both the PCA and the LDA were run in the free software PAST4 v.4.17 (Hammer *et al.* 2001). Given that the measurements used different units and can have different scales, the analyses were performed using a correlation matrix. Missing values were treated with the iterative imputation option, as recommended by Hammer *et al.* (2001). To explore how morphology and ecology could be associated, extant limbed lizards were categorized according to their substrate using SquamBase (Meiri 2024). In this database, substrate or microhabitat use is represented by seven categories (arboreal, terrestrial, saxicolous, semi-aquatic, marine, fossorial, and cryptic), but taxa can also be given a combination of these categories (e.g. arboreal & terrestrial, terrestrial & saxicolous). In our study, the categories were simplified to five, for ease of analysis and comparison to fossil taxa (Supporting Information, Supplementary Data 1): (i) arboreal ($N = 21$ specimens); (ii) semi-arboreal (all taxa that have a combination of arboreal and other categories; $N = 21$ specimens); (iii) terrestrial (all terrestrial, and the cryptic-terrestrial, *Xantusia wigginsi* Savage, 1952, taxa, because the latter uses mainly leaf litter as its substrate; $N = 18$ specimens); (iv) saxicolous (all saxicolous and combined terrestrial and saxicolous; $N = 16$ specimens); and (v) semi-aquatic (as in the study by Meiri 2024, with the addition of the marine iguana, *Amblyrhynchus cristatus* Bell, 1825; $N = 9$ specimens). Substrate use by *Sphenodon* is terrestrial, although they do spend time in burrows and can dig their own (e.g. Cree 2014). Measurements of fossil specimens were included in the PCA, without specifying their substrate use. The principal component (PC) scores from the PCA were used to perform the LDA, to determine whether the substrates ascribed to the extant specimens could be differentiated and whether fossil specimens could be classified to these substrates. To test our results in the LDA further, two analyses were done, the first one using the five abovementioned substrate uses, and a second one in which semi-aquatic squamates were assigned a 'secondary' substrate use, following the SquamBase (e.g. semi-aquatic lizards that are mainly terrestrial when not in the water were assigned the terrestrial substrate use in this second analysis). In these analyses, *Acrosaurus*, *Palaeopleurosaurus* Carroll, 1985, and *Pleurosaurus* specimens were assigned the marine substrate use, following the current consensus that these animals were fully marine (e.g. Carroll and Wild 1994, Beccari *et al.* 2025). The confusion matrix of the LDA was corrected using jackknifed resampling (leave-one-out cross-validation procedure; Hammer *et al.* 2001).

A second PCA was run for the *Sphenodon* specimens in this study to understand possible influences of ontogeny and skeletal maturity in our complete analysis. This analysis followed the same methods as stated above.

## Nomenclatural acts

This publication and its nomenclatural acts are registered at ZooBank (zoobank.org). The publication is registered as 'zoobank.org/urn:lsid:zoobank.org:pub:3DD80139-4BB3-411A-8380-9AE0C1A26D00'; the new genus *Sphenodraco* as 'zoobank.org/urn:lsid:zoobank.org:act:A8D02D03-462B-4046-BF0C-7062429FF0FF'; and the new species *Sphenodraco scandentis* as 'zoobank.org/urn:lsid:zoobank.org:act:8558457C-E048-4126-B9D3-727752ABC29A'.

## Institutional abbreviations

AMNH FARB, American Museum of Natural History, Paleontology: Fossil Amphibians, Reptiles, and Birds, New York, NY, USA; AMNH Herpetology, American Museum of Natural History, Department of Herpetology; DM and DINO, Dinosaur National Monument, Vernal, UT, USA; HT, Helmut

Tischlinger private collection, Germany; LMU, Ludwig-Maximilians-Universität München, Munich, Germany; MB.R, Paläontologische Sammlungen am Museum für Naturkunde, Berlin, Germany; MCM and MNHN, Muséum national d'Histoire naturelle, Paris, France; NHMLA, Natural History Museum of Los Angeles County, Los Angeles, CA, USA; NHMUK, Natural History Museum London, Collection Specimen, London, UK; MPN, Museo di Paleontologia, Naples, Italy; QMUL QMBC, Queen Mary University of London, Queen Mary Biology Collection, London, UK; SMF, Senckenberg Naturmuseum, Frankfurt, Germany; SMNS, Staatliches Museum für Naturkunde Stuttgart, Stuttgart, Germany; SNSB-BSPG, Bayerische Staatssammlung für Paläontologie und Geologie, Munich, Germany; SNSB-ZSM, Zoologische Staatssammlung München Sammlungen, Bavarian State Collection of Zoology Collections, Munich, Germany; StIPB, Museum Koenig, Bonn, Germany; TM, Tylers Museum, Haarlem, The Netherlands; UF.Herp, University of Florida, Florida Museum of Natural History, Division of Herpetology, Gainesville, FL, USA; USNM, National Museum of Natural History (formerly United States National Museum), Smithsonian Institution, Washington, DC, USA; YPM, Yale Peabody Museum, New Haven, CT, USA; ZMB, Museum für Naturkunde, Zoological Collection, Berlin, Germany.

## RESULTS

## SYSTEMATIC PALAEONTOLOGY

**Lepidosauria Haeckel, 1866**

**Rhynchocephalia Günther, 1867 *sensu* DeMar *et al.* (2022)**

**Neosphenodontia Herrera-Flores *et al.*, 2018**

### *Sphenodraco* gen. nov.

*Derivation of name:* The genus name combines the prefix *spheno-* (which composes the name Sphenodontia) and *draco* (Latin for 'dragon', but also in reference to the arboreal gliding lizards, whose limb proportions are similar to that of the new taxon) and translates to 'the sphenodontian dragon'. The genus name is masculine.

*Type species: Sphenodraco scandentis* gen. et sp. nov., by monotypy.

*Diagnosis:* As for type and only known species.

### *Sphenodraco scandentis* sp. nov.

*Derivation of name:* The species name comes from the Latin word *scandens*, meaning 'climber'.

*Holotype:* The holotype of *Sphenodraco scandentis* is divided into two slabs (Figs 1, 3; Supporting Information, Supplementary Data 2: Table S1): the counter slab (*NHMUK PV R 2741*), containing most of the skeletal remains, and a main slab (*SMF R414*), including the mould of the skeleton and some of the remaining bones. *NHMUK PV R 2741* represents a small and articulated rhynchocephalian preserved in ventral view, containing some skull bones (i.e. right premaxilla, left and right maxillae, right jugal, right quadratojugal, left palatine, left and right pterygoids, basisphenoid, left and right mandibles, and ceratobranchials), most of the postcranial elements (i.e. the complete axial series, pectoral and pelvic girdles, and fore- and hindlimbs), and soft-tissue impression in the tail region. *SMF R414* contains the distal phalanges (unguals) of manual digits IV and V (left side) and III and IV (right side), fragments of the left ischium, the proximal half of the right femur, a fragment of right metatarsal V, pedal phalanges I and II of the right digit IV, and a fragment of the ungual of left pedal digit V.

*Locality and horizon:* According to Cocude-Michel (1963: p. 11), the holotype comes from the area of Eichstätt, although the exact locality has not been reported. It is thus derived from the Altmühltal Formation (*eigeltigense* horizon of the Riedense ammonite zone of the Early Tithonian; Schweigert 2015); given that the lower part of the Eichstätt Member of this formation (*sensu* Niebuhr and Pürner 2014) is largely covered and there are no active quarries in this unit, it most probably comes from the Upper Eichstätt Member.

*Diagnosis:* Small rhynchocephalian with the following unique combination of traits: (i) maxillary dentition with posterior flanges decreasing in size posteriorly among the last three teeth; (ii) bases of the maxillary teeth are oblique to the tooth row (in labial view)*; (iii) short posterior process of the pleurapophysis of sacral vertebra 2; (iv) tall, funnel-shaped proximal epiphysis of the humerus; (v) tall acetabular region of the ilium, with posteriorly oriented iliac blade; (vi) short pubic process of the ilium*; (vii) slender stylopodia and zeugopodia, with the diameter being <.06 of the length between metaphyses; and (viii) metacarpal and metatarsal IV longer than III. An asterisk (*) represents autapomorphic features.

### Description

#### *Skull*

Considering that only a limited number of bone elements are preserved in the main slab, *SMF R414*, the description of the new taxon (both cranial and postcranial elements) is mainly based on the counterslab, *NHMUK PV R 2741*. The exposed portion of the skull (Fig. 4) is elongate and triangular in ventral view, as in *Kallimodon pulchellus*, *Leptosaurus*, *Pleurosaurus*, and *Vadasaurus*, and different from the rounded skull outline of *Homoeosaurus*, *Oenosaurus* Rauhut *et al.*, 2012, *Sapheosaurus*, and *Sphenofontis* Villa *et al.*, 2021 (Cocude-Michel 1963, Fabre 1981, Rauhut *et al.* 2012, Villa *et al.* 2021).

#### *Premaxilla*

Only a small, posterior part of the right premaxilla is preserved (Fig. 4). The dentigerous portion of the bone is absent. The posterior process of the premaxilla contacts the anterior process of the maxilla, although the ventralmost contact is not preserved in *NHMUK PV R 2741*.

#### *Maxilla*

The anterior region of the left maxilla is only exposed in part in ventral view, with the posterior half obscured by the left mandible (Fig. 4). This portion has one poorly preserved tooth. The right maxilla is well preserved and visible in ventrolateral view. The maxilla is elongated and increases in height posteriorly. The

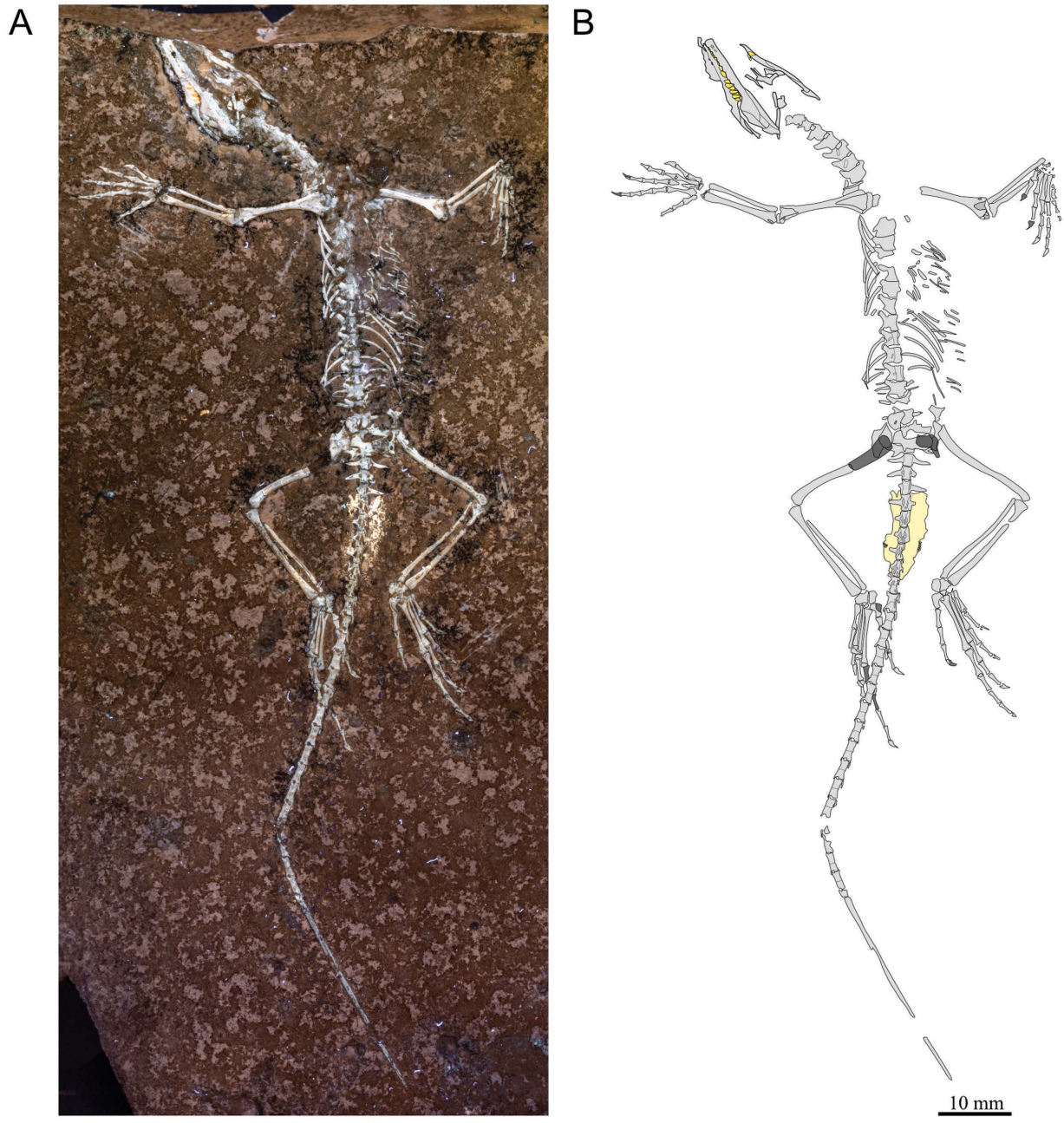


**Figure 3.** The holotype counterslab of ***Sphenodraco scandentis*** *NHMUK PV R 2741*. A, photograph under ultraviolet light. B, schematic illustration. The dark (black) bones in the illustration represent the bones preserved in the main slab *SMF R414*.

anterior premaxillary process of the maxilla tapers to a point anteriorly. This process extends slightly further anteriorly than in *Kallimodon pulchellus*, which has a short anterior process ending flush with the anterior margin of the facial process of the maxilla, but is not as developed anteriorly as in *Homoeosaurus* and *Pleurosaurus* (Cocude-Michel 1963, Fabre 1974, 1981). The visible part of the facial process of the maxilla is shallow rectangular and about half of the total length of the maxilla. It has at least three anteroposteriorly aligned oval foramina along its base, the anteriormost of which is the largest. The suborbital portion of the maxilla bows laterally, resulting in a gently concave lateral margin in ventral view. The posterior process of the maxilla is short and tapers posteroventrally. It contacts the jugal mediodorsally and obscures the lateral surface of the anterior process of the latter bone in lateral view. Its general morphology is similar to that of *Kallimodon pulchellus* and *H. maximiliani* (Cocude-Michel 1963).

### *Jugal*

Only the ventral portion of the right jugal can be seen in *NHMUK PV R 2741* (Fig. 4). This bone is lateromedially narrow. The anterior process is shorter than the ascending (dorsal) process; it is similar in morphology to the anterior process of most rhynchocephalians, but different from the bifid one of *Pleurosaurus* (Beccari *et al.* 2025). The ascending process extends posterodorsally and overlaps the anterior end of the squamosal laterally. The quadratojugal (posterior) process of

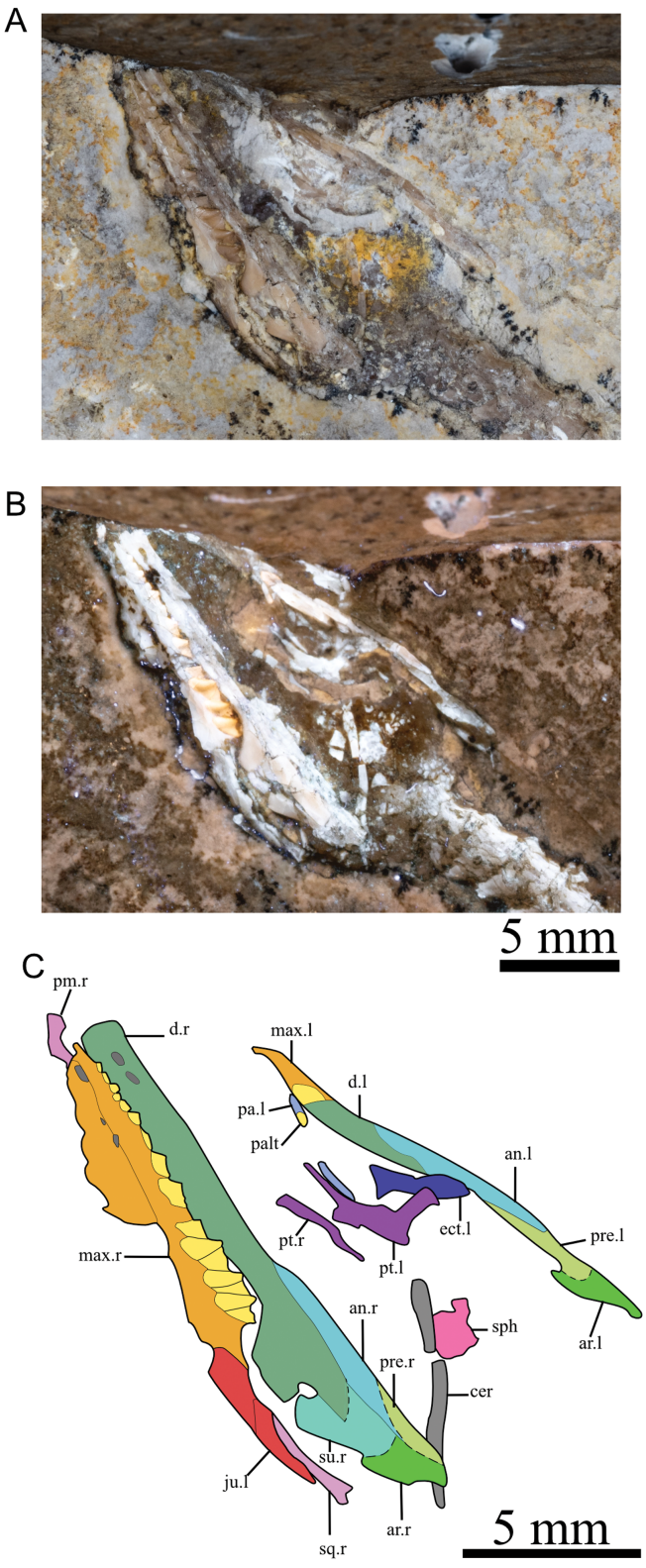


**Figure 4.** Skull of the holotype of ***Sphenodraco scandentis*** *NHMUK PV R 2741*. A, photograph of the skull under normal lighting. B, photograph of the skull under ultraviolet light. C, schematic illustration of the skull. Abbreviations: an, angular; ar, articular; cer, ceratobranchial; d, dentary; ect, ectopterygoid; ju, jugal; max, maxilla; pa, palatine; palt, palatine tooth; pm, premaxilla; pre, prearticular; pt, pterygoid; sph, sphenoid; sq, squamosal; su, surangular. Note that .l and .r after the respective abbreviations indicate left and right elements, respectively. Hatched lines represent uncertain bone contacts.

the jugal is not present in *NHMUK PV R 2741*. Instead, a small posterior 'bump' lies at the base of the ascending process, as was observed in *Pleurosaurus* (Beccari *et al.* 2025). The lack of a quadratojugal process of the jugal seems to be shared between Jurassic rhynchocephalians of the Solnhofen Archipelago (e.g. *Kallimodon*, *Homoeosaurus*, and *Sapheosaurus*; see the discussion below), except for *Sphenofontis*, which shows the elongated and straight posterior (quadratojugal) process found in *Sphenodon* (Evans 2008, Jones *et al.* 2011, Villa *et al.* 2021). The posterior margin of the jugal of *NHMUK PV R 2741* is therefore concave, and the lower temporal fenestra is open in this specimen.

### *Squamosal*

Only a small portion of the anterior process of the right squamosal is visible in ventral view (Fig. 4). This process contacts the ascending process of the jugal medially, as in *Pleurosaurus* (Beccari *et al.* 2025), but differently from *Sphenodon* (Evans 2008, Jones *et al.* 2011).

### *Palatine*

Only two small portions of the left palatine are preserved in ventral view (Fig. 4). The anterior portion preserves a tooth, and the posterior one flanks the anterior ramus of the pterygoid laterally. This posterior portion is slender but does not appear to be broken laterally, suggesting that the articular portion (i.e., the articular facet to the pterygoid) of the palatine tapers posteriorly, as in *Kallimodon pulchellus* (e.g. SNSB-BSPG 1922 I 15) and *Oenosaurus* (Rauhut *et al.* 2012), but different from the broad posterior region of the palatine of *Sphenodon* and *Sphenofontis* (Evans 2008, Villa *et al.* 2021).

### *Pterygoid*

Both pterygoids are poorly preserved, with the left element being slightly more complete (Fig. 4). The pterygoid shows a slender palatine process, which contacts the palatine laterally, and an elongated ectopterygoid flange. The flange contacts the ectopterygoid anterolaterally; it is longer than in *Oenosaurus* and *Kallimodon pulchellus* SNSB-BSPG 1922 I 15, but is similar to that of *Sphenodon* and *Pleurosaurus* cf. *Pleurosaurus ginsburgi* SNSB-BSPG 2018 I 179 (Evans 2008, Beccari *et al.* 2025). However, it differs from the latter *Pleurosaurus* specimen in being laterally straight, rather than posterolaterally oriented (Beccari *et al.* 2025).

### *Ectopterygoid*

The left ectopterygoid is preserved disarticulated from the pterygoid and slightly rotated, such that the ventromedial view is exposed (Fig. 4). The lateral and ventral processes (lateral and ventral heads *sensu* Evans 2008) are visible and elongated, as in *Sphenodon*, but different from the stout, bifid process of *Oenosaurus* (Rauhut *et al.* 2012) and from the short ectopterygoid of *Kallimodon pulchellus* SNSB-BSPG 1922 I 15 (Evans 2008). The lateral process of the ectopterygoid is anteroposteriorly broad and lateromedially flattened.

### *Sphenoid*

A small fragment of the sphenoid is preserved in ventral view (Fig. 4). It is square in ventral view and shows a well-developed, anterolateroventrally directed basipterygoid process.

### *Lower jaw*

The left mandible is poorly preserved and exposed in ventral and slightly medial view (Fig. 4). The right mandible is almost complete, lacking the posterior region of the prearticular. It is preserved in ventrolateral view. The posterior end of the mandible is poorly preserved. The coronoid process of the dentary is obscured by sediment, and the coronoid is obscured by the dentary and surangular laterally. The mandibular foramen is enlarged and placed slightly above mid-height of the mandible at the posterior base of the coronoid process, as in most rhynchocephalians.

### *Dentary*

The dentary is the largest mandibular bone of *NHMUK PV R 2741* (Fig. 4). It is elongated and shallow, and the ventral margin is only slightly convex ventrally. The symphysial end is broken in this specimen, but its outline is still visible in *SMF R414*. The ventral margin of the anterior end of the dentary is slightly expanded ventrally, forming the ventral 'chin' (*sensu* Villa *et al.* 2021), which is also present in *H. maximiliani*, *Kallimodon pulchellus*, *Oenosaurus*, *Sphenodon*, and *Sphenofontis*, but not in *Pleurosaurus* and *Vadasaurus* (Cocude-Michel 1963, Fabre 1981, Evans 2008, Rauhut *et al.* 2012, Villa *et al.* 2021, Beccari *et al.* 2025). At the anterior end, the lateral surface of the right dentary is pierced by two large, anteroposteriorly aligned oval foramina. The coronoid process of the dentary is triangular in lateral view, with a concave anterior and slightly convex posterodorsal margin. Posteriorly, the dentary forms the anterior and ventral margins of the mandibular foramen and is thus bifurcated, with a smaller dorsal and a larger ventral posterior process. The ventral posterior process of the dentary tapers distally and is triangular in lateral view. In contrast to many rhynchocephalians (e.g. *Sphenodon*: Evans 2008; *Sphenofontis*: Villa *et al.* 2021), the process does not reach the area of the articular glenoid of the mandible.

### *Angular*

The angular is slender and forms most of the posteroventral margin of the mandible (Fig. 4).

### *Surangular*

Only a small portion of the lateral wall of the right surangular is exposed (Fig. 4). The surangular has a well-developed anterior process that articulates medially with the coronoid process of the dentary. As in most rhynchocephalians, the surangular, articular, and prearticular are unfused, different from the articular complex of *Pleurosaurus* (Beccari *et al.* 2025).

### *Prearticular*

Only a small portion of the prearticular is visible (Fig. 4). Its poor preservation hampers description of the bone. It is located ventrolaterally to the articular, but it is unclear whether it contributes to the posterior end of the lower jaw.

### *Articular*

In lateral view, the articular is short and tall in *NHMUK PV R 2741* (Fig. 4), and the retroarticular process is short and triangular, similar to that of *Kallimodon pulchellus*, but different from the relatively longer, posteriorly oriented process of *Pleurosaurus* (Cocude-Michel 1963, Fabre 1974, 1981, Dupret 2004, Beccari *et al.* 2025). Although it is not possible to identify confidently whether a medial ridge is present on the dorsal surface of the articular, the overall lateral aspect of this bone resembles that of other rhynchocephalians, e.g. *Diphydontosaurus* Whiteside, 1986, *Gephyrosaurus bridensis* Evans, 1980, *H. maximiliani*, *Kallimodon pulchellus*, *Oenosaurus muehlheimensis*, and *Sphenodon* (*Evans 1981a*, *Whiteside 1986*, *Evans 2008*, *Rauhut et al. 2012*). Therefore, it is possible that *Sphenodraco* also showed this ridge, which is associated with proal jaw action (e.g. Jones *et al.* 2011, 2012, Simões *et al.* 2022).

### *Dentition*

Only the maxillary and a small part of the palatine dentition are exposed in *NHMUK PV R 2741* (Figs 4, 5A, B). At least 13 teeth are present in the right maxilla. The five anteriormost teeth show some alternation in size, whereas the posterior seven teeth generally increase in size posteriorly, with the three distalmost teeth being the largest. The five anterior teeth might represent a hatchling series, but it is also possible that it has been replaced fully or in part by successional teeth.

The anterior teeth are small, worn down, and conical. The third tooth in this anterior series is taller than the other ones, but the apex is broken. It is possible that this tooth is a worn-down caniniform, as present in other rhynchocephalians, such as *Navajosphenodon* Simões *et al.*, 2022, *Sphenodon*, and *Sphenofontis* (Howes and Swinnerton 1901, Rieppel 1992, Villa *et al.* 2021, Simões *et al.* 2022), and in JME-Scha 100 (Fig. 5G, H), assigned to the *Kallimodon–Leptosaurus* complex (Renesto and Viohl 1997, Rauhut and López-Arbarello 2016). No successional teeth are present in specimens assigned to *Homoeosaurus*, *Kallimodon*, and *Pleurosaurus* (Cocude-Michel 1963, Fabre 1981, Beccari *et al.* 2025). Although the anterior teeth possibly pertain to hatchling dentition, there is no clear boundary between those and additional teeth in *NHMUK PV R 2741*. Teeth 6 and 7 are here regarded as displaying a transitional morphology between the anterior hatchling teeth and the posterior additional teeth, although they might represent anterior additional teeth, because the anteriormost additional teeth are usually smaller and can alternate in size (Robinson 1976). The eighth tooth and more posterior teeth are likely to be additional teeth, which were added to the back of the growing jaw bone during ontogeny. These are similar in morphology to one another but increase in size posteriorly. These teeth have a triangular outline in labial view and comprise an anterior cone and a posterior flange. The anterior cone occupies half of the tooth length. It has an apicobasally slightly concave mesial border and a rounded labial surface. The posterior flanges are lower than the respective cone and decrease in size posteriorly. Their apical margin is slightly concave, different from the convex margin of *H. maximiliani* (Fig. 5E, F) and *Kallimodon pulchellus* (Fig. 5C, D) and from the straight margin of JME-Scha 100 (Fig. 5G, H). As in other rhynchocephalians, the additional teeth have an *en echelon* arrangement, with the flange of the preceding tooth being overlapped labially by the cone of the following tooth.

A single palatine tooth is preserved in *NHMUK PV R 2741* (Fig. 4). This tooth is conical, with an ovoid cross-section at the

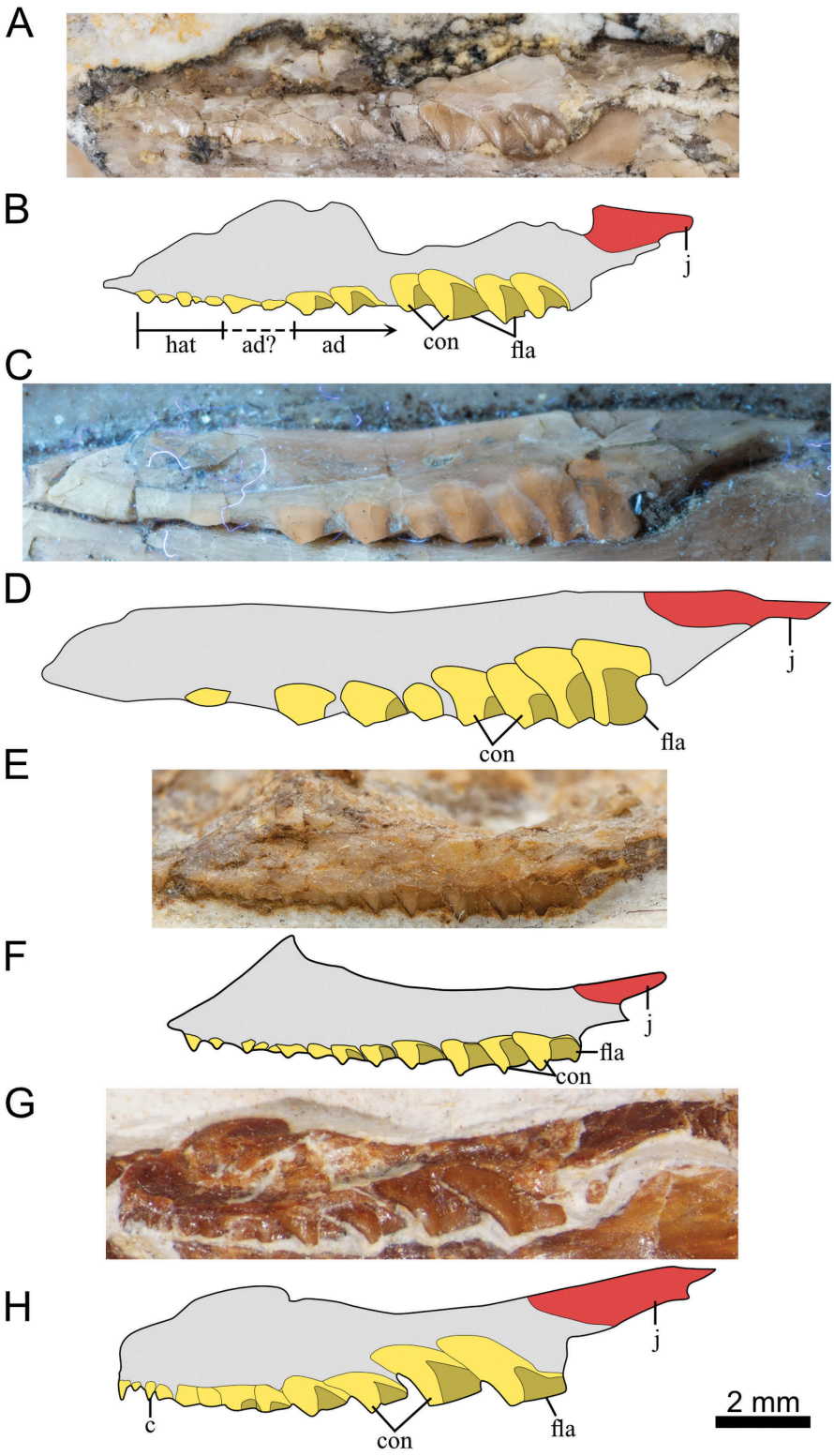


**Figure 5.** Comparison of the dentition of ***Sphenodraco scandentis*** and other fossil rhynchocephalians. A, B, photograph (A) and schematic illustration (B) of mirrored right maxilla of *NHMUK PV R 2741*. C, D, photograph under ultraviolet light (C) and schematic illustration (D) of the mirrored right maxilla of *Kallimodon pulchellus SNSB-BSPG 1887 VI 1*. E, F, photograph (E) and schematic illustration (F) of the left maxilla of *Homoeosaurus maximiliani* SNSB-BSPG 1937 I 40. G, H, photograph (G) and schematic illustration (H) of the mirrored right maxilla of JME-Scha 100 (*Kallimodon–Leptosaurus* complex specimen from Rauhut and LópezArbarello 2016). All photographs and illustrations are up-to-scale. Abbreviations: ad, additional teeth; ad?, possible additional teeth; c, caniniform; con, anterior cone; fla, posterior flange; hat, hatchling dentition; j, jugal; tran, transitional dentition.

base. It is similar in morphology to the single palatine tooth of *Kallimodon pulchellus* (SNSB-BSPG 1922 I 15).

### *Hyoid*

A single, incomplete ceratobranchial is preserved in *NHMUK PV R 2741* (Fig. 4). This bone is slender and slightly bowed, similar to the one observed in *Kallimodon pulchellus SNSB-BSPG 1887 VI 1* (Cocude-Michel 1963), *Microsphenodon bonapartei* Chambi-Trowell *et al.*, 2021, *Sphenodon* (Evans 2008), and *Sphenofontis* (Villa *et al.* 2021), but different from the robust and wide ceratobranchials of *Pleurosaurus* cf. *Pleurosaurus ginsburgi* SNSB-BSPG 2018 I 179 (Beccari *et al.* 2025).

### *Axial skeleton*

*NHMUK PV R 2741* preserves most of its presacral, sacral, and caudal vertebral series in articulation, with only a few presacrals and caudals missing. However, both sacral vertebrae are partly obscured by the pelvic girdle (Fig. 6). All preserved vertebrae appear to be amphicoelous. The vertebral count includes 23 preserved presacral vertebrae (24 in total, including the obscured atlas), two sacral vertebrae, and 25 caudal vertebrae, in addition to a long, calcified distal tail region, representing a possible regrown tail, as it has been described in other Solnhofen rhynchocephalians (Tischlinger and Wild 2009, Villa *et al.* 2021). The exact position of the cervical–dorsal transition and thus the precise number of cervical vertebrae cannot be determined for *NHMUK PV R 2741* owing to the absence of a preserved sternum and cervical ribs.

### *Presacral vertebrae, ribs, and gastralia*

The atlas cannot be observed in *NHMUK PV R 2741* because it is poorly preserved and obscured by matrix and other bones. The axis is poorly preserved, with its anterior half fragmented (Fig. 6). The odontoid process cannot be observed. The axial centrum widens posteriorly. It is shorter than the following presacral vertebrae and lacks diapophyseal protuberances.

All presacral vertebrae are exposed in ventral view, but slightly deflected such that the right lateral sides of the centra and pre- and postzygapophyses are exposed. The presacral vertebral centra are hourglass shaped in ventral view and slightly longer than wide. The length of the presacral series centra increases slightly posteriorly until at least presacral vertebra 8, from where on it remains constant in length until the last presacral vertebra. The centra lack ventral ridges. Presacral vertebra 6 and following vertebrae show a posterodorsal–anteroventral oriented synapophysis. This feature is similar to *Kallimodon pulchellus*, but different from the *Oenosaurus* aff. *muehlheimensis* specimen SNSB-BSPG 2009 I 69 (first synapophysis on presacral vertebra 5), *Pleurosaurus* (first synapophysis on presacral vertebrae 3), and *Sphenodon* (first synapophysis on presacral vertebra 4, but presacral vertebrae 3 shows a lateral protuberance, possibly an incipient synapophysis not associated with ribs; Cocude-Michel 1963, Hoffstetter and Gasc 1969, Fabre 1974, 1981, Beccari *et al.* 2025). The synapophyseal articulation facet is slightly posterolaterally oriented, as in *Kallimodon pulchellus* and SNSB-BSPG 1993 XVIII 3, but different from the laterally oriented synapophysis in other rhynchocephalians. The pre- and postzygapophyses are elongated, with the prezygapophyses expanding anterolaterally and the postzygapophyses posterolaterally. This elongated condition is similar to that of *Kallimodon pulchellus*, but differs from *H. maximiliani*, which shows short, less expanded zygapophyses (Cocude-Michel 1963, Fabre 1981).

It is not possible to see the intercentrum of presacral 3, but presacrals 4–8 show wedge-like intercentra. The posterior presacral vertebrae lack intercentra.

The anteriormost ribs (short cervical ribs), if present, cannot be identified. The single-headed dorsal ribs are elongated and bowed. These ribs are tubular throughout their length, with an anteroposterior flattening at their distal ends. The dorsal ribs are similar in length until reaching presacral vertebra 21, then decrease rapidly in size posteriorly. The last pair of ribs (presacral vertebra 24) is partly fused to the synapophysis. In *Sphenodon*, the last pair of presacral ribs is totally fused only in adult individuals, but the fusion starts in late juveniles (V.B., personal observations). At least four bits of bone recovered in the vicinity of the dorsal ribs are here interpreted as mineralized sternocostal segments. These are similar to the ones in *Sphenodon*: elongated and Y-shaped.

Gastralia are preserved in *NHMUK PV R 2741* (Fig. 6). These bones are slender and slightly recurved posteriorly at their distal end. The chevrons (contact between left and right elements) are not preserved.

### *Sacral vertebrae*

Both sacral vertebral centra are obscured by the pelvic girdle, and their morphology cannot be accessed (Fig. 6). The first sacral vertebra bears a long pleurapophysis (fused rib, *sensu* Hoffstetter and Gasc 1969) that is directed laterally. This process does not deflect posteriorly or expand towards its distal end. The pleurapophysis of the second sacral vertebra is bifid, with a tubular anterior process reaching the ilium and a posterolaterally oriented posterior process. The anterior process extends only laterally and does not expand anteriorly at its distal end, similar to *H. solnhofensis*, but different from *Kallimodon pulchellus*, *H. maximiliani*, *H. parvipes*, *Pleurosaurus*, and *Vadasaurus*, all of which have anteriorly deflected distal ends in this process, sometimes reaching the transverse process of the first presacral vertebra (Cocude-Michel 1963, Fabre 1974, 1981, Bever and Norell 2017). The posterior process tapers distally. It extends only until the midlength of the anterior process. This condition is similar to that of *Leptosaurus* sp. SMF R 4108, *Pleurosaurus*, and *Vadasaurus* (Cocude-Michel 1963, Fabre 1974, Bever and Norell 2017), but different from the more laterally elongated posterior process of *Kallimodon pulchellus*, *Homoeosaurus*, *Oenosaurus* aff. *muehlheimensis* SNSB-BSPG 2009 I 69, and *Sphenofontis* (Cocude-Michel 1963, Villa *et al.* 2021; V.B., personal observations).

### *Caudal vertebrae*

The first eight caudal vertebrae are exposed in ventral view, caudal vertebra nine in right ventrolateral view, and all posterior caudals in right lateral view (Fig. 6). The anterior caudal vertebral centra are slightly longer than wide, with a gradual increase in length posteriorly. The centra are hourglass shaped in ventral view, with the constriction between the articular ends increasing from the first caudal posteriorly in those vertebrae that are exposed in ventral view. Different from the presacral

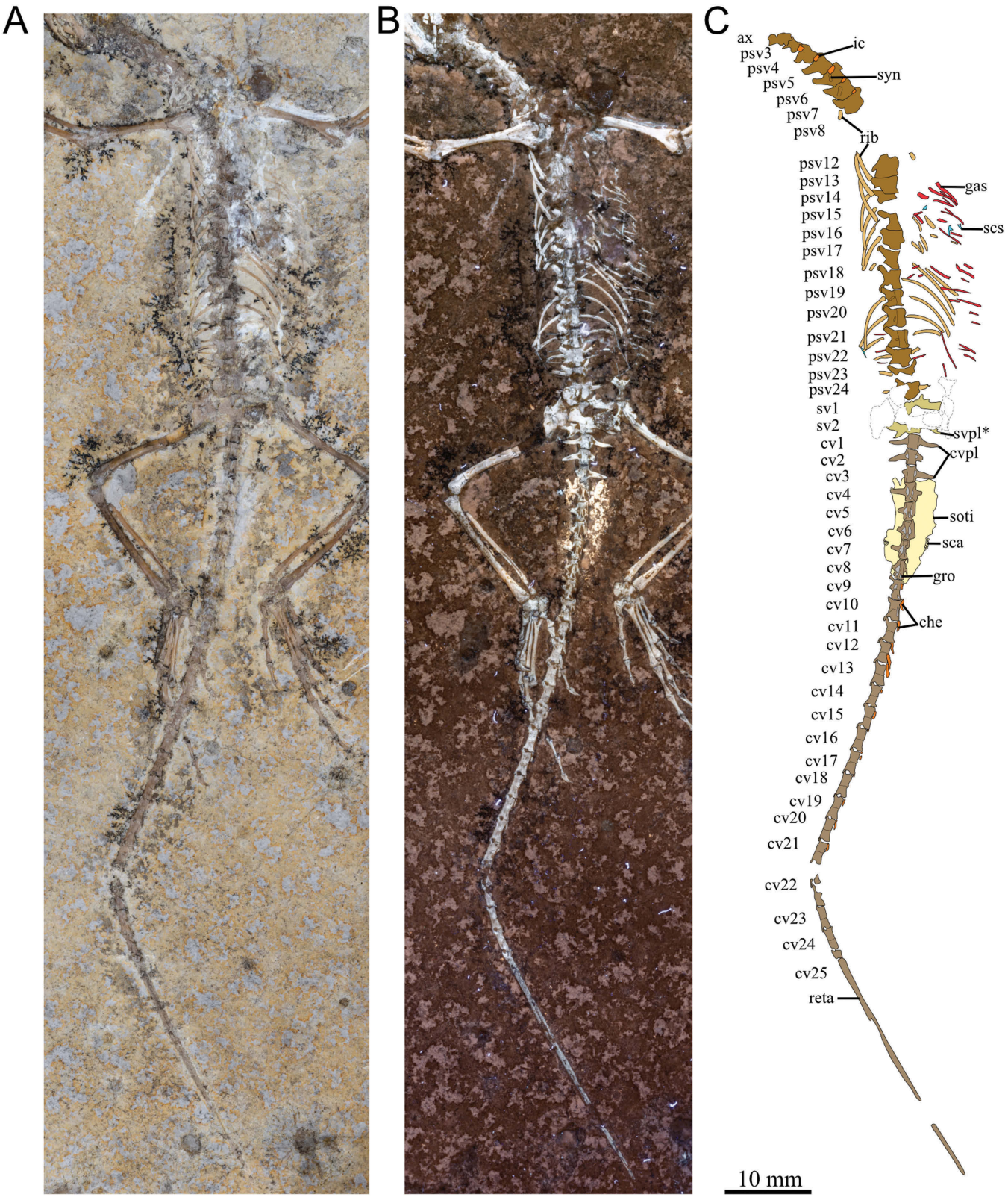


**Figure 6.** Axial skeleton of the holotype of ***Sphenodraco scandentis*** *NHMUK PV R 2741*. A, photograph under normal lighting. B, photograph under ultraviolet light. C, schematic illustration. Abbreviations: ax, axis; che, chevron; cv, caudal vertebra; cvpl, caudal vertebra pleurapophysis; gas, gastralia; gro, groove; ic, intercentrum; psv, presacral vertebra; reta, regrown tail; rib, ribs; sca, scales impression; scs, sternocostal segment; soti, soft tissue impression; sv, sacral vertebra; svpl, sacral vertebra pleurapophysis. Asterisk (*) indicates diagnostic features of ***Sphenodraco scandentis***. Preserved soft tissue impression is marked in yellow.

vertebrae, the ventral surface of the caudal centra is excavated by a shallow median groove, starting in the second caudal. This groove is also observed in the caudal vertebrae of the *Kallimodon pulchellus* holotype (V.B., personal observations). The posterior caudals (caudal vertebra 10 and onwards) are similar in shape, being much longer than tall. The prezygapophyses are shorter than the postzygapophyses. Autotomic planes are clearly visible and present from caudal vertebra 9 onwards posteriorly. The eighth caudal appears to lack such a plane. In *Sphenodon* and *Sphenofontis*, the autotomy plane appears in caudal 8 and 7, respectively (Hoffstetter and Gasc 1969, Seligmann *et al.* 2008, Villa *et al.* 2021). *Homoeosaurus parvipes*, *H. solnhofensis*, *Kallimodon pulchellus*, and *Pleurosaurus* lack autotomy planes in their caudal vertebrae (Cocude-Michel 1963, Fabre 1974, 1981, Dupret 2004, Beccari *et al.* 2025; V.B., personal observations). Autotomy planes are known in isolated caudal vertebrae of *Gephyrosaurus bridensis*, but the starting position along the tail is unknown (Evans 1981a).

Caudal vertebra 25 is represented only by its portion anterior to the autotomy plane. Posterior to this, an elongated calcified portion of regrown tail is present (Fig. 6).

The anterior nine caudal vertebrae have long pleurapophyses (sometimes referred to as transverse processes, e.g. Villa *et al.* 2021). These processes change in orientation along the caudal series, with the first three pleurapophysis pairs directed slightly posterolaterally, the pleurapophyses 4 and 5 directed laterally, and from caudals 6 to 9 directed slightly anterolaterally. The pleurapophyses of the first caudal vertebra differ from the others in showing a markedly concave anterior margin, whereas this margin is convex in the following vertebrae. In *Sphenodon*, the orientation of the pleurapophyses of the anterior caudal series does not change throughout ontogeny and follows the pattern of first two directed laterally, and the following ones directed anteriorly (Villa *et al.* 2021; V.B., personal observations). In *Sphenofontis*, all anterior caudal pleurapophyses are bowed anteriorly at their distal half (Villa *et al.* 2021). All *Kallimodon pulchellus* and *Leptosaurus* specimens observed show different patterns of caudal pleurapophyses compared with *NHMUK PV R 2741*, with the ribs of caudals 6–9 directed posteriorly in these taxa. Two specimens of *H. maximiliani*, SNSB-BSPG 1887 VI 502 and MB.R.893, show the same pattern as *NHMUK PV R 2741*.

The intercentra of the first caudal vertebrae are missing in *NHMUK PV R 2741*. In the posterior caudals, the intercentrum is modified into a chevron. The chevrons are relatively short and seem to have been more posteriorly than ventrally directed.

### *Appendicular skeleton*

The appendicular skeleton of *NHMUK PV R 2741* is almost entirely preserved, with only a few elements missing (Figs 7, 8). The left scapula and coracoid, the interclavicle, and left clavicle are missing or not exposed in *NHMUK PV R 2741*. The right clavicle, scapula, and coracoid are preserved, but mostly obscured by the right humerus. The right elements of the pelvic girdle are better preserved and unfused to each other, whereas the left elements are either unpreserved or poorly preserved in this specimen. The long bones are extremely slender and elongated in comparison to other rhynchocephalians, even the ones with longer limbs, such as *H. maximiliani*, *H. solnhofensis*, and *Navajosphenodon*. The carpus is not fully ossified, but some of the distal elements are preserved.

#### *Pectoral girdle*

Owing to the preservation of the pectoral girdle, little can be said about its morphology (Fig. 7). A slender, bent rod-like bone associated with the right scapula is here interpreted as the right clavicle. The scapular blade is wide and rectangular, at least as far as what can be said of the exposed portion. Only the ventral margin of the coracoid is visible, and it is concave.

#### *Humerus*

Both humeri are incompletely preserved (Fig. 7). The left humerus is preserved in anterior view and lacks the proximal end, and the right humerus is preserved in anteroventral view, lacking the distal epiphysis. The humerus is only slightly longer than the ulna (accounting for the olecranon). The humeral ends are only slightly twisted relative to one another, with the bicipital fossa being visible on the same plane as the radioulnar fossa. The same condition is observed in the holotype of *Kallimodon pulchellus* (*SNSB-BSPG 1887 VI 1*), but not in the probably conspecific referred specimen SNSB-BSPG 1922 I 15, whose proximal and distal ends are twisted and almost perpendicular to one another. Although taphonomy could play a part in bringing the proximal and distal ends to the same plane, these differences in the humeral torsion are better explained by either intraspecific or interspecific variation. In *Sphenodon*, the angle of torsion between the proximal and distal ends of the humerus has been reported to be ~40°, but this trait might vary with ontogeny (Günther 1867, Russell and Bauer 2008).

Both ends of the humerus are strongly dorsoventrally expanded compared with the humeral shaft. The proximal end is funnel shaped in ventral view, being more strongly expanded posteriorly than anteriorly, with a wide and deep bicipital fossa. The deltopectoral crest is well developed and slightly expanded anteriorly. The humeral condyle is poorly ossified. This condyle is anteroposteriorly wide and dorsoventrally short, being rectangular in ventral view. The humeral shaft is slender and relatively long. The shaft appears to be cylindrical in cross-section, as can be observed by the broken left humerus, and its diameter-to-length proportion is the smallest among rhynchocephalians, even when comparing with the slender limbs of *H. maximiliani* and *H. solnhofensis* (Cocude-Michel 1963, Fabre 1981). The distal end of the humerus is anteroposteriorly wide, but not to the same extent as the proximal end of the bone. The entepicondyle is bulbous and well developed. It expands further distally than the ectepicondyle and is more markedly expanded from the shaft than the latter. The epicondyles are separated by a deep radioulnar fossa. The ectepicondylar foramen is fully open anteriorly and posteriorly. The entepicondylar foramen is open at least at the ventral end, but its dorsal opening is obscured by sediment. The humerus lacks a developed radial condyle, as in other Solnhofen Archipelago rhynchocephalians (e.g. *Kallimodon*, *Homoeosaurus*, and *Pleurosaurus*), but different from the well-developed radial condyle of *Sphenodon* (Russell and Bauer 2008).

#### *Radius and ulna*

Both radii and ulnae are preserved in posterior view (Fig. 7). Without accounting for the olecranon process, both radius and

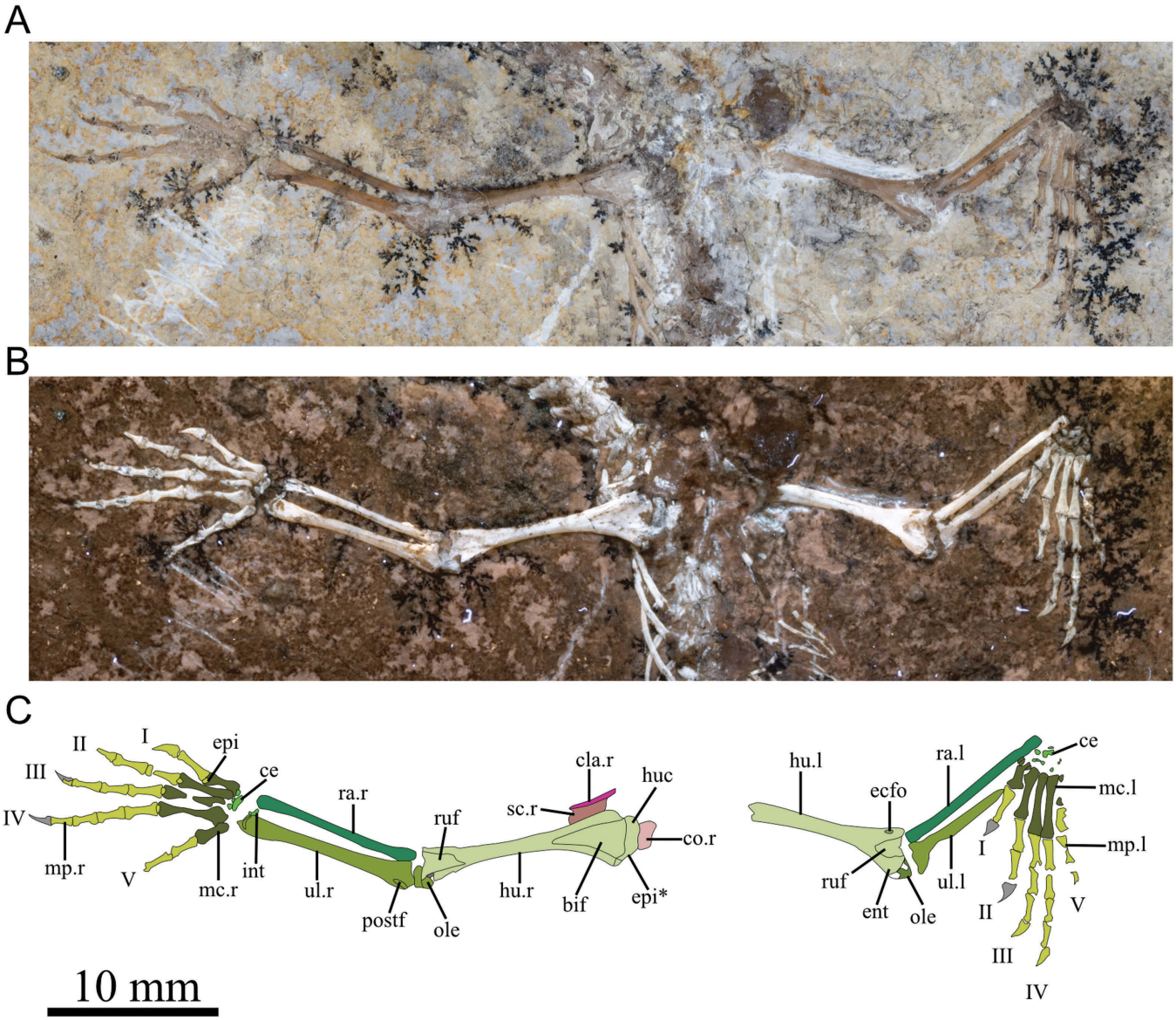


**Figure 7.** Forelimbs and pectoral girdle of ***Sphenodraco scandentis*** *NHMUK PV R 2741*. A, photograph under normal lighting. B, photograph under ultraviolet light. C, schematic illustration. Abbreviations: IV, digits I–V; bif, bifid fossa; ce, medial centrale; cla, clavicle; co, coracoid; ecfo; ectepicondylar foramen; ent, entepicondyle; epi, epiphysis; hu, humerus; huc, humeral condyle; int, intermedium; mc, metacarpal; mp, manual phalanx; ole, olecranon process; postf, posterior fossa; ra, radius; ruf, radioulnar fossa; sc, scapula; ul, ulna. Note that .l and .r after the respective abbreviations indicate left and right elements, respectively. Asterisk (*) indicates diagnostic features of ***Sphenodraco scandentis***. In dark grey, bones preserved in the main slab, *SMF R414*.

ulna are similar in length, being elongated and slender bones. The ulna is slightly wider than the radius. Both radial ends are slightly dorsoventrally expanded. However, this expansion is barely noticeable, as is the case for *Homoeosaurus*, but different from other rhynchocephalians, such as *Kallimodon*, *Oenosaurus*, *Pleurosaurus*, *Sphenodon*, and *Sphenofontis* (Cocude-Michel 1963, Fabre 1981, Russell and Bauer 2008, Villa *et al.* 2021; V.B., personal observations). The radius is mainly straight throughout its length, with only a slight ventral flexure at the proximal end of the bone.

Both ulnar ends are dorsoventrally expanded. The proximal end is well developed, with a ventral expansion that overlaps the proximal end of the radius in posterior view and with a robust, but poorly ossified, olecranon process. The olecranon process is ossified, but not fused to the ulnar end. The sigmoid notch is concave and deep. The posterior fossa is deep and oval. This fossa lies at the dorsal end of the posterior surface of the proximal end. The distal end of the ulna is rounded and not fully ossified.

### *Carpus*

Only some elements of the carpus are preserved in *NHMUK PV R 2741* (Fig. 7). The lack of most elements here is interpreted as being attributable to poor ossification of the cartilaginous carpal components, which could indicate that the specimen possibly represents a subadult individual. At least two larger carpal bones are distinguishable, a proximal carpal interpreted here as an intermedium between the distal ends of the ulna and radius, and the medial centrale. The centrale is wide and short, rectangular

in palmar view, and concave proximally. It contacts the distal carpals I–III. These distal carpals are small and circular.

### *Metacarpus*

All metacarpals are preserved in *NHMUK PV R 2741*, the left ones exposed in dorsomedial view and the right ones in ventrolateral view (Fig. 7). Metacarpal IV is the longest, followed by III, II, V, and I (Fig. 9). In *H. maximiliani*, *H. solnhofensis*, *Kallimodon pulchellus*, *Leptosaurus*, and *Oenosaurus* aff. *muehlheimensis* SNSB-BSPG 2009 I 69, metacarpal IV is also the longest (Cocude-Michel 1963, Fabre 1981; V.B., personal observations), but in *Navajosphenodon*, *Opisthiamimus* DeMar *et al.*, 2022, *Pleurosaurus*, *Sphenodon*, and *Sphenofontis*, the longest metacarpal is the third one (Cocude-Michel 1963, Russell and Bauer 2008, Villa *et al.* 2021, DeMar *et al.* 2022, Simões *et al.* 2022). In *Kallimodon*, the first metacarpal is longer than the fifth, different from *NHMUK PV R 2741*, whose metacarpals I and V are subequal in length, with the latter slightly longer. The proximal epiphyses of metacarpals I–V are not fully ossified.

Although all metacarpals are elongated, slender bones, whose proximal and distal ends are mediolaterally expanded relative to the shaft, their overall morphology diverges slightly. Both metacarpals I and V have asymmetrical proximal and distal ends. Both proximal and distal mediolateral expansions in metacarpal I are more pronounced laterally. The proximal lateral expansion is overlapped ventrolaterally by the proximal end of metacarpal II. The head of metacarpal I is rounded in dorsal view. The medial margin of the shaft of metacarpal I is almost straight, being gently concave in ventral view, whereas the lateral margin is strongly concave. The lateral expansion of the distal end in metacarpal I advances further distally than its medial expansion. A groove separates the lateral and medial expanded ends in ventral view.

Metacarpals II and III are similar to each other in morphology. Both show symmetrical proximal and distal ends. Proximally, the lateral surface of these metacarpals is overlapped ventrolaterally by the subsequent metacarpal. The proximal end of metacarpals II and III is slightly compressed in a dorsolateral to ventromedial direction.

Metacarpal IV shows a distinct morphology from the other metacarpals. The proximal end shows a well-developed dorsolateral expansion and is triangular in lateral view. This expansion is different from the rounded proximal end of all other metacarpals in *NHMUK PV R 2741* and seems to be unique to metacarpal IV in this specimen when compared with other rhynchocephalians, including *Homoeosaurus*, *Kallimodon*, *Navajosphenodon*, *Oenosaurus* sp., *Opisthiamimus*, *Pleurosaurus*, *Sphenodon*, *Sphenofontis*, and *Vadasaurus*.

Metacarpal V shows almost a mirrored condition to metacarpal I, having both proximal and distal ends expanded further medially than laterally. Metacarpals I–IV are almost parallel and diverge only slightly distally, whereas metacarpal V strongly diverges laterally from metacarpal IV. The lateral margin of metacarpal V is almost straight, whereas its medial margin is strongly concave.

The distal end of all metacarpals shows a prominent mesial groove between the lateral and medial expansions. This groove forms a saddle joint articulation to the first phalanx of the manual digits.

### *Manual digits*

Most phalanges are preserved in *NHMUK PV R 2741*, with some distal phalanges (unguals) preserved in the main slab, *SMF R414* (Figs 3–7). The phalangeal formula is 2-3-4-5-3, as is typical for rhynchocephalians (Cocude-Michel 1963, Fabre 1981, Russell and Bauer 2008). The fingers are long and slender, with digit four being the longest. The proximal phalanges are the longest of each digit, especially in digits I, III, and IV, with a gradual decrease in length throughout the distal phalanges (Fig. 9).

The proximal phalanges are well ossified, but their proximal epiphyses are unfused. Proximally, the articular condyle of these phalanges is ventrally expanded, forming a proximally oriented joint that slots into the distal groove of the metacarpals. The distal sequential phalanges show a concave articular margin proximally and no proximoventral expansion.

The distal articulation of the non-ungual phalanges is composed of a pair of condyles, the lateral of which is slightly wider than the medial. The lateral margin of the shaft in these phalanges is slightly more concave than their medial margins.

The manual unguals are short, tall at the base, and strongly concave ventrally. This differs from the short but ventrally flattened unguals of *Pleurosaurus* and from the long and flattened unguals of *Kallimodon* and *Oenosaurus* aff. *muehlheimensis* (Cocude-Michel 1963, Fabre 1981; V.B., personal observations). The proximal articulation is ginglymoid, with a tall dorsal condyle and a shorter ventral one.

### *Pelvic girdle*

*NHMUK PV R 2741* displays the left ilium, both pubes, and the right ischium in ventral view, in addition to the right ilium in lateral view (Figs 3–8). The left ischium is preserved in dorsal view in *SMF R414*. All pelvic bones are in articulation, but unfused.

The ilium contributes the most to the acetabulum (Fig. 8C, D). As observed in *NHMUK PV R 2741*, the ilium is divided into a deep iliac blade posteriorly, whose full length cannot be evaluated because it is broken distally, an acetabular region that is slightly longer than tall (Supporting Information, Supplementary Data 2: Table S1), and a short anterior pubic process. The iliac blade is directed posteriorly, being parallel to the axial series. This seems to be the same orientation as the ilium of *Kallimodon* (e.g. SNSB-BSPG 1887 VI 2), *Oenosaurus* aff. *muehlheimensis* (SNSB-BSPG 2009 I 69), and *Sapheosaurus* (MB.R.1950), but differs from the posterodorsally oriented iliac blade of *H. maximiliani* (SNSB-BSPG 1937 I 40), *H. parvipes* (MB.R.1007), *Pleurosaurus* (e.g. SNSB-BSPG 1977 X 40), and *Sphenodon* (Cocude-Michel 1963, Fabre 1974, Russell and Bauer 2008). The anterior pubic process is relatively short compared with other rhynchocephalians, such as *Kallimodon*, *Pleurosaurus*, and *Sphenodon* (Cocude-Michel 1963, Fabre 1974, 1981, Russell and Bauer 2008). Especially in *Kallimodon*, the anterior pubic process is similar in length to the iliac blade (e.g. in specimens *SNSB-BSPG 1887 VI 1* and SNSB-BSPG 1922 I 15; V.B., personal observations). The anterior margin dorsal to the pubic process is concave anteriorly and forms a distinct bulging preacetabular process in the dorsal margin of the ilium.

Both pubes are poorly preserved, with the proximal end of the right pubis being the best-preserved portion (Fig. 8C, D). The articular facet to the ilium in the pubis is convex. An

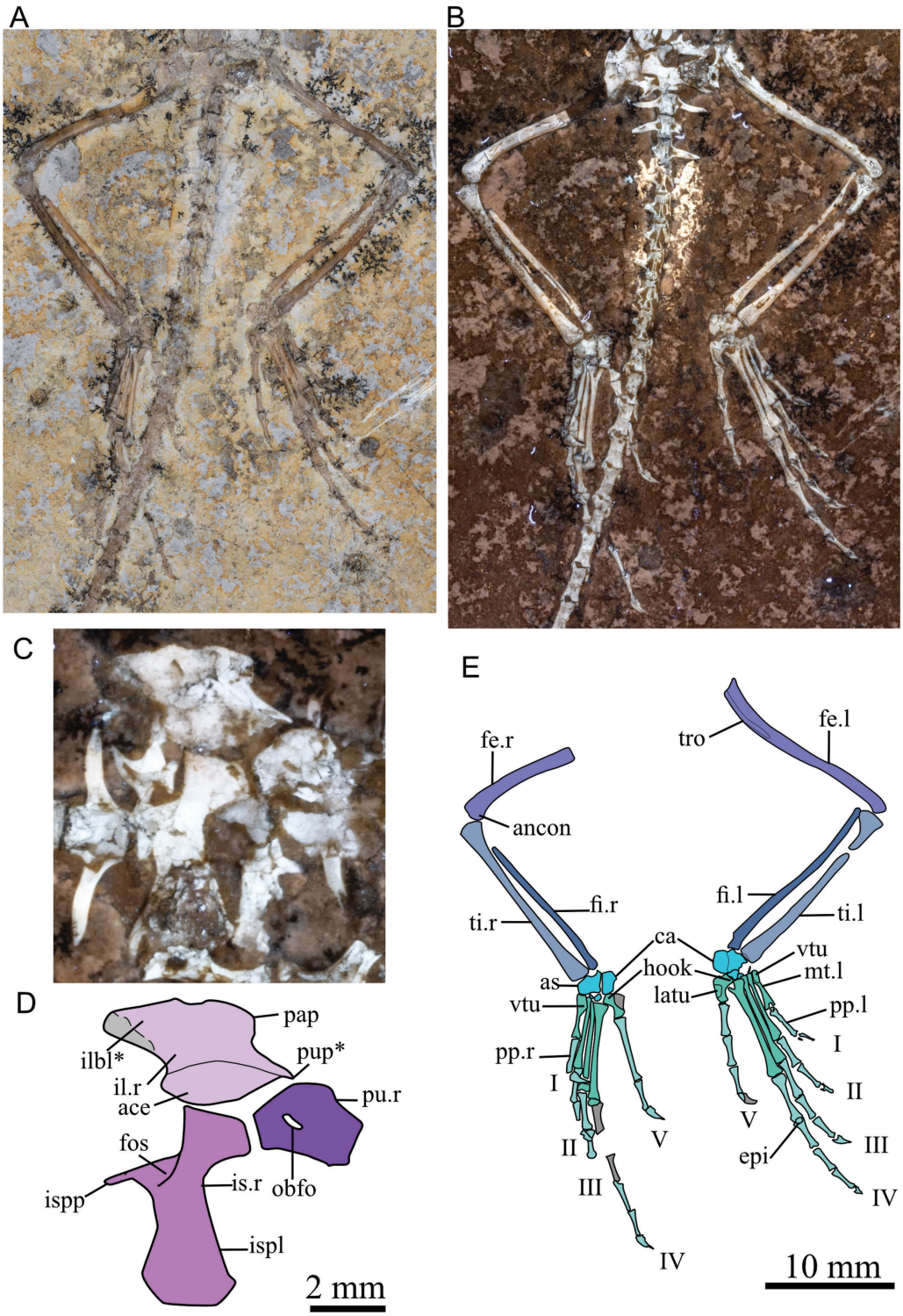


**Figure 8.** Hindlimbs and pelvic girdle of ***Sphenodraco scandentis*** *NHMUK PV R 2741*. A, photograph under normal lighting. B, photograph under ultraviolet light. C, detailed photograph of the right pelvic girdle elements under ultraviolet light. D, schematic illustration of the right pelvic girdle elements. E, schematic illustration of the hindlimbs. Abbreviations: I–V, digits I–V; ace, acetabulum; ancon, anterior condyle; as, astragalus; ca, calcaneum; epi, epiphysis; fe, femur; fi, fibula; fos, fossa; hook, hook of metatarsal V; il, ilium; ilbl, iliac blade; is, ischium; ispl, ischiadic plate; ispp, ischium posterior process; latu, lateral tubercle; mt; metatarsal; obfo, obturator foramen; pap, preacetabular process; pp, pedal phalanx; pu, pubis; pup, pubic process of the ilium; ti, tibia; tro, trochanter; vtu, ventral tubercle. Note that .l and .r after the respective abbreviations indicate left and right elements, respectively. Asterisk (*) indicates diagnostic features of ***Sphenodraco scandentis***. In dark grey, bones preserved in the main slab *SMF R414*.

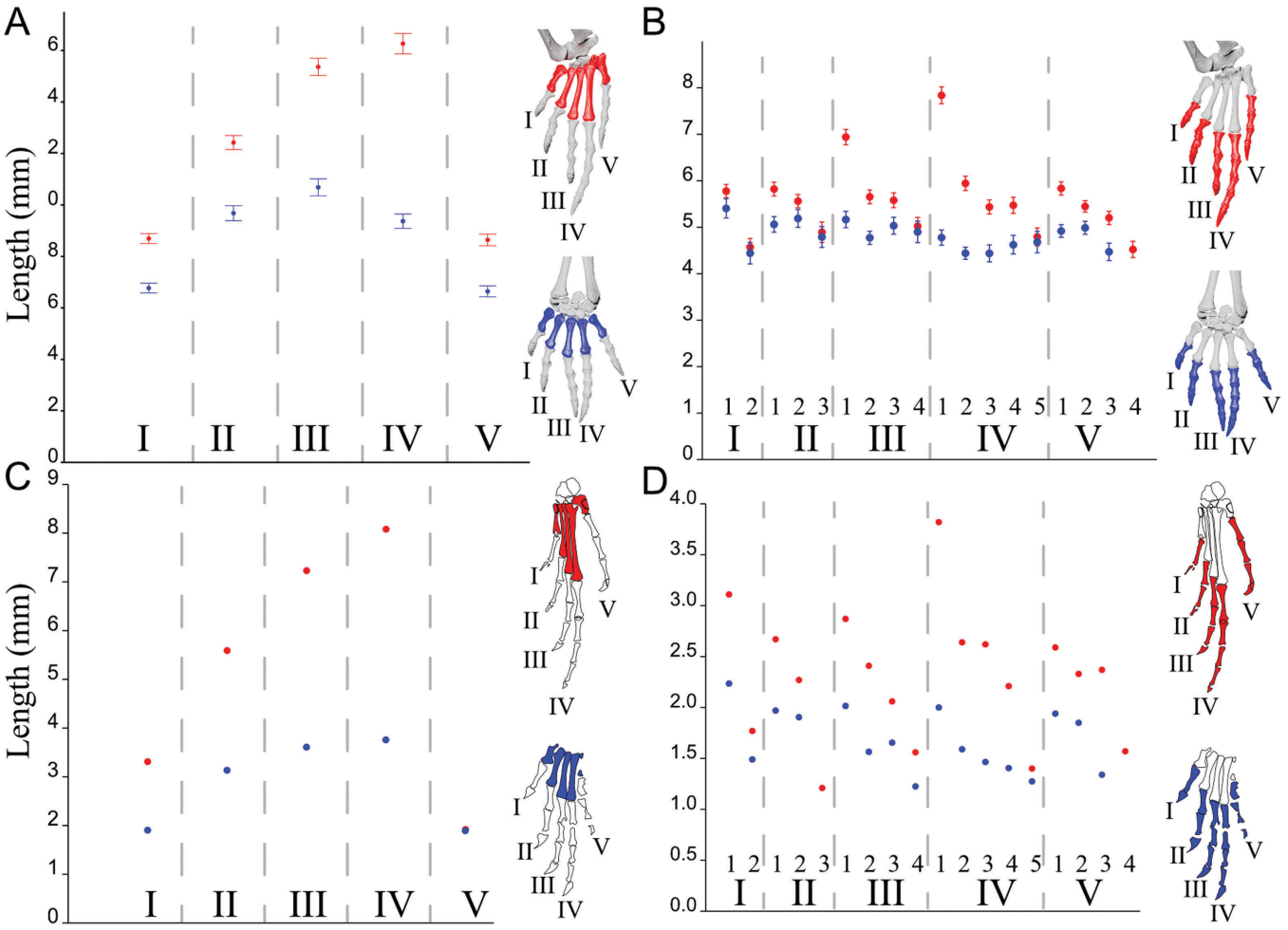


**Figure 9.** Graph with the measurements of the manus and pes of *Sphenodon punctatus* and ***Sphenodraco scandentis***. A, mean plot with error bar of the metacarpals (blue) and metatarsals (red) of 21 *Sphenodon punctatus* specimens in this study, with visual representation of the three-dimensional model of the adult *Sphenodon punctatus* specimen ZMB 13837. B, plot of the mean with error bars of the manual phalanges (blue) and pedal phalanges (red) of 21 *Sphenodon punctatus* specimens in this study, with visual representation of the three-dimensional model of the adult *Sphenodon punctatus* specimen ZMB 13837. C, mean values of the metacarpals (blue) and metatarsals (red) of ***Sphenodraco scandentis***, with schematic illustration of the pes and manus of *NHMUK PV R 2741*. D, mean values of the manual phalanges (blue) and pedal phalanges (red) of ***Sphenodraco scandentis***, with schematic illustration of the pes and manus of *NHMUK PV R 2741*.

ovoid obturator foramen is present close to the articular surface to the ischium. This foramen is also ovoid in *Kallimodon*, *Pleurosaurus*, and *Sphenofontis* (Cocude-Michel 1963, Villa *et al.* 2021). It is circular in *H. maximiliani*, *H. parvipes*, *Oenosaurus* aff. *muehlheimensis*, *Sapheosaurus*, and *Sphenodon* (Cocude-Michel 1963, Russell and Bauer 2008; V.B., personal observations). In some *Kallimodon* specimens (e.g. *SNSB-BSPG 1887 VI 1*, MB.R.1008.1, and MB.R.1012), the obturator foramen seems to be open only ventrally, differing from the fully opened obturator foramen of *NHMUK PV R 2741*.

The right ischium is the only complete pelvic bone, although its symphysial end is poorly preserved (Fig. 8C, D). The articular facet for the pubis lies at the anterolateral corner of the proximal end, followed posterodorsally by the articular facet for the ilium. Both facets are straight. The ischium is then constricted into a neck posteromedioventrally to the articular facets. The anterior margin of this neck is concave and delimits the posterolateral border of the thyroid fenestra. Posterior to the constricted neck lies a deep lateral fossa. This fossa is not observed in *Sphenodon*, but it is present in *Kallimodon pulchellus* (specimens *SNSB-BSPG 1887 VI 1*, SNSB-BSPG 1922 I 15, and MB.R.1012). The ischiadic tuberosity is better observed in *SMF R414*. The tuberosity is well developed, slender, and posteriorly expanded into a distinct posterior process (*sensu* Fraser 1988). It is significantly shorter than the ischiadic plate. In *Kallimodon* and *Pleurosaurus*, the ischiadic tuberosity is very strongly developed and almost as long as the ischiadic plate. The ischiadic plate in *NHMUK PV R 2741* expands anteroposteriorly at its distal end, having a straight symphysial margin and convex anterior and posterior margins.

### *Femur*

Both femora are preserved in anterior view in *NHMUK PV R 2741* (Fig. 8), and the proximal half of the right femur is preserved in posterior view in *SMF R414*. The femur is only slightly longer than the humerus, similar to *H. maximiliani*, *Oenosaurus* aff. *muehlheimensis*, and *Sphenodon* (Cocude-Michel 1963; V.B., personal observations) and different from the substantially longer femur in relationship to humerus in *Kallimodon*,

*Leptosaurus*, and *Pleurosaurus*, especially *Pleurosaurus ginsburgi* (Cocude-Michel 1963, Fabre 1974, 1981, Dupret 2004).

The femur is very slender and slightly sigmoidal in anterior view. Both femoral ends are expanded in comparison to the shaft. The proximal epiphysis of the femur is well ossified, but not fused to the diaphysis. The internal trochanter is well developed and marked as an anteriorly expanded shelf. The femoral shaft is bowed and slightly sigmoidal, with the dorsal surface concave proximally and convex distally. The anterior condyle of the femur is rounded and bulges ventrally. It is well ossified and fused to the diaphysis.

### *Tibia and fibula*

Both the tibia and the fibula are extremely elongated (Fig. 8). The tibia is longer than the humerus (HML/TML = 0.85), as in *Homoeosaurus*, *Kallimodon*, and some *Pleurosaurus* specimens (e.g. MB.R.1949, *MNHN CNJ 67*, and SNSB-BSPG 1978 I 7), but different from *Oenosaurus* aff. *muehlheimensis*, *Palaeopleurosaurus*, some *Pleurosaurus* specimens (e.g. NHMUK PV R 37008 and SNSB-BSPG 1926 I 18), *Sphenodon*, and *Sphenofontis* (Cocude-Michel 1963, Fabre 1974, Carroll 1985, Villa *et al.* 2021; Supporting Information, Supplementary Data 1), and almost as long as the femur (FML/TML = 1.06), which is similar only to the juvenile Brunn specimen (SNSB-BSPG 1993 XVIII P12; FML/TML = 1.05) and some specimens of *H. maximiliani* (MB.R.893 and TM F03955; FML/TML = 1.07 and 1.03, respectively). In all other observed rhynchocephalians, the femur is substantially longer than the tibia (FML/TML > 1.15). The proximal end of the tibia is wide in comparison to the shaft and the distal end, with the strongest constriction of the shaft being found about one-sixth of the length of the bone distal to the proximal end. This constriction is much lower (about one-quarter of the tibial length) and happens gradually in most other Solnhofen rhynchocephalians, except for *Homoeosaurus*, which shows a similar condition to *NHMUK PV R 2741* (Cocude-Michel 1963, Fabre 1981, Villa *et al.* 2021). The tibia is nearly straight throughout its length, whereas the fibula is slightly bowed. Both bones expand gradually anteroposteriorly towards the distal end, the tibia more so than the fibula. The tibia and the fibula are separated from each other at the distal end.

### *Tarsus*

The tarsus is well preserved in *NHMUK PV R 2741*, with the astragalus, calcaneum, and distal tarsals 3 and 4 preserved in plantar view (Fig. 8). The astragalus and calcaneum are unfused. Together, the astragalocalcaneum is trapezoidal in ventral (= plantar) view. The calcaneum is subcircular, with a convex lateral margin and a straight medial margin, where it contacts the astragalus. The astragalus is lateromedially wide, and both lateral and medial margins are straight and perpendicular. The lateral margin of the astragalus is proximodistally longer than the medial one. The articular facet to the tibia is set in a proximolateral to mesiodistal slope. This articular facet is straight, whereas the distal margin that articulates with the distal tarsals is slightly concave mediolaterally in ventral view. The suture between the astragalus and calcaneum is straight and divides the fibular articular facet. The calcaneum participates almost twice as much as the astragalus in the fibular articular facet. A deep concavity separates the tibial and fibular articular facets, similar to that observed in *Kallimodon*, *Leptosaurus*, and *Sphenodon* (Cocude-Michel 1963, Fabre 1981; V.B., personal observations), but different from the shallow concavity of *Oenosaurus* aff. *muehlheimensis* SNSB-BSPG 2009 I 69 and *Sphenofontis* (Villa *et al.* 2021). *Homoeosaurus* and *Pleurosaurus* lack this concavity between the tibial and fibular facets (Cocude-Michel 1963). Only two distal tarsals are present in *NHMUK PV R 2741*, representing the distal tarsals 3 and 4. These tarsals are well ossified. The distal tarsal 4 is lateromedially elongated and twice the size of the distal tarsal 3, which is circular.

### *Metatarsus*

All metatarsal bones are preserved in ventrolateral view, except for the right metatarsal I, which rotated slightly inwards and is exposed in medial view (Fig. 8). Except for metatarsal V, all metatarsals are slender and long, with metatarsal IV being the longest, followed by III, II, I, and V. As for the metacarpals, this is the same pattern as seen in *H. maximiliani*, *H. solnhofensis*, *Kallimodon*, and *Leptosaurus* (Cocude-Michel 1963, Fabre 1981). In *Sphenodon*, the metatarsals I and V are subequal in length, whereas in *NHMUK PV R 2741* the fifth metatarsal is substantially shorter than the first (Fig. 9). The elongate metatarsal IV (MTIV) is ~2.5 times the length of metatarsal I (MTI). This proportion is higher than in other rhynchocephalians, e.g. *Kallimodon*, *Leptosaurus*, *Sphenofontis*, and *Sphenodon* (MTIV/MTI ranging from 1.7 to 2.1), and much higher than *Pleurosaurus* (MTIV/MTI ≈ 1.4), but similar to that of *H. maximiliani* (MTIV/MTI ≈ 2.6) and a single specimen of *Kallimodon pulchellus* (identification according to Cocude-Michel 1963), MB.R.1009.1-2 (MTIV/MTI = 2.7; Supporting Information, Supplementary Data 1).

Metatarsals I and V are asymmetrical, whereas metatarsals II–IV are symmetrical. Metatarsal I shows a prominent ovoid ventral tubercle at the medial margin of the proximal end. This tubercle has a flat ventral surface and is slightly expanded laterally at its ventral end. This tubercle is similar to that of *Kallimodon pulchellus* but is less developed in *NHMUK PV R 2741* (V.B., personal obserations). *Homoeosaurus maximiliani*, *Oenosaurus* aff. *muehlheimensis* SNSB-BSPG 2009 I 69, and *Sphenofontis* show a ventral tubercle in metatarsal I, but to a much lesser degree than in *NHMUK PV R 2741* and *Kallimodon pulchellus*. In *Sphenodon*, this tubercle is absent. The shaft of metatarsal I is straight at the medial margin and concave at the lateral one in *NHMUK PV R 2741*. The distal end of metatarsal I is expanded laterally and medially, with the lateral expansion advancing further distally than the medial one.

Metatarsals II–IV share similar morphologies. The proximal end of these metatarsals is dorsoventrally expanded and mediolaterally flattened. In metatarsals II and III, this proximal expansion decreases gradually into the shaft, whereas in metatarsal IV this expansion is more abrupt and occurs closer to the metatarsal proximal end. The shaft of metatarsals II–IV is straight throughout its length. The distal end of these bones is mediolaterally expanded and symmetrical. They are similar in morphology to the distal ends of metacarpals II–IV, but with a less prominent ventral groove for the articulation with the first pedal phalanx.

Metatarsal V is curved proximomedially and articulates with the tarsals more proximally than the other metatarsals, forming the typical lepidosaurian hook. This hook is less than two-thirds the length of metatarsal V and offsets from the main shaft at an obtuse angle, forming a rounded concavity distally. This is similar to the condition in *H. maximiliani*, but different from the perpendicular hook of *Kallimodon*, *Leptosaurus*, and *Oenosaurus* aff. *muehlheimensis*. In *Kallimodon* and *Leptosaurus*, the hook is prominent and almost the same length as the metatarsal V main shaft. In pleurosaurids, especially *Pleurosaurus*, the metatarsal V hook appears greatly reduced. Metatarsal V shows a prominent lateral tubercle, which is positioned at the level of the hook. In *Sphenodon*, it is located slightly distally. The distal end of metatarsal V is rounded, and it does not expand laterally, only medially.

### *Pedal digits*

Most pedal phalanges are preserved in *NHMUK PV R 2741*, with some phalanges of the right digits III and IV preserved in the counter slab, *SMF R414* (Figs 3–8). The phalangeal formula is 2-3-4-5-4, as is typical for rhynchocephalians (Cocude-Michel 1963, Russell and Bauer 2008). All digits are extremely long, especially the fourth one. As for the manus, the proximal phalanges are the longest of each digit, especially in digit IV, where this phalanx is at least one-third longer than any other in the pes.

The general morphology of the pedal phalanges is similar to that of the manus, with the main difference being the overall length. The proximal pedal phalanges show the proximoventral expanded condyle, and differently from the manus, the second phalanges of digits II–IV also show this proximoventral condyle. The distal articulation of the pedal phalanges shows two symmetrical condyles.

The pedal unguals are slightly longer than the manual unguals, different from the subequal unguals of *Sphenodon* (Fig. 9). These unguals are much shorter than their preceding phalanges; they are tall at the base and strongly downturned. The ungual articulation is ginglymoid, as in the manus.

### *Soft tissue remains*

From caudal vertebra 4 to 8, a small patch of soft tissue impression is preserved in *NHMUK PV R 2741*. This can be observed only under UV light (Figs 3, 6B, C, 10). Most of this patch is poorly defined but probably represents roughly the outline of the tail of the animal when alive. At least three rows of scales are visible on both sides, and these show that the scales are approximately homogeneous in size and have a hexagonal arrangement, such that each scale is bounded by six others. This scale arrangement is similar to that observed in *Sphenodon* (Ali 1941), *Pamizinsaurus tlayuaensis* Reynoso, 1997, and *Pleurosaurus* (Cocude-Michel 1963, Reynoso 1997), but differs from the squared scales of *Kallimodon pulchellus SNSB-BSPG 1887 VI 1* (Fig. 10C), and *Piocormus* TM F 03954 (Fig. 10D).

## Phylogenetic analysis

The results of the New Technology Search analysis with implied weighting ($k = 8$; Fig. 11A) recovered 25 trees, with the best score of 17.76308, retention index (RI) of 0.691, and consistency index (CI) of 0.459. The reduced consensus found four rogue OTUs, *Cynosphenodon huizachalensis* Reynoso, 1996, *Eilenodon robustus* Rasmussen and Callison, 1981, *Kawasphenodon* Apesteguía *et al.*, 2014, and *Toxolophosaurus cloudi* Olson, 1960 (Supporting Information, Supplementary Data 2). Removal of these OTUs from the analysis results in a single most parsimonious tree, with the best score of 17.54086, RI = 0.692, and CI = 0.496 (Fig. 11A). The non-clock analysis resulted in a similar topology to that of the most parsimonious tree, but with less support for some clades. The majority rule consensus tree from the non-clock Bayesian inference is poorly resolved (Fig. 11B).

Both analyses recovered a monophyletic Rhynchocephalia *sensu* DeMar *et al.* (2022). This is congruent with some recent phylogenetic studies (i.e. Herrera-Flores *et al.* 2017, Chambi-Trowell *et al.* 2021, DeMar *et al.* 2022, Sues and Schoch 2023). The position of *Gephyrosaurus* has been unstable in some analyses (i.e. Simões *et al.* 2020, 2022, Martínez *et al.* 2021), with the clade Sphenodontia Williston, 1925 (*sensu* Simões *et al.* 2020) being preferred instead of Rhynchocephalia in some studies. However, here we recovered a stable Rhynchocephalia, with *Gephyrosaurus* at the base as a non-sphenodontian rhynchocephalian. This placement is supported by five unambiguous synapomorphies: (i) the presence of a laterally oriented posteroventral process of the jugal (character 12, state 1); (ii) contact between the ascending process of the jugal and the squamosal (new character 13, state 1); (iii) presence of a dorsally expanding coronoid process in the dentary (character 59, state 1); (iv) presence of a posteroventral process of the dentary (character 60, state 1); and (v) amphicoelous presacral centra (character 98, state 0).

Both analyses recovered a monophyletic Neosphenodontia Herrera-Flores *et al.*, 2018, which includes all the Solnhofen Archipelago OTUs, *Sphenodon*, and closely related taxa. The clades Pleurosauridae, Sapheosauridae, and Sphenodontidae (all *sensu* Simões *et al.* 2020), were recovered in both analyses.

In both our analyses, the Pleurosauridae contain *Acrosaurus*, *Ankylosphenodon* Reynoso, 2000, *Derasmosaurus*, *Palaeopleurosaurus*, *Pleurosaurus ginsburgi*, and *Pleurosaurus goldfussi*. This clade is supported by two unambiguous synapomorphies: (i) lack of an autotomic septum in the caudal vertebrae (character 103, state 0); and (ii) absence of an anterior emargination in the scapula (character 114, state 0).

The clade Sapheosauridae was recovered in both analyses and includes *Oenosaurus muehlheimensis*, *Oenosaurus* aff. *muehlheimensis* SNSB-BSPG 2009 I 69, *Piocormus*, and *Sapheosaurus*. This clade is supported by four unambiguous synapomorphies: (i) palatines contacting at midline (character 43, state 1, not scored in *Piocormus*); (ii) marginal dentition fused into a single element (character 80, state 1); (iii) posterior process of the second sacral rib terminating distally at the same level as the anterior process (new character 145, state 0, not scored in *Oenosaurus muehlheimensis*); and (iv) posteriorly oriented pleurapophyses of caudal vertebra 4 (new character 148, state 2, not scored in *Oenosaurus muehlheimensis*). In the maximum parsimony analysis, sapheosaurids are recovered in a clade with *Vadasaurus* and *Leptosaurus* MNHN CNJ 72 at its base, sister to pleurosaurids. In the non-clock Bayesian inference, MNHN

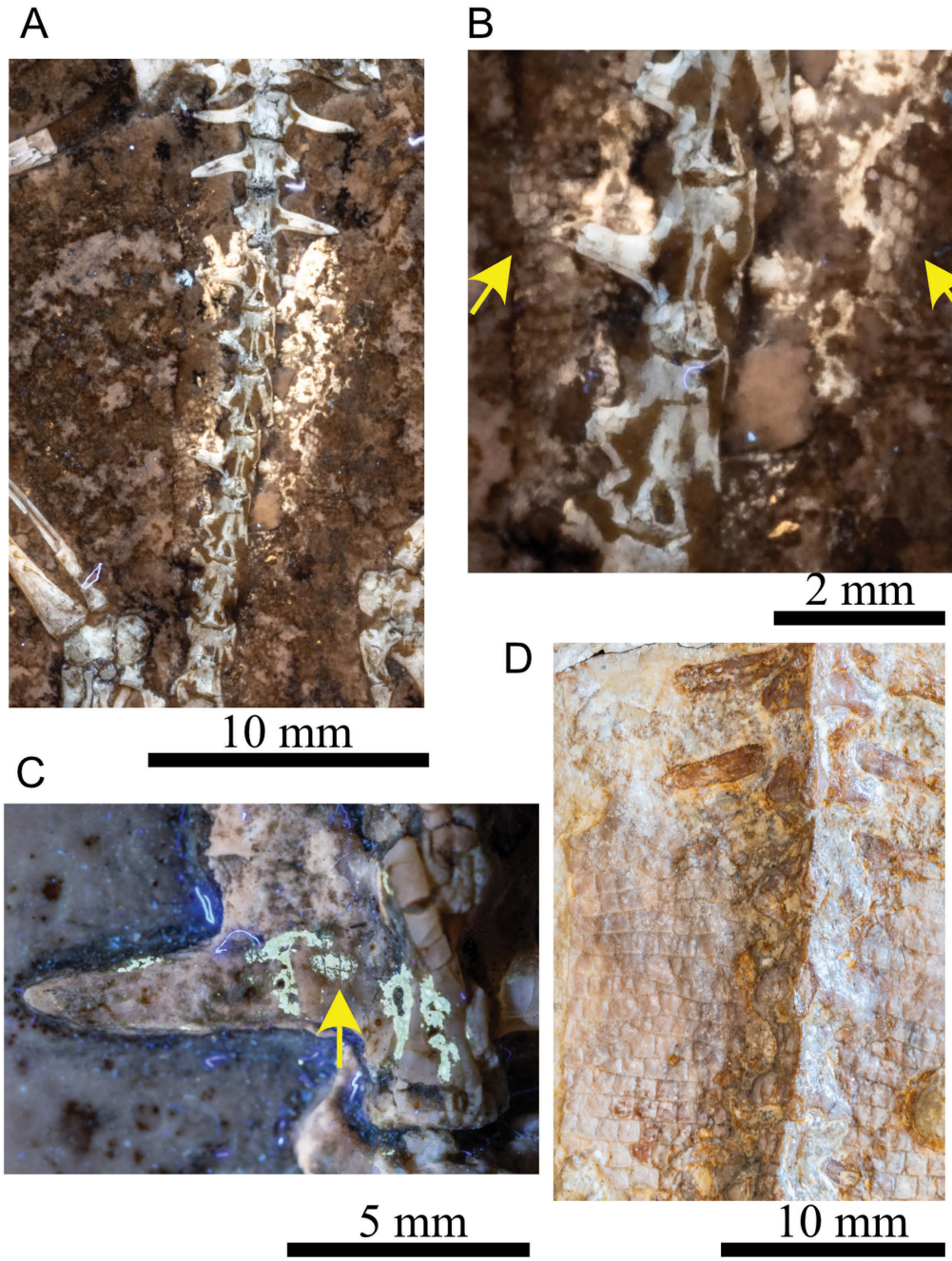


**Figure 10.** Soft tissue imprint of ***Sphenodraco scandentis*** *NHMUK PV R 2741* (A, B), with comparison to *Kallimodon pulchellus SNSB-BSPG 1887 VI 1* (C) and *Piocormus laticeps* TM F 03954 (D). A, B, tail region of ***Sphenodraco scandentis*** under ultraviolet light. C, tail region of *Kallimodon* under ultraviolet light. D, tail region of *Piocormus*. The yellow arrows point to the preserved scales.

CNJ 72 is recovered at the base of Pleurosauridae instead, with *Vadasaurus* in an unresolved position within Neosphenodontia.

The clade Sphenodontinae (*sensu* Simões *et al.* 2020) includes *Navajosphenodon*, *Opisthiamimus*, *Sphenodon*, and *Sphenofontis* in both analyses. The placement of *Opisthiamimus* in our analyses differs from the one found by DeMar *et al.* (2022), where this taxon was recovered at the base of Eusphenodontia Herrera-Flores *et al.*, 2018. This taxon is recovered at the base of Sphenodontinae, followed by *Navajosphenodon*, then *Sphenodon* + *Sphenofontis* in the most parsimonious tree, and an unresolved clade of *Navajosphenodon* + *Sphenodon* + *Sphenofontis* in the Bayesian inference. These relationships among sphenodontines are congruent with the analyses of Simões *et al.* (2022: fig. 8 therein). In our analysis, the Sphenodontinae are supported by two unambiguous synapomorphies: (i) presence of a dentary caniniform (character 87, state 1); and (ii) presence of the radial condyle in the humerus (character 123, state 0). Additionally, two ambiguous synapomorphies are present: (i) absence of lateral flanges in the palatine dentition (character 74, state 0); and (ii) presence of posteromedial flanges in the posterior maxillary teeth (character 85, state 1, reversed to state 0, flanges absent, in *Sphenofontis*).

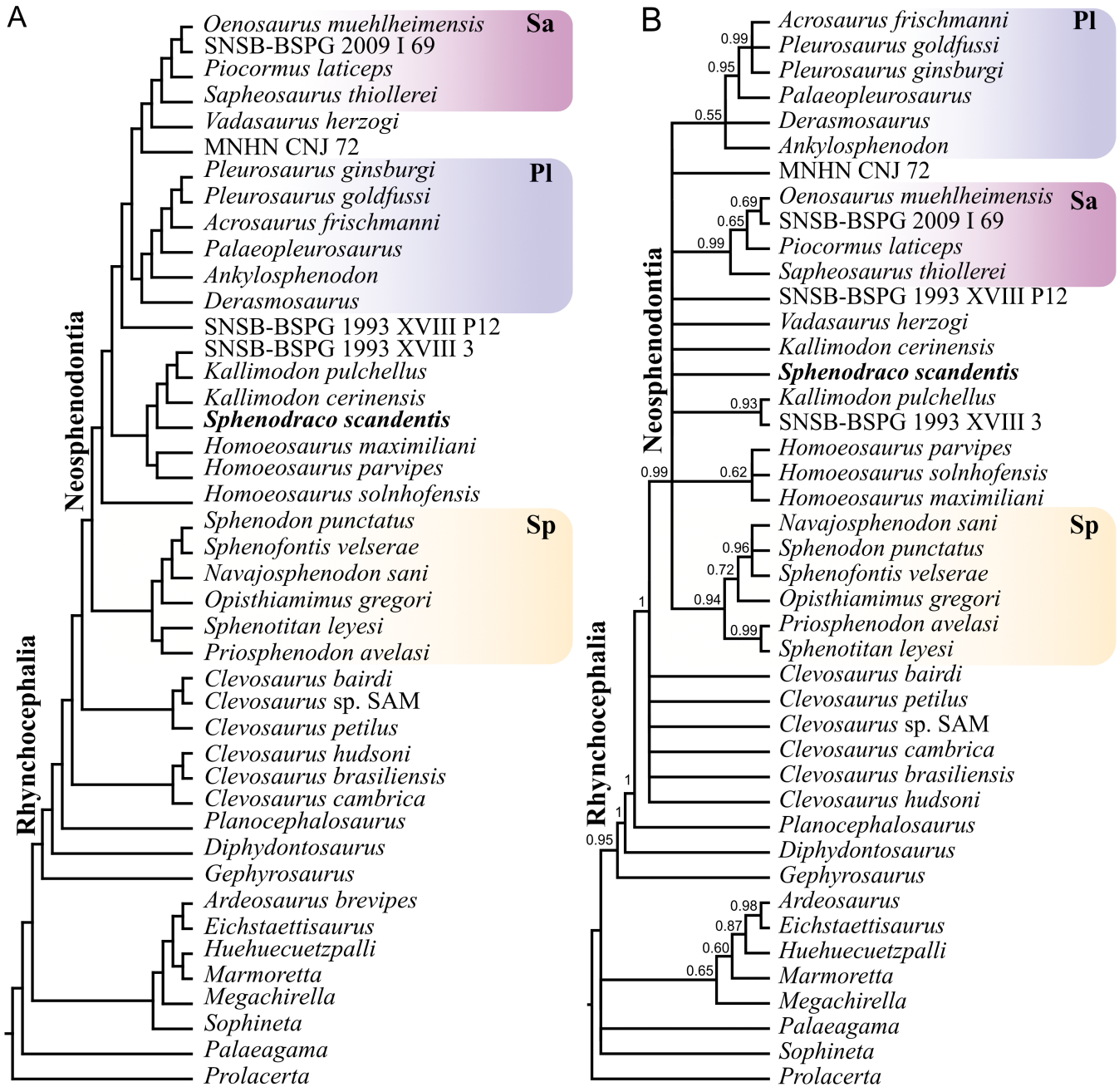


**Figure 11.** Phylogenetic analysis of fossil rhynchocephalians. A, most parsimonious tree with implied weightings ($k = 8$). B, majority rule consensus tree from the non-clock Bayesian inference analysis, with clade posterior probabilities (values under the branches). Abbreviations: Pl, Pleurosauridae; Sa, Sapheosauridae; Sp, Sphenodontinae.

A clade containing *H. maximiliani*, *H. parvipes*, *Kallimodon cerinensis*, *Kallimodon pulchellus*, SNSB-BSPG 1993 XVIII 3, and *Sphenodraco* was recovered in the maximum parsimony analysis, but not in the Bayesian inference. This clade is supported by two unambiguous synapomorphies: (i) lack of contact between prefrontal and jugal (character 14, state 0, not scored in SNSB-BSPG 1993 XVIII 3 and *Sphenodraco*); and (ii) post-axial presacral intercentra restricted to the anterior (cervical) presacral vertebrae (new character 142, state 1, not scored in *H. parvipes* and *Kallimodon cerinensis*). In the most parsimonious tree, *H. maximiliani* and *H. parvipes* cluster together in a clade that is sister to *Sphenodraco* + (*Kallimodon cerinensis* + (*Kallimodon pulchellus* + SNSB-BSPG 1993 XVIII 3)). In this analysis, *Homoeosaurus* is paraphyletic, with *H. solnhofensis* recovered outside this clade. In the non-clock analysis, *Homoeosaurus* is monophyletic, but the relationships of *Sphenodraco*, *Kallimodon cerinensis*, and *Kallimodon pulchellus* + SNSB-BSPG 1993 XVIII 3 are unresolved. *Sphenodraco* shares exclusively with the *Kallimodon* species three characters: (i) lack of ventral concavity in the parabasisphenoid (character 50, state 2, not scored in *H. parvipes*); (ii) presence of the symphyseal spur (character 53, state 1, not scored in *H. parvipes*); and (iii) posterolaterally oriented synapophyseal articulation in the presacral vertebrae

(new character 137, state 1). *Sphenodraco* does not share any characters exclusively with *Homoeosaurus*.

## Ecomorphological analysis

In this section, results of the ecomorphological analysis are reported for squamates and rhynchocephalians. Figure 12 presents the general morphology of selected rhynchocephalians from the Solnhofen Archipelago, exemplifying different ecomorphological groups, and how they compare to *Sphenodraco*. To illustrate this, the following five fossil specimens are used: (i) *NHMUK PV R 2741*, the holotype of *Sphenodraco scandentis* (Fig. 12A); (ii) SNSB-BSPG 1887 VI 502, the neotype of *Homoeosaurus maximiliani* (Fig. 12B); (iii) SNSB-BSPG 2009 I 69, an *Oenosaurus* aff. *muehlheimensis* sapheosaurid specimen (Fig. 12C); (iv) *SNSB-BSPG 1887 VI 1*, the holotype of *Kallimodon pulchellus* (Fig. 12D); and (v) SNSB-BSPG 1977 X 40, a specimen referred to the pleurosaurid *Pleurosaurus ginsburgi* (Fig. 12E). In the subsequent figures, these specimens and the groups they represent will be coloured consistently, following the respective outlines in Figure 12.

### *General trends in squamates*

To test whether the inclusion of rhynchocephalians modifies the results of squamate ecomorphospaces in the PCA, the same analysis was done twice, first using only squamates (PCA1; Fig. 13), and second including rhynchocephalians (PCA2; Fig. 14). Both analyses show congruent results, and only small changes are seen in the graphs (Figs 13A, 14A). In both analyses, the first five PCs of the PCA account for 95% of the total variation in body shape, with 85.5% and 82.8% of the variation explained by the first three PCs in PCA1 and PCA2, respectively (see Supporting Information, Supplementary Data 1). Given that no significant differences were found between both analyses, the results below describe PCA2, which includes the target taxa (i.e. fossil rhynchocephalians).

There is considerable overlap between extant limbed lizard ecologies, being the most pronounced according to PC2–PC3 axes, suggesting that this combination of axes does not signal substrate preferences. Nevertheless, climbing taxa (arboreal, saxicolous, and semi-arboreal) tend to be grouped together towards positive values of PC1, with arboreal taxa more spread into positive values of PC2 and PC3, semi-arboreal taxa widespread across positive and negative values of PC2 and PC3, and saxicolous taxa spread more into negative values of PC2 but positive values of PC3. On the contrary, terrestrial and semi-aquatic taxa are mostly grouped into negative values of PC1. Terrestrial taxa seem to be spread evenly across negative and positive values of PC2 but spread more in negative values of PC3, whereas semi-aquatic taxa are more spread into positive values of PC2 and negative values of PC3.

PC1 (50.1% of variance explained) represented variation in limb length and body size, with elongated limbs and short body sizes (presacral vertebral length) at positive values of PC1 and with robust limbs (wide mid-shaft diameter) and elongated body size at negative values of PC1. In terms of habitat/substrate use, climbing (i.e. arboreal, saxicolous, and semi-arboreal) squamates fall into positive values of PC1 and terrestrial species into negative values of PC1, with large overlap of categories around the centre. PC2 (20.2% of variance explained) is related to forelimb and hindlimb size, with positive values of PC2 representing relatively longer forelimbs in relationship to hindlimbs and body size, and the opposite, i.e. relatively longer hindlimbs and longer body size, for negative values of PC2. PC3 (12.5% of variance explained) represents differences in body size; specimens with relatively shorter body size have positive values of PC3, whereas specimens with longer body size have negative values.

Owing to the overlap across substrate use categories (especially semi-aquatic and semi-arboreal lizards), the LDA shows only an average confusion matrix, 49.57% when using semi-aquatic (SA) as the substrate use , and 57.26% when assigning the secondary substrate (SS) use to semi-aquatic lizards. Arboreal, marine, and terrestrial taxa were more often classified accurately in both analyses, with 52% of arboreal lizards being classified correctly in both respective analyses, and 62% and 74% of terrestrial animals (*Sphenodon* included in this category) in the respective analyses. Semi-aquatic lizards were the least accurately classified lizards to their assigned substrate use in the first analysis (11%). Saxicolous and semi-arboreal lizards also show low accuracy of classification in both analyses (31% and 33% in the first analysis, and 35% and 33% in the second, respectively).

### *General trends in morphospace position for rhynchocephalians*

Most fossil rhynchocephalian specimens (e.g. the Brunn juvenile, *H. parvipes*, all *Kallimodon–Leptosaurus* complex specimens, *Oenosaurus* aff. *muehlheimensis*, *Piocormus*, and *Sapheosaurus*) are recovered in the centre of PC1, PC2, and PC3 (Fig. 14A), where the overlap between habitat preferences of squamates is predominant. However, there are notable exceptions. The fully marine taxa (i.e. *Acrosaurus* and *Pleurosaurus*: Carroll and Wild 1994, Gutarra *et al.* 2023, Beccari *et al.* 2025) occupy mainly the negative values of PC1, PC2, and PC3; morphospaces characterized by elongated bodies, long and gracile hindlimb bones, and short and robust forelimb bones. It is worth noting that both specimens of *Acrosaurus* and specimens of *Pleurosaurus* displays a larger range of variability than that observed in *Sphenodon* (Fig. 14A). *Homoeosaurus maximiliani*, *H. solnhofensis*, *Navajosphenodon*, and *Sphenodraco* occupy positive values in PC1. These taxa have slender limb bones and proportionally shorter bodies in comparison to other rhynchocephalians and occupy the same ecomorphospace as climbing lizards. In particular, *Sphenodraco* shows the highest values in PC1 among rhynchocephalians (Fig. 14A) and is positioned close to the strictly arboreal lizards *Bronchocela cristatella* (Kuhl, 1820) and members of the genus *Draco* Linnaeus, 1758.

To test for possible ontogenetic changes in the limb and body size proportions in *Sphenodon*, a separate PCA was done using only this taxon (Fig. 15). The three first axes of the PCA account for 77% of the total variation, with the first six axes accounting for 96%. PC1 (45.5% of variance explained) is positively correlated with elongated and gracile limbs and long body sizes. PC2 (17.1% of variance explained) is positively correlated with elongated stylopodia (humerus/femur) and short zeugopodia (radius/tibia), but also correlated with rather robust forelimbs and gracile hindlimbs, and slightly correlated with short body sizes. PC3 (14.4% of variance explained) is also positively correlated with short body sizes, in addition to elongated hindlimbs,

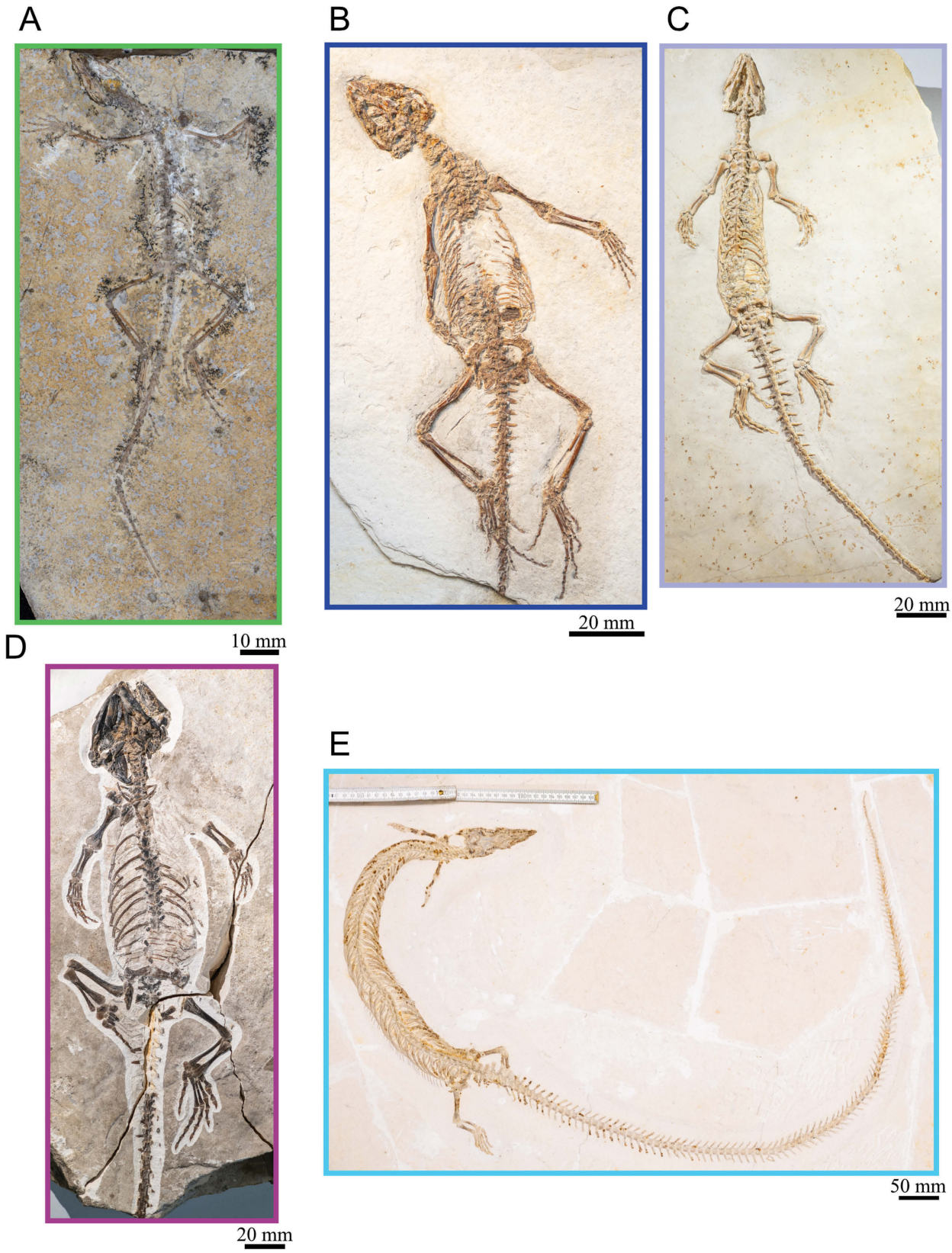


**Figure 12.** Rhynchocephalian specimens used for comparison. A, ***Sphenodraco scandentis*** *NHMUK PV R 2741*. B, *Homoeosaurus maximiliani* SNSB-BSPG 1887 VI 502. C, *Kallimodon pulchellus SNSBBSPG 1887 VI 1*. D, *Oenosaurus* aff. *muehlheimensis* SNSB-BSPG 2009 I 69. E, *Pleurosaurus ginsburgi* SNSB-BSPG 1977 X 40.

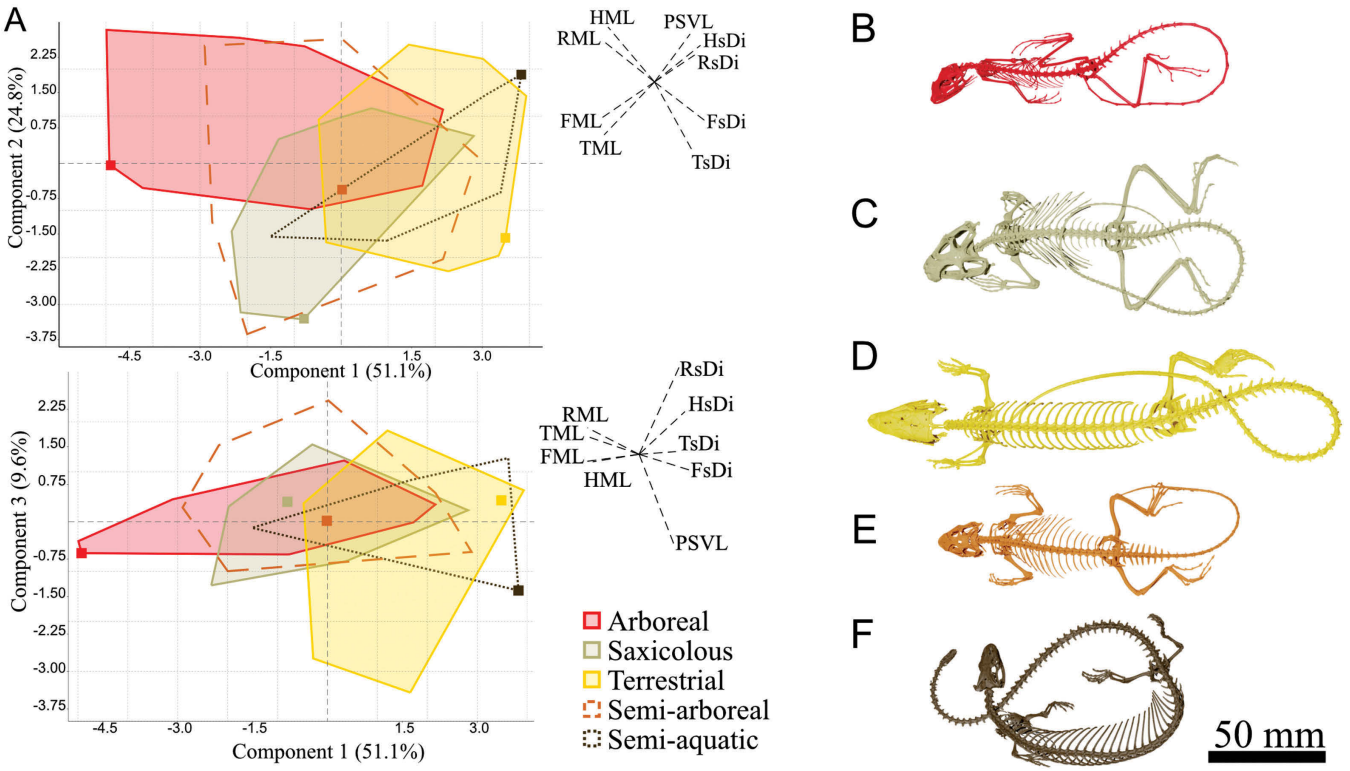


**Figure 13.** Principal component analysis (PCA) of extant limbed squamates, and comparative limb proportions. A, PCA graphs (scaling 1) of combinations PC1 × PC2 and PC1 × PC3, with biplots (scaling 2). B, *Bronchocela cristatella* UF.Herp 112989 (arboreal). C, *Crotaphytus collaris* YPM HERR 7496 (saxicolous). D, *Gerrhosaurus flavigularis* UF.Herp 90238 (terrestrial). E, *Tropidurus torquatus* UF.Herp 60944 (semi-arboreal). F, *Lanthanotus borneensis* UF.Herp 16268 (semi-aquatic). Abbreviations: FML, femur length between metaphyses; FsDi, femur mid-shaft diameter; HML, humerus length between metaphyses; HsDi, humerus mid-shaft diameter; PSVL, presacral vertebrae total length; RML, radius length between metaphyses; RsDi, radius mid-shaft diameter; TML, tibia length between metaphyses; TsDi, and tibia mid-shaft diameter.

robust femora, and gracile radia. Hatchlings tend to have negative values of PC1 and positive values of PC2 and PC3. There is a considerable overlap between other ontogenetic stages, with all of them spreading to similar extents across negative and positive values of PC1, suggesting that this axis is not related to any ontogenetic signal. Nevertheless, adult morphospace tends to be recovered more into negative values of PC2 and PC3, and juveniles are clearly grouped in positive values of PC2. More importantly, there seems not to be a continuous range of morphospaces through which an individual would develop during growth: juvenile, subadult, and adult individuals largely overlap with each other.

The LDA classified fossil rhynchocephalians across all available substrate uses (Supporting Information, Supplementary Data 1). Some specimens were assigned the same substrate use irrespective of the analyses (both SA and SS). The terrestrial substrate use was classified in both analyses for *Kallimodon cerinensis*, some *Kallimodon pulchellus* specimens (i.e. the holotype *SNSB-BSPG 1887 VI 1*, MB.R.1008.1, and SNSB-BSPG 1911 I 34), *Leptosaurus neptunius* and *Leptosaurus*-like specimens (except for JME Scha-100), *Oenosaurus* aff. *muehlheimensis* SNSB-BSPG 2009 I 69, *Palaeopleurosaurus*, and *Sapheosaurus* MB.R.1949. Only *Sphenodraco scandentis* was classified as arboreal in both SA and SS. All *H. maximiliani* specimens were classified as semi-arboreal in both analyses, except for the neotype SNSB-BSPG 1887 VI 502, which was classified as arboreal in SS. *Leptosaurus*-like JME-Scha 100 was classified as semi-aquatic in SA and arboreal in SS, and *Oenosaurus* aff. *muehlheimensis* SNSB-BSPG 2020 I 48 was classified as arboreal in SA and saxicolous in SS. *Homoeosaurus solnhofensis*, *Navajosphenodon*, *Sphenofontis*, and *Vadasaurus* were classified as saxicolous in both analyses. In SA, *Homoeosaurus parvipes*, two specimens of *Kallimodon pulchellus* (i.e. SNSB-BSPG 1887 VI 2 and SNSB-BSPG 1922 I 15), the *Kallimodon*-like specimen SNSB-BSPG 1993 XVIII P11, *Piocormus*, and *Sapheosaurus* were classified as semi-aquatic. In both analyses, 91% of marine (pleurosaurids) were correctly classified.

## DISCUSSION

### A new rhynchocephalian species from the Solnhofen Archipelago

The new information extracted from the description of *SMF R414* together with the counterslab of the same individual, *NHMUK PV R 2741*, here reported for the first time, supports the identification of a new rhynchocephalian taxon from the Solnhofen Archipelago: *Sphenodraco scandentis* (Fig. 16). Previously, *SMF R414* was assigned to *H. maximiliani* owing to its elongated limbs (Cocude-Michel 1963, Fabre 1981). However, the individual represented by this slab and its counterslab differs

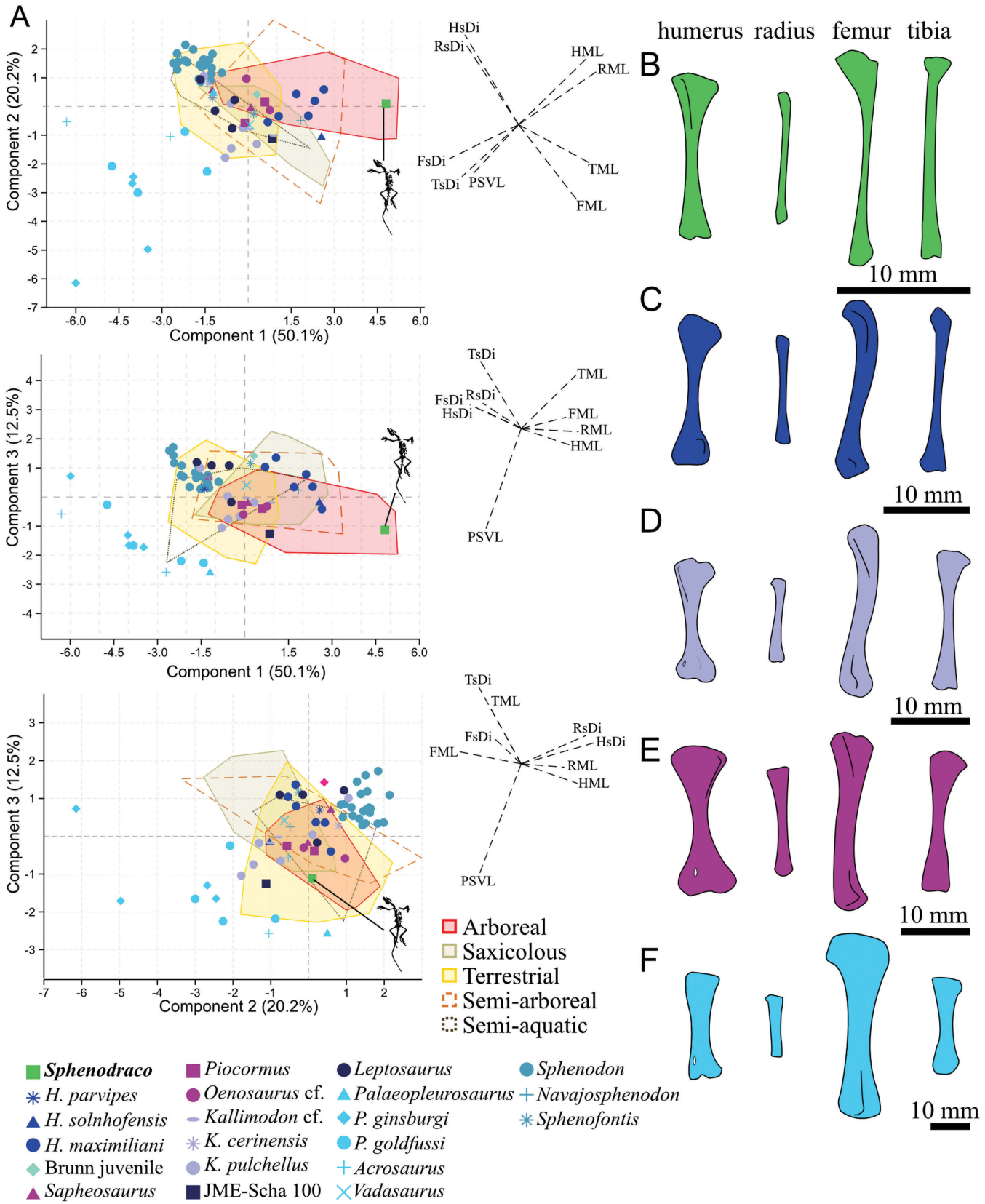


**Figure 14.** Principal component analysis (PCA) of fossil rhynchocephalians, and comparative limb proportions. A, PCA graphs (scaling 1) of combinations PC1 × PC2, PC1 × PC3, and PC2 × PC3, with biplots (scaling 2). B–F, measured limbs of: B, ***Sphenodraco scandentis*** *NHMUK PV R 2741*; C, *Homoeosaurus maximiliani* SNSB-BSPG 1887 VI 502; D, *Kallimodon pulchellus SNSB-BSPG 1887 VI 1*; E, *Oenosaurus* aff. *muehlheimensis* SNSB-BSPG 2009 I 69; and F, *Pleurosaurus ginsburgi* SNSB-BSPG 1977 X 40. Abbreviations: FML, femur length between metaphyses; FsDi, femur mid-shaft diameter; HML, humerus length between metaphyses; HsDi, humerus mid-shaft diameter; PSVL, presacral vertebrae total length; RML, radius length between metaphyses; RsDi, radius mid-shaft diameter; TML, tibia length between metaphyses; TsDi, tibia mid-shaft diameter.

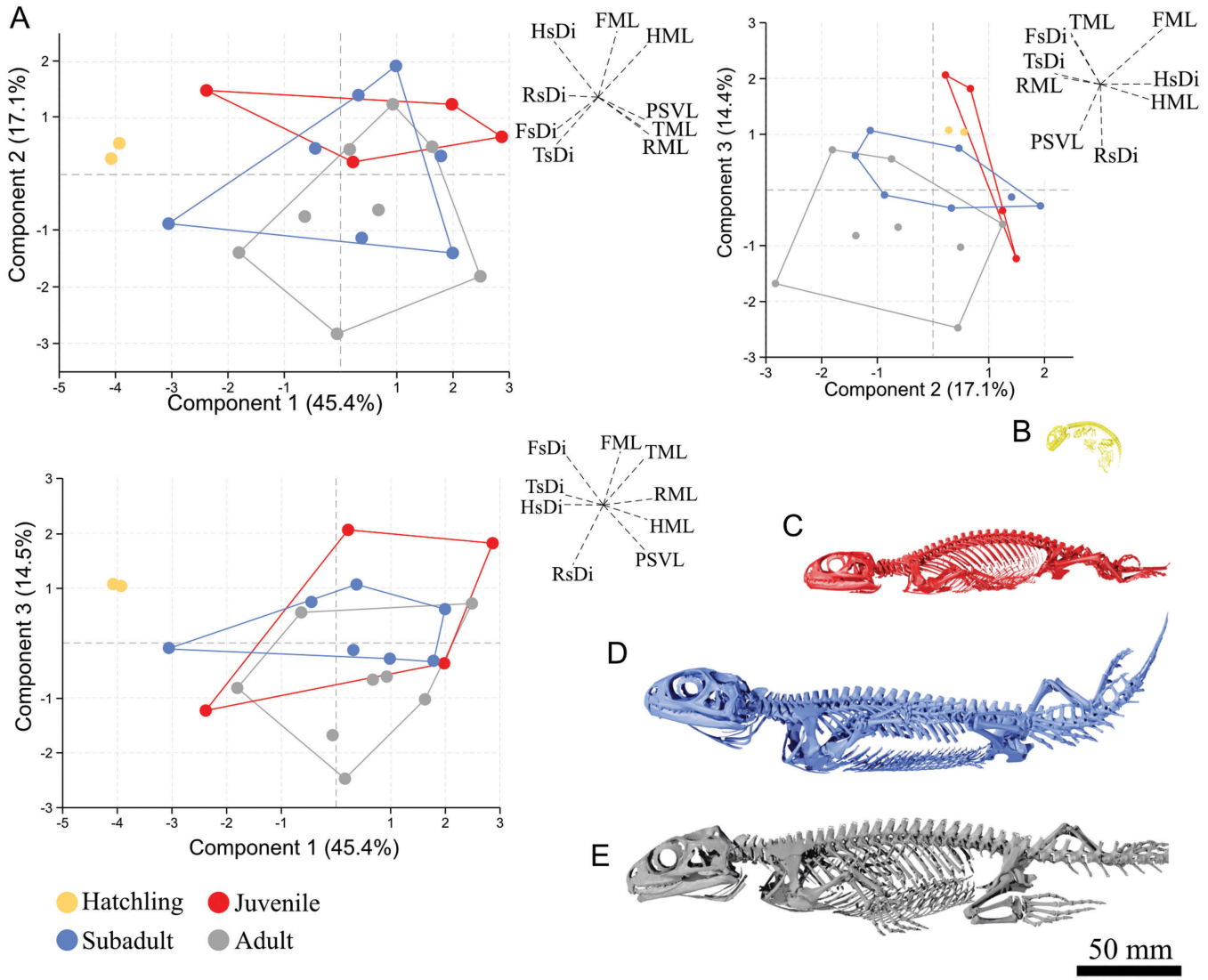


**Figure 15.** Principal component analysis (PCA) of the extant tuatara *Sphenodon punctatus* of different ontogenetic stages using their limb proportions. A, PCA graphs of combinations PC1 × PC2, PC1 × PC3, and PC2 × PC3. B, hatchling SNSB-ZSM 20/1959. C, juvenile LDKCL 11. D, subadult SNSB-ZSM 1318 2006. E, adult IDHRN NH 84.19. Abbreviations: FML, femur length between metaphyses; FsDi, femur midshaft diameter; HML, humerus length between metaphyses; HsDi, humerus mid-shaft diameter; PSVL, presacral vertebrae total length; RML, radius length between metaphyses; RsDi, radius mid-shaft diameter; TML, tibia length between metaphyses; TsDi, tibia mid-shaft diameter.

in many osteological features from the neotype of *H. maximiliani* and from all other rhynchocephalians described so far by two autapomorphic features, i.e. maxillary teeth oriented obliquely at their base, and an ilium with a short pubic process and square acetabulum. *Sphenodraco* shares a mosaic of features with other rhynchocephalians, especially *Homoeosaurus*, *Kallimodon*, and *Leptosaurus*. It shares with *Homoeosaurus*, to which the fossil was previously referred: (i) the lack of the quadratojugal process of the jugal and the open temporal fenestra (also shared by most other Solnhofen rhynchocephalians, except for *Sphenofontis*; see below); (ii) the presence of posterior flanges in the dentition (also shared with *Kallimodon* and *Leptosaurus*); (iii) the direction of the pleurapophyses of the first four caudal vertebrae (different from the condition of *Kallimodon*, *Leptosaurus*, *Oenosaurus*, *Sapheosaurus*, *Sphenodon*, and *Sphenofontis*); (iv) elongated limbs relative to body size; (v) longer metacarpal and metatarsal IV compared with III (also shared with *Kallimodon* and *Leptosaurus*); (vi) strongly curved unguals (different from the flattened unguals of *Kallimodon*, *Leptosaurus*, and *Pleurosaurus*); and (vii) complete obturator foramen in the pubis (different from the dorsally closed foramen observed in at least some *Kallimodon* specimens, e.g. *SNSB-BSPG 1887 VI 1* and MB.R.1012). However, the new taxon differs from *Homoeosaurus* in many aspects, such as: (i) the triangular outline of the skull (similar to *Kallimodon*, *Leptosaurus*, *Pleurosaurus*, and *Vadasaurus*); (ii) the oblique orientation of the maxillary teeth (different also from *Kallimodon* and *Leptosaurus*); (iii) a short posterior process of the transverse process of the second sacral vertebra (different also from *Kallimodon* and *Leptosaurus*); (iv) the presence of an autotomic septum in the caudal vertebrae, different also from *Kallimodon pulchellus*, *Leptosaurus*, and *Pleurosaurus* [although *Kallimodon pulchellus* has been

**Figure 16.** Life representation of ***Sphenodraco scandentis*** in the palaeoenvironment of the Solnhofen Archipelago. Artwork by Gabriel Ugueto.

described with an autotomic septum by Cocude-Michel (1963), further examination of the holotype showed no signs of this feature; V.B., personal observations]; (v) a triangular proximal epiphysis of the humerus; and (vi) a tall, but more or less horizontally oriented ilium (different also from *Pleurosaurus*). It is also worth mentioning that the placement of *Sphenodraco* both in our phylogenetic (Fig. 11) and ecomorphological (Fig. 14A) analyses differs from that of *H. maximiliani*. In the implied weightings phylogenetic analysis, *Sphenodraco* is recovered in a clade with *Kallimodon*. In the PCA, *Sphenodraco* is recovered consistently with PC values more comparable to strictly arboreal squamates (e.g. the gliding lizards) than any *Homoeosaurus* specimen, in a position further away from the latter than would be expected for intraspecific variation (assuming a similar pattern to that of *Sphenodon*, in addition to the reduced morphological variation in *H. maximiliani* and *Kallimodon pulchellus* specimens; Fig. 14A).

As mentioned above, *Sphenodraco* was recovered at the base of a clade with *Kallimodon cerinensis*, *Kallimodon pulchellus*, and the undescribed specimen SNSB-BSPG 1993 XVIII 3 in our

maximum parsimony analysis, and the relationships between *Sphenodraco* and the *Kallimodon* species are poorly resolved in the Bayesian analysis. *Sphenodraco* differs from *Kallimodon pulchellus* in five characters used in our phylogenetic analysis: (i) character 79 (alternating teeth in the marginal dentition); (ii) character 103 (presence of an autotomic septum); (iii) character 108 (absence of uncinate processes); (iv) character 118 (presence of an anterior pubic process in the ilium); and (v) character 145 (distal forking of the pleurapophysis of sacral vertebra 2 terminating proximally). *Sphenodraco* differs from *Kallimodon cerinensis* in a single phylogenetic character, character 122 (fully open entepicondylar foramen in the humerus). The diagnosis for the genus *Kallimodon* is vague and poorly informative, being a combination of morphological traits, such as an elongated, triangular skull, narrow parietals, elongated upper temporal fenestra, short limbs, and caudal autotomy (Cocude-Michel 1963). As mentioned above, caudal autotomy is absent in all specimens assigned to *Kallimodon pulchellus*, including the holotype (*SNSB-BSPG 1887 VI 1*), and is present only in *Kallimodon cerinensis*. Narrow parietals, elongate upper temporal fenestra, and short limbs are morphological traits shared among many fossil rhynchocephalians, especially those from the Solnhofen Archipelago, e.g. *Pleurosaurus ginsburgi*, *Piocormus*, and *Vadasaurus* (Cocude-Michel 1963, Fabre 1981, Rauhut *et al.* 2012, Bever and Norell 2017, Beccari *et al.* 2025), and, therefore, not exclusive to *Kallimodon*. In our Bayesian analysis (Fig. 11B), *Kallimodon* is paraphyletic, which might question the generic attribution of *Kallimodon cerinensis*. It is worth mentioning that, although most recent works consider *Kallimodon* as a valid taxon (Rauhut *et al.* 2012, 2017, Simões *et al.* 2020, 2022, Chambi-Trowell *et al.* 2021, Villa *et al.* 2021, DeMar *et al.* 2022), it has been proposed that this genus is a junior synonym of *Leptosaurus* (Fabre 1981). As of this moment, the holotype of *Leptosaurus neptunius* is missing (Rauhut and López-Arbarello 2016). One specimen (MNHN CNJ 72) from Canjuers, France (Tithonian), previously assigned to *Leptosaurus pulchellus* (Fabre 1981), has been regarded as *Leptosaurus neptunius* and scored in recent phylogenetic studies in place of the holotype (i.e. Simões *et al.* 2020, 2022). However, this specimen might pertain to a new taxon, not closely related to *Kallimodon* (according to our personal observations and phylogenetic analyses; Fig. 11). It is also difficult to compare MNHN CNJ 72 with the holotype of *Leptosaurus neptunius* (*StIPB 1305*), because these specimens are preserved in different views, with MNHN CNJ 72 preserved in dorsal view, whereas *StIPB 1305* is preserved in ventral view. Therefore, some important features of *Leptosaurus neptunius* (e.g. its dentition; Cocude-Michel 1963, Fabre 1981) cannot be compared. A proper redescription of *Kallimodon* and *Leptosaurus* falls outside the scope of the present work. Nevertheless, *Sphenodraco scandentis* differs from known *Kallimodon cerinensis*, *Kallimodon pulchellus*, and *Leptosaurus neptunius* specimens in a set of morphological traits, as mentioned above, i.e. oblique maxillary dentition, the orientation of the caudal pleurapophyses, presence of a well-developed preacetabular process of the ilium, extremely elongated limbs (differing from the current diagnosis for *Kallimodon* and *Leptosaurus*; Cocude-Michel 1963, Fabre 1981), and flat unguals. The limb proportions of *Sphenodraco* fall outside of the expected variability of *Kallimodon*, if an ontogenetic and intraspecific pattern similar to that of *Sphenodon* is inferred (Fig. 15). In fact, some subadult specimens of *Kallimodon pulchellus* (e.g. SNSB-BSPG 1922 I 15 and MB.R.1008-1), in addition to the juvenile specimen JME-Scha 100, previously assigned to the *Kallimodon–Leptosaurus* complex (Renesto and Viohl 1997, Rauhut and López-Arbarello 2016), show drastically different limb proportions from *NHMUK PV R 2741* (Fig. 14). The maxillary dentition of SNSB-BSPG 1922 I 15 is similar to that of the holotype of *Kallimodon pulchellus* (*SNSB-BSPG 1887 VI 1*, adult; Fig. 5), both differing from that of *Sphenodraco scandentis* (*NHMUK PV R 2741*). Therefore, *NHMUK PV R 2741* and *SMF R414* can be assigned confidently to a new genus, different from both *Kallimodon* and *Leptosaurus*.

### Ontogenetic inferences

The development of many osteological features is associated with ontogeny in rhynchocephalians, such as skull proportions, the dental wear and arrangement, bone fusion, and the ossification of epiphyses and sesamoids (Carroll 1985, Reynoso 2003, Jones 2008, Regnault *et al.* 2016, 2017, Chambi-Trowell *et al.* 2019, Griffin *et al.* 2021, Villa *et al.* 2021, Simões *et al.* 2022, Beccari *et al.* 2025). The holotype of *Sphenodraco scandentis* shows the degree of ossification of a yet not fully skeletally mature specimen; this can be inferred by the presence of: well-ossified but unfused humeral condyle, olecranon process of the ulna, and epiphyses of the first manual phalanges; presence of some, but not all, ossified carpal elements; and unfused pelvic girdle. Therefore, the holotype and only known specimen of *Sphenodraco scandentis* pertains possibly to a subadult individual.

### Lower temporal bar in Solnhofen rhynchocephalians

Previous studies have reconstructed the skull of some Solnhofen rhynchocephalians, such as *Kallimodon*, *Homoeosaurus*, and *Sapheosaurus*, with a complete lower temporal bar (e.g. Cocude-Michel 1963), and these taxa have been scored accordingly in phylogenetic matrices with this feature (e.g. Simões *et al.* 2020, Chambi-Trowell *et al.* 2021, DeMar *et al.* 2022). A closed temporal fenestra was assumed historically to be the plesiomorphic condition of lepidosauromorphs (e.g. Moazen *et al.* 2009); however, it is absent in Triassic forms (see Whiteside 1986, Müller 2003, Schaerlaeken *et al.* 2008, Moazen *et al.* 2009) but present (at least to some extent) in at least some species of *Clevosaurus* Swinton, 1939 (Herrera-Flores *et al.* 2018, O'Brien *et al.* 2018, Chambi-Trowell *et al.* 2019), *Opisthias* Gilmore, 1909 (DINO 16454), *Opisthiamimus* (DeMar *et al.*, 2022), *Navajosphenodon*, *Sphenofontis*, and *Sphenodon* (Evans 2008, Jones 2008, Jones *et al.* 2011, Villa *et al.* 2021, Simões *et al.* 2022). In our observations, all non-sphenodontine rhynchocephalians from the Solnhofen Archipelago, i.e. *Acrosaurus*, *Kallimodon*, *H. maximiliani*, *H. parvipes*, *H. solnhofensis*, *Oenosaurus* (here observed in *Oenosaurus* aff. *muehlheimensis* SNSB-BSPG 2009 I 69), *Piocormus*, *Pleurosaurus*, *Sapheosaurus*, and *Vadasaurus*, show a completely open lower temporal fenestra and the lack of a quadratojugal process of the jugal. This has been observed previously in *Pleurosaurus* and *Vadasaurus* ( Jones 2008; Bever and Norell 2017, Villa *et al.* 2021, Beccari *et al.* 2025), but little has been said about the condition in the other taxa above. It is worth mentioning that, owing to dorsoventral compression of the

skull in most specimens from Solnhofen, the ascending process of the jugal is visible ventrally and has been interpreted as the quadratojugal process of the jugal (e.g. Cocude-Michel 1963). The variation in temporal structure within Rhynchocephalia is likely to be related to the arrangement of muscles and distribution of loading rather than the magnitudes of loading *per se* (Jones and Lappin 2009, Curtis *et al.* 2011).

### Inter- and intraspecific variation and the taxonomy of fossil rhynchocephalians

Limb proportions alone are not good diagnostic features for extinct taxa, but this study shows that the variability in *Sphenodon* is usually much lower than in fossil rhynchocephalians assigned to the same species (e.g. *Acrosaurus frischmanni*, *H. maximiliani*, and *Pleurosaurus* species). This, combined with morphological features observed in our sample of fossil specimens, suggests that the diversity of Jurassic rhynchocephalians from the Solnhofen Archipelago is underestimated.

In our analysis, all *Acrosaurus* and *Pleurosaurus* specimens show a large amplitude of variation in their limb and body size proportions. Both *Acrosaurus* specimens in this study represent young individuals, possibly post-hatchlings (Cocude-Michel 1963, Beccari *et al.* 2025). These specimens display a much greater variability in the PCA than that of the *Sphenodon* ontogenetic series. Indeed, when comparing the humeral length with radial length, and femoral length with tibial length (Supporting Information, Supplementary Data 1), *Acrosaurus* shows a larger amplitude of values than that measured in *Sphenodon*. The same applies to *Pleurosaurus ginsburgi* and *Pleurosaurus goldfussi*. The holotype of *Pleurosaurus ginsburgi* (*MNHN CNJ 67*) shows the highest hindlimb/forelimb proportion among *Pleurosaurus* specimens, having a femoral length almost four times the humeral length (FML/HML = 3.70). In the PCA, at least three separate clusters of *Pleurosaurus* specimens can be observed, probably indicating the existence of a further species within this genus. *Pleurosaurus* specimens are abundant in the fossil record, but species diagnoses within the genus are problematic (Beccari *et al.* 2025). Furthermore, *Pleurosaurus* specimens have a wide range in both geographical and stratigraphical distribution (Cocude-Michel 1963, Fabre 1974, Carroll 1985, Dupret 2004, Beccari *et al.* 2025). Taking all of this into consideration and including *Palaeopleurosaurus*, it is possible to recognize at least five species of European pleurosaurids in the Jurassic.

*Homoeosaurus* specimens considered in this study show a similar trend to that of pleurosaurids, with their variability falling outside the one measured for *Sphenodon*. When described, the main difference between *H. maximiliani* and *H. solnhofensis* was in the skull shape and proportions (Cocude-Michel 1963). However, it is possible that some specimens currently assigned to *H. maximiliani* (i.e. MB.R.893, MB.R.1011, SNSB-BSPG 1937 I 40, and TM F03955) might pertain to *H. solnhofensis* instead, or even to a new, undescribed species.

### Defining habitat use in rhynchocephalians and sampling limitations

The lack of diverse ecomorphological representation within extant rhynchocephalians hinders any habitat preference assessment for fossil taxa. Nevertheless, ecomorphological inferences have been made for many groups of extinct reptiles (e.g. dinosaurs: Birn-Jeffery *et al.* 2012; pseudosuchians and lepidosauromorphs: Gutarra *et al.* 2023; and pterosaurs: Smyth *et al.* 2024) and, because of their anatomical similarities and phylogenetic affinity, lizards might offer important insight into rhynchocephalian ecomorphology. However, despite this, it is not possible to certify that fossil rhynchocephalians would show the same functional morphology trends as extant squamates. Notably, the tuatara shows some marked differences from extant terrestrial lizards, especially regarding body size (Fig. 14A). Therefore, any inferences drawn here should be considered as being tentative, and future studies are required.

Postcranial morphology has been correlated with ecomorphology multiple times in extant lizards, but not much has been done for rhynchocephalians (notable examples come from the aquatic rhynchocephalians, e.g. Gutarra *et al.* 2023). Our PCA is a good initial step for defining the habitat use in some fossil rhynchocephalians, i.e. marine rhynchocephalians and some possibly climbing ones, such as *Homoeosaurus*, *Navajosphenodon*, and *Sphenodraco*. However, one major limitation for the available measurements in our study is the incompleteness of fossil specimens. Most of the fossil rhynchocephalians used in our analysis have a high degree of skeletal preservation, owing to their provenance from Konservat-Lagerstätten, such as the Solnhofen Archipelago (Mäuser 2015, Tischlinger and Rauhut 2015, Viohl 2015, Rauhut *et al.* 2017). However, many specimens have incomplete manus and pes, and the length of the longest digits is important to infer habitat preferences in lizards (e.g. Goodman *et al.* 2008, Goodman 2009, Fontanarrosa and Abdala 2016, Foster *et al.* 2018), which limits the resolution of our analysis.

Another limitation concerns the ontogeny of the sampled specimens. The lizard and rhynchocephalian specimens in this study represent a heterogeneous sample of ontogenetic stages, with juvenile, subadult, and adult individuals. To tackle this issue, the sample was standardized using the length between the proximal and distal metaphyses for appendicular bones (see the Material and Methods section above). For the lizard sample, we further minimized the impact of ontogeny by selecting and measuring only subadult and adult specimens. However, some fossil rhynchocephalians are represented by early juveniles (e.g. both *Acrosaurus* specimens, the Brunn juvenile SNSB-BSPG 1993 XVIII P12, *Navajosphenodon*, and some *Homoeosaurus*, *Kallimodon*, and *Leptosaurus* specimens). Habitat use may change during ontogeny, as is the case for some lizards (e.g. in some arboreal anoles, juveniles and females are known to forage on the ground; Schettino *et al.* 2010). Therefore, any ecomorphological categorization for these young specimens could change throughout development.

To test possible trends in rhynchocephalian morphological variability throughout ontogeny, we analysed possible ontogenetic trends in *Sphenodon*, which is represented here by a comprehensive sample of different ontogenetic stages. In our analysis, we did not find any compelling changes throughout the skeletal development in the tuatara (Fig. 15). Note that early juvenile and adult tuataras show similar ecomorphologies (e.g. Castanet *et al.* 1988, Herrel *et al.* 2010, Cree 2014) and, therefore, this might reflect on the PCA results herein. It also appears that limb shafts

are proportionally wider in hatchlings than in post-hatchling individuals. Despite this, we cannot be certain that ontogeny would not influence substrate use in fossil rhynchocephalians.

Phylogeny also plays a part in limb morphology, with some lizards (e.g. anoles, geckos, and lacertids) possibly showing unexpected limb proportions. In general, anoles show longer limbs relative to body size even in fully terrestrial taxa (Feiner *et al.* 2020, Ríos-Orjuela *et al.* 2020, Huie *et al.* 2021), whereas geckos and lacertids usually show shorter limbs relative to body size, even in good climbers (Zaaf and Van Damme 2001, Hagey *et al.* 2017, Cordero *et al.* 2021). These evolutionary trends in the appendicular skeleton of lizards influence the morphospace in our analysis, because they create further overlap across substrate use ecomorphospaces. It is possible that closely related fossil rhynchocephalians would show such phylogenetically driven trends in limb proportions, and their ecomorphology would be masked or difficult to interpret.

Finally, limb length alone is not the only metric to evaluate and understand substrate preferences in squamates. Previous studies have shown that terrestrial lizards tend to have shorter, more robust forelimbs than climbing ones (e.g. Fontanarrosa and Abdala 2016, Foster *et al.* 2018). Furthermore, the length and proportions of the longest digit have been shown to be correlated with climbing capabilities in some of these squamates (e.g. Goodman *et al.* 2008, Hagey *et al.* 2017, Ríos-Orjuela *et al.* 2020). Therefore, differences between the longest digits of rhynchocephalians (Fig. 17) should be also taken into consideration for the attribution of habitat use. The claws in ground-dwelling lizards are shown to be relatively longer than tall and straighter than in climbing and clinging lizards (Zani 2000, Tulli *et al.* 2009, Birn-Jeffery *et al.* 2012). Some morphological traits, such as a narrower, streamlined skull, elongation of the presacral vertebral series, late ossification in the appendicular skeleton, more robust metacarpal and metatarsal I compared with V, and reduction of the hook of metatarsal V, have been associated with an aquatic lifestyle in lepidosaurs (e.g. Reynoso 2000, Lee *et al.* 2016, Bever and Norell 2017, Beccari *et al.* 2025). Therefore, results of the PCA were considered in conjunction with the LDA and osteological features in order to infer more accurately the possible substrate use in these animals.

### Climbing rhynchocephalians

In our PCA, climbing lizards show great overlap among each other. Strictly arboreal lizards usually show relatively longer forelimbs than saxicolous lizards (Fig. 13A). This could be an artefact of sampling, because a large number of saxicolous lizards in our analyses are bipedal runners, whose hindlimbs have an important role in locomotion (e.g. Villaseñor-Amador *et al.* 2021). Semi-arboreal lizards are evenly distributed (Fig. 14A). However, as mentioned above, most semi-arboreal lizards are found in the positive values of PC1, meaning that their limbs are relatively longer and their body size shorter than terrestrial lizards.

Arboreal, saxicolous, and semi-arboreal lizards (i.e. climbing lizards) are common, with more than one-third of the limbed lizard species being arboreal or semi-arboreal, and ~20% being rock dwellers (saxicolous), according to the data published in SquamBase (Meiri 2024). However, climbing has not been proposed as a mode of life for many rhynchocephalians, with the notable exception of *Gephyrosaurus bridensis* (Evans 1981b). In our analysis, at least some specimens assigned to the genus *Homoeosaurus*, in addition to *Navajosphenodon* and *Sphenodraco*, show the expected morphology of arboreal, saxicolous, or semi-arboreal lepidosaurs, i.e. elongated and slender limbs, slender phalanges, and short and curved claws.

The neotype of *H. maximiliani* (SNSB-BSPG 1887 VI 502) and one referred specimen (MB.R.1014) show proportionally shorter limbs than other *H. maximiliani* specimens. However, the tibial length in these specimens is proportionally longer than any other specimens referred to this species. The elongated tibia is similar to that of bipedal running lizards (e.g. Grinham 2020, Villaseñor-Amador *et al.* 2021). Indeed, the neotype of *H. maximiliani* shares close PC1, PC2, and PC3 values with bipedal running lizards, i.e. *Chlamydosaurus kingii* Gray, 1825 and lizards of the genus *Crotaphytus* Holbrook, 1842. In the LDA, these two specimens of *H. maximiliani* were classified as semi-arboreal, with the neotype being classified as arboreal in SS. Therefore, *H. maximiliani* might represent a bipedal runner, or at least a well-adapted climbing taxon.

The specimens MB.R.893, MB.R.1011, SNSB-BSPG 1937 I 40, and TM F03955, currently also referred to *H. maximiliani* (Cocude-Michel 1963, Fabre 1981), and *Navajosphenodon* show similar limb and body proportions to each other and to *H. solnhofensis* SMF 4073. These specimens occupy the same morphospace as the arboreal, saxicolous, and semi-arboreal lizards. Among these specimens, *Navajosphenodon MNA.V.12442* and SNSB-BSPG 1937 I 40 represent young, possibly juvenile individuals (Cocude-Michel 1963, Simões *et al.* 2022), whereas the other three *H. maximiliani* specimens and *H. solnhofensis* SMF 4073 represent older, subadult to adult specimens (Cocude-Michel 1963). These specimens also have short, dorsoventrally deep, and curved unguals, which are associated with an arboreal lifestyle in lizards (Zani 2000, Tulli *et al.* 2009, Birn-Jeffery *et al.* 2012). The LDA classifies these specimens as saxicolous or semi-arboreal. Therefore, it is possible that *H. solnhofensis*, *Navajosphenodon*, and the abovementioned *H. maximiliani* specimens were good climbers, but no precise habitat preferences can be assigned.

*Sphenofontis* and *Vadasaurus* also show relatively longer limbs, especially hindlimbs, when compared with other rhynchocephalians. The LDA classifies these taxa as saxicolous, which could imply good climbing capabilities, which was suggested at least for *Sphenofontis* (Villa *et al.* 2021). It is worth noting that *Vadasaurus* has been recovered as a pleurosaurid or closely related to this clade in previous phylogenetic studies (i.e. Bever and Norell 2017, Chambi-Trowell *et al.* 2021) and suggested to be at least a semi-aquatic rhynchocephalian. Given that semi-aquatic lizard ecomorphospaces show great overlap with other substrate use ecomorphospaces and considering the poor accuracy in classifying semi-aquatic lizards in the LDA, we cannot discard the possibility that *Vadasaurus* could be a semi-aquatic animal, although our phylogenetic analysis disagrees with the close relationship between this taxon and pleurosaurids (Fig. 11).

*Sphenodraco* has extremely elongated limb bones, all of which are similar in length to each other, as opposed to the relatively

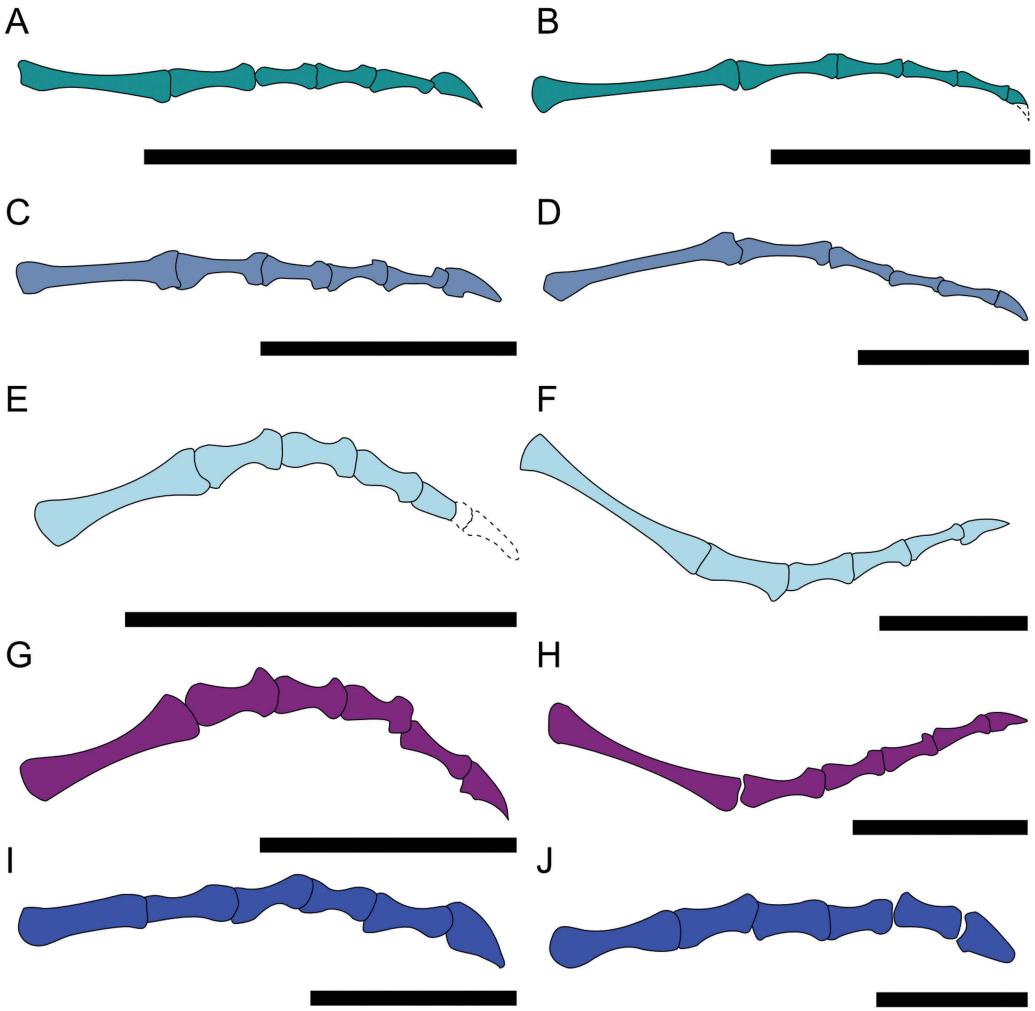


**Figure 17.** Comparison of the longest digit (digit IV) of the manus (left) and pes (right) of different rhynchocephalian specimens. A, B, ***Sphenodraco scandentis*** *NHMUK PV R 2741*. C, D, *Homoeosaurus maximiliani* SNSB-BSPG 1887 VI 502. E, F, *Kallimodon pulchellus SNSB-BSPG 1887 VI 1*. G, H, *Oenosaurus* aff. *muehlheimensis* SNSB-BSPG 2009 I 69. I, J, *Pleurosaurus ginsburgi* SNSB-BSPG 1977 X 40.

longer hindlimbs in comparison to forelimbs of *H. maximiliani*, *H. solnhofensis*, and *Navajosphenodon* (Fig. 12). A small body size with long limbs has been shown to be advantageous for strictly arboreal lizards (e.g. Hagey *et al.* 2017, Ríos-Orjuela *et al.* 2020). *Sphenodraco* has further possible adaptations to the arboreal environment, such as relatively longer forelimbs, elongated digits (especially manual and pedal digits IV), and recurved unguals (Zani 2000, Birn-Jeffery *et al.* 2012, Fontanarrosa and Abdala 2016, Foster *et al.* 2018), and is also closely located to the strictly arboreal lizards *Bronchocela cristatella* and *Draco* in the main combination of PCs. *Sphenodraco* is the only rhynchocephalian classified as arboreal in our LDA. Therefore, *Sphenodraco* is regarded here as the first strictly arboreal rhynchocephalian described to date.

### Terrestrial rhynchocephalians

In our PCA, most terrestrial squamates display relatively shorter and more robust limbs. These animals also have longer body sizes than climbing lizards, especially arboreal ones. Furthermore, there seems to be no or little detectable trend between fore- and hindlimb proportions to each other in terrestrial squamates. In other words, some terrestrial taxa may display proportionally longer forelimbs than hindlimbs, whereas others would display the opposite condition.

Unfortunately, it is not possible to assign fossil rhynchocephalians confidently to strict terrestrial habitat preferences through our PCA. Some *Kallimodon* and *Leptosaurus* specimens are positioned among strictly terrestrial lizards, but most specimens of these taxa, in addition to *H. parvipes*, the Brunn *Kallimodon*-like specimens, *Oenosaurus* aff. *muehlheimensis* specimens, *Piocormus*, and *Sapheosaurus*, are recovered at the centre of the main combination of PCs, where all lizard ecomorphospaces overlap. However, these taxa and specimens have significantly shorter limbs and proportionally longer bodies than the rhynchocephalians assigned to climbing ecomorphology, which is congruent with what is observed in terrestrial lizards and would hint either at this habitat preference or at a more generalist lifestyle. In agreement with this, the LDA classifies most of the specimens assigned to these taxa as terrestrial. Owing to the high accuracy when classifying terrestrial lizards and the tuatara, it is plausible that these fossil rhynchocephalians are indeed terrestrial, but more diverse

measurements and morphological traits would be required to confirm this observation.

### Aquatic and semi-aquatic rhynchocephalians

Our PCA results suggest that semi-aquatic extant lizard taxa are characterized by elongated bodies with long and robust forelimbs and with short and gracile hindlimbs (Fig. 14A), although their ecomorphospace overlaps with most of the other substrate use ecomorphospaces.

Most authors agree that pleurosaurids (i.e. *Acrosaurus*, *Pleurosaurus*, and *Palaeopleurosaurus*) were fully marine rhynchocephalians because they share a set of morphological traits correlated with this type of living habits in other vertebrates: e.g. streamlined, elongated skull; elongated presacral vertebral series; and reduced forelimbs with poorly ossified epiphyses (Carroll and Wild 1994, Reynoso 2000, Lee *et al.* 2016, Bever and Norell 2017, Simões *et al.* 2020, Beccari *et al.* 2025). Even young individuals have these adaptations, in addition to robust ceratobranchials associated with aquatic feeding (Delsett *et al.* 2023, Beccari *et al.* 2025). The position of *Acrosaurus*, *Pleurosaurus ginsburgi*, and *Pleurosaurus goldfussi* in our PCA is different from that expected for terrestrial or semi-aquatic lizards. These animals have extremely elongated bodies and reduced limbs, including stout manual and pedal digits V (Fig. 17). It is worth mentioning that *Palaeopleurosaurus*, although sharing many morphological features with *Pleurosaurus*, is found in the combination of PC1 and PC2 at the centre of the morphospace, but shows strong negative PC3 values, making it one of the extremes in the pleurosaurid ecomorphospace. In the LDA, this taxon is the only pleurosaurid classified as terrestrial instead of marine. One previous study on the histology of *Palaeopleurosaurus* (i.e. Klein and Scheyer 2017) has found no osteosclerosis in the femur, and only slightly more osteosclerosis in the ribs when compared with the tuatara. It is, therefore, possible that this taxon was not as fully adapted to the marine environment as *Acrosaurus* and *Pleurosaurus*, although it shows many expected aquatic adaptations and was recovered from a fully marine depositional environment (Carroll 1985).Thus, *Palaeopleurosaurus* might not be considered a terrestrial or semi-aquatic animal, but an early marine form among rhynchocephalians that had not yet adapted fully to this environment, although more studies are needed to confirm this claim.

Although *Kallimodon* has been proposed as an aquatic, or at least semi-aquatic, rhynchocephalian (e.g. Carroll and Wild 1994, Gutarra *et al.* 2023), no compelling arguments have been provided for this classification. As mentioned above, all *Kallimodon*, in addition to other *Kallimodon–Leptosaurus* complex specimens, are found in or close to the centre of the morphospaces in our PCA. Therefore, the skeletal proportions of *Kallimodon* are different from the aquatic pleurosaurids (except for *Palaeopleurosaurus*) and not specialized enough to infer an aquatic lifestyle for this taxon. However, there are some morphological features that support this hypothesis. *Kallimodon*, as is the case for pleurosaurids, has a triangular skull in dorsal view, poorly ossified limb bone epiphyses even in adult individuals, and relatively more robust and longer metacarpal and metatarsal I compared with metapodial V, all features associated with an aquatic lifestyle (Reynoso 2000, Lee *et al.* 2016, Bever and Norell 2017, Beccari *et al.* 2025). Additionally, specimen SNSB-BSPG 1887 VI 2, referred to *Kallimodon pulchellus*, preserves fish skeletal remains between its ribs and gastralia (possibly juvenile of *Tharsis* Blainville, 1818, although no confident identification can be made owing to the fragmentary aspect of the specimen; Adriana López-Arbarello, personal communication, 2022), suggesting that this individual ate a fish at some point shortly before death (Fig. 18). Although it is possible for a terrestrial animal to have scavenged or even captured the fish at the shore, taken together these arguments support the hypothesis that *Kallimodon* was, at the very least, semi-aquatic. Owing to the similar morphology of most *Leptosaurus* specimens and the complex taxonomic status of these two genera and their species, it is possible that all, or at least most, of the components of the *Kallimodon–Leptosaurus* complex were also semi-aquatic animals.

## CONCLUSION

Here, we describe a new genus and species of rhynchocephalian from the Solnhofen Archipelago, *Sphenodraco scandentis*. This was a small, long-limbed animal that differs from all other known rhynchocephalians by two autapomorphies (the obliquely oriented maxillary teeth in labial view, and short pubic process of the ilium), in addition to a combination of morphological traits, i.e. posterior flanges in the dentition decreasing in size posteriorly, extremely elongated limbs, and funnel-shaped proximal epiphysis of the humerus. Part of the holotype of *Sphenodraco scandentis*, composed by a main slab and a counterslab, was previously assigned to the species *Homoeosaurus maximiliani*. However, it differs from this taxon in having a long and narrow (triangular) skull, presence of well-developed posterior flanges in the maxillary dentition, short posterior process of the second sacral transverse process, presence of autotomic septa in the tail, wider and triangular-shaped proximal end of the humerus, and robust ilium with perpendicular iliac blade. Our phylogenetic analysis recovered *Sphenodraco scandentis* in a clade with *Kallimodon cerinensis*, *Kallimodon pulchellus*, and specimen SNSB-BSPG 1993 XVIII 3. Although *Sphenodraco* shares many morphological traits with *Kallimodon*, it differs from this taxon in having elongated limbs, in addition to the abovementioned autapomorphies. A revision of *Kallimodon* and *Leptosaurus* is suggested, because there are lingering taxonomic issues regarding these taxa.

To test possible habitat preferences in *Sphenodraco* and other extinct rhynchocephalians, we studied a comprehensive sample of fossil specimens and extant limbed lizards, in addition to the extant tuatara. For extant squamates, our analysis shows similar results to previous studies based solely on these reptiles, with major overlaps between ecomorphospaces for lizards with different habitat preferences and some distinction between long-limbed taxa (usually climbing species in the arboreal, saxicolous, or semi-arboreal categories) and short-limbed terrestrial taxa. Most fossil rhynchocephalians have average limb proportions relative to body size and occupy a central position in the morphospace graphs, which hinders confident assessment of ecological preferences. However, some taxa, especially the long-limbed *Homoeosaurus maximiliani*, *H. solnhofensis*, *Navajosphenodon*, and *Sphenodraco*, can be suggested, at least

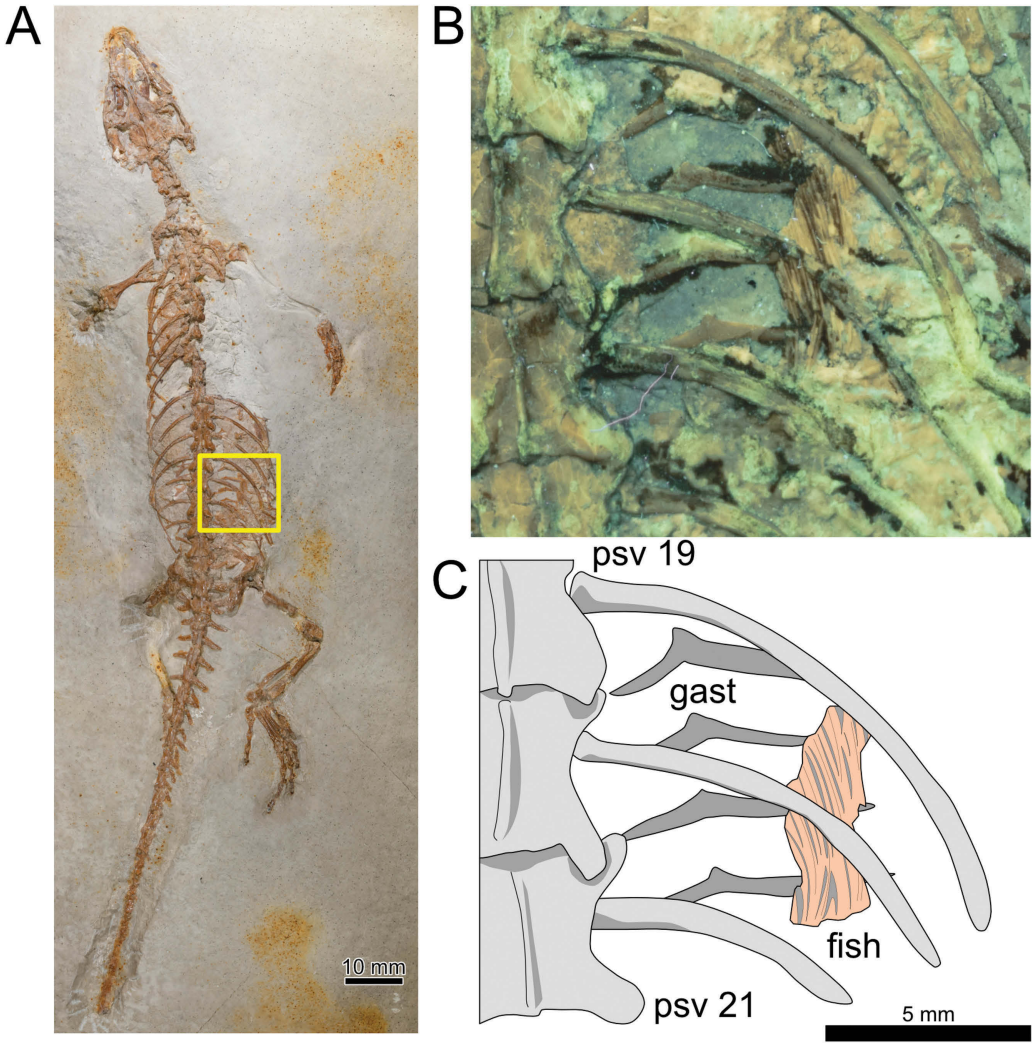


**Figure 18.** *Kallimodon pulchellus* specimen SNSB-BSPG 1887 VI 2. A, photograph under normal lighting. B, photograph of the abdominal region (yellow square in A) under ultraviolet light. C, schematic illustration of the abdominal region. Abbreviations: fish, fossil remains of an actinopterygian fish; gast, gastralia; psv, presacral vertebra.

tentatively, to represent climbing rhynchocephalians, whether saxicolous, semi-arboreal, or fully arboreal. We argue that the new species *Sphenodraco scandentis* represents the first identified fully arboreal rhynchocephalian. Another group that clearly occupies a morphospace distinctly separate from the lizards and other rhynchocephalians in our study are the pleurosaurids, especially the fully marine *Acrosaurus*, *Palaeopleurosaurus*, and *Pleurosaurus*. This ecomorphological distinction is attributable mainly to their elongated bodies and reduced limbs. We also propose that *Kallimodon* and *Leptosaurus* were semi-aquatic animals, based on their skeletal morphology and the presence of fish remains associated with the gut area of one *Kallimodon* specimen (SNSB-BSPG 1887 VI 2).

Our PCA also highlights low intraspecific variability in limb and body size proportions of *Sphenodon*. All tuatara specimens in our sample occupy a small area of morphospace in our analysis, and no ontogenetic trends are found in this taxon, meaning that limb and body size proportions show little change throughout skeletal development. Many fossil rhynchocephalians, which are currently assigned to the same taxon (e.g. specimens of *Acrosaurus*, *Pleurosaurus ginsburgi*, *Pleurosaurus goldfussi*, *Kallimodon pulchellus*, and *H. maximiliani*), show larger variation in limb bone proportions than observed in *Sphenodon*. This could either mean that extinct taxa had higher intraspecific variability than *Sphenodon* or that the diversity of extinct rhynchocephalians in the Jurassic of Europe is still underestimated. The identification of a new taxon in our study, previously referred to *H. maximiliani*, is in line with the latter hypothesis, and further assessment of other specimens will be likely to increase our understanding of the past diversity of these reptiles.

## ACKNOWLEDGEMENTS

VB thanks the following colleagues for access to specimens: Anne Schulp and Tim de Zeeuw (TM); Rainer Brocke and Gunnar Riedel (SMF); Karin Peyer and Nour-Eddine Jalil (MNHN); Michael O. Day and Susannah Maidment (NHMUK); Rebecca Hunt-Foster (DM); Maureen Walsh and Nathan Smith (NHMLA); and Daniel Brinkman and Vanessa Rhue (YPM). We would like to thank Adriana López-Arbarello (SNSB-BSPG) for the identification

of the fossil fish preserved in the *Kallimodon pulchellus* specimen SNSB-BSPG 1887 VI 2. We would like to thank Tiago R. Simões for sharing the 3D models of *Navajosphenodon sani* used for measurements in this study. We would also like to thank Basanta Khakurel (LMU) and Gustavo Darlim (LMU) for help with the Bayesian inference. Finally, we would like to thank the two anonymous reviewers and the editors for comments that greatly improved the current manuscript.

## FUNDINGS

VB is financed by the Deutsche Forschungsgemeinschaft (DFG grant RA 1012/28). AV was supported by a Humboldt Research Fellowship from the Alexander von Humboldt Foundation during part of the development of this work; he is now funded by Secretaria d'Universitats i Recerca of the Departament de Recerca i Universitats, Generalitat de Catalunya, through a Beatriu de Pinós postdoctoral grant (2021 BP 00038). AV further acknowledges support by the CERCA Programme/Generalitat de Catalunya and the Agència de Gestió d'Ajuts Universitaris i de Recerca of the Generalitat de Catalunya (2021 SGR 00620).

## SUPPLEMENTARY DATA

Supplementary data is available at *Zoological Journal of the Linnean Society* online.

## CONFLICT OF INTEREST

No conflict of interest is present.

## DATA AVAILABILITY STATEMENT

Both parts of the holotype, i.e. the main slab *SMF R414* and the counter slab *NHMUK PV R 2741*, are housed in public institutions and available for research. As stated in the Materials and Methods section, CT scans of *Sphenodon* are publicly available at https://osf.io/bds35.
All specimen measurements, PCA values, and the dataset used for the phylogenetic analysis are available online as Supplementary materials.

## REFERENCES

Ali SM. Studies on the comparative anatomy of the tail in Sauria and Rhynchocephalia I. *Sphenodon punctatus* Gray. *Proceedings of the Indian Academy of Sciences-Section B* 1941;**13**:171–92.

Anantharaman S, Demar DG, Sivakumar R *et al.* First rhynchocephalian (Reptilia, Lepidosauria) from the Cretaceous–Paleogene of India. *Journal of Vertebrate Paleontology* 2022;**42**:e2118059. https://doi.org/10.1080/02724634.2022.2118059

Apesteguía, S. Rhynchocephalians: the least known South American lepidosaurs. In: Agnolin FL., Lio G, Brissón Egli F *et al.* (eds.), *Historia Evolutiva y Paleobiogeográfica de los vertebrados de América del Sur*., Argentina: Contribuciones del MACN N°6. 2016, 7–19.

Bardet N, Falconnet J, Fischer V *et al.* Mesozoic marine reptile palaeobiogeography in response to drifting plates. *Gondwana Research* 2014;**26**:869–87. https://doi.org/10.1016/j.gr.2014.05.005

Beccari V, Glaw F, Rauhut OWM. On a complete specimen of *Oenosaurus* from the Late Jurassic of the Solnhofen Archipelago, with implications for its palaeoecology. In Alba DM, Marigó J, Nacarino-Meneses C *et al.* (eds), *Book of Abstracts of the 20th Annual Conference of the European Association of Vertebrate Palaeontologists, 26th June–1st July 2023, Sabadell (Barcelona), Spain. Special Volume 1, 2023*. PalaeoVertebrata, p. 31, 2023. https://doi.org/10.18563/pv.eavp2023

Beccari V, Villa A, Jones MEH *et al.* A juvenile pleurosaurid (Lepidosauria: Rhynchocephalia) from the Tithonian of the Mörnsheim Formation, Germany. *Anatomical Record (Hoboken, N. J.: 2007)* 2025;**308**:844–67. https://doi.org/10.1002/ar.25545

Bever GS, Norell MA. A new rhynchocephalian (Reptilia: Lepidosauria) from the Late Jurassic of Solnhofen (Germany) and the origin of the marine Pleurosauridae. *Royal Society Open Science* 2017;**4**:170570. https://doi.org/10.1098/rsos.170570

Birn-Jeffery AV, Miller CE, Naish D *et al.* Pedal claw curvature in birds, lizards and Mesozoic dinosaurs – complicated categories and compensating for mass-specific and phylogenetic control. *PLoS One* 2012;**7**:e50555. https://doi.org/10.1371/journal.pone.0050555

Blackburn DC, Boyer DM, Gray JA *et al.*; openVert Project Team. Increasing the impact of vertebrate scientific collections through 3D imaging: the openVertebrate (oVert) Thematic Collections Network. *BioScience* 2024;**74**:169–86. https://doi.org/10.1093/biosci/biad120

Bolet A, Stubbs TL, Herrera-Flores JA *et al.* The Jurassic rise of squamates as supported by lepidosaur disparity and evolutionary rates. *eLife* 2022;**11**:e66511. https://doi.org/10.7554/eLife.66511

Caldwell MW, Simões TR, Palci A *et al. Tetrapodophis amplectus* is not a snake: re-assessment of the osteology, phylogeny and functional morphology of an Early Cretaceous dolichosaurid lizard. *Journal of Systematic Palaeontology* 2021;**19**:893–952. https://doi.org/10.1080/14772019.2021.1983044

Camaiti M, Evans AR, Hipsley CA *et al.* A farewell to arms and legs: a review of limb reduction in squamates. *Biological Reviews of the Cambridge Philosophical Society* 2021;**96**:1035–50. https://doi.org/10.1111/brv.12690

Camaiti M, Evans AR, Hipsley CA *et al.* Macroecological and biogeographical patterns of limb reduction in the world's skinks. *Journal of Biogeography* 2023;**50**:428–40. https://doi.org/10.1111/jbi.14547

Capobianco A, Höhna S. On the Mkv model with among-character rate variation. *Systematic Biology* 2025;**syaf038**. https://doi.org/10.1093/sysbio/syaf038: 1–17.

Carroll RL. A pleurosaur from the Lower Jurassic and the taxonomic position of the Sphenodontida. *Palaeontographica. Abteilung A, Paläozoologie, Stratigraphie* 1985;**189**:1–28.

Carroll RL, Wild R. Marine members of the Sphenodontia. In Fraser NC, Sues H-D (eds), *In the Shadow of the Dinosaurs: Early Mesozoic Tetrapods*. Cambridge, UK: Cambridge University Press, 1994, 70–83.

Castanet J, Newman DG, Girons HS. Skeletochronological data on the growth, age, and population structure of the tuatara, *Sphenodon punctatus*, on Stephens and Lady Alice islands, New Zealand. *Herpetologica* 1988;**44**:25–37.

Chambi-Trowell SAV, Whiteside DI, Benton MJ. Diversity in rhynchocephalian *Clevosaurus* skulls based on CT reconstruction of two Late Triassic species from Great Britain. *Acta Palaeontologica Polonica* 2019;**64**:41–64. https://doi.org/10.4202/app.00569.2018

Chambi-Trowell SAV, Whiteside DI, Benton MJ *et al.* Biomechanical properties of the jaws of two species of *Clevosaurus* and a re-analysis of rhynchocephalian dentary morphospace. *Palaeontology* 2020;**63**:919–39. https://doi.org/10.1111/pala.12493

Chambi-Trowell SAV, Martinelli AG, Whiteside DI *et al.* The diversity of Triassic South American sphenodontians: a new basal form, clevosaurs, and a revision of rhynchocephalian phylogeny. *Journal of Systematic Palaeontology* 2021;**19**:787–820. https://doi.org/10.1080/14772019.2021.1976292

Cocude-Michel M. Les rhynchocéphales et les sauriens des calcaires lithographiques (Jurassique supérieur) d'Europe occidentale. *Nouvelles archives du Muséum d'histoire naturelle de Lyon* 1963;**7**:3–224. https://doi.org/10.3406/mhnly.1963.992

Cordero GA, Maliuk A, Schlindwein X *et al.* Phylogenetic patterns and ontogenetic origins of limb length variation in ecologically

diverse lacertine lizards. *Biological Journal of the Linnean Society* 2021;**132**:283–96. https://doi.org/10.1093/biolinnean/blaa183
Cree A. Tuatara – biology and conservation of a venerable survivor. *Canterbury University Press* 2014;**160**:1–583.
Curtis N, Jones MEH, Shi J *et al.* Functional relationship between skull form and feeding mechanics in *Sphenodon*, and implications for diapsid skull development. *PLoS One* 2011;**6**:e29804. https://doi.org/10.1371/journal.pone.0029804
Delsett LL, Pyenson N, Miedema F *et al.* Is the hyoid a constraint on innovation? A study in convergence driving feeding in fish-shaped marine tetrapods. *Paleobiology* 2023;**49**:765–765. https://doi.org/10.1017/pab.2023.17
DeMar DG, Jones MEH, Carrano MT. A nearly complete skeleton of a new eusphenodontian from the Upper Jurassic Morrison Formation, Wyoming, USA, provides insight into the evolution and diversity of Rhynchocephalia (Reptilia: Lepidosauria). *Journal of Systematic Palaeontology* 2022;**20**:1–64. https://doi.org/10.1080/14772019.2022.2093139
Dickson BV, Sherratt E, Losos JB *et al.* Semicircular canals in *Anolis* lizards: ecomorphological convergence and ecomorph affinities of fossil species. *Royal Society Open Science* 2017;**4**:170058. https://doi.org/10.1098/rsos.170058
Drevermann F. Drei *Homoeosaurus*-Skelette im Senckenberg-Museum. *Natur Museum Senckenberg Gesellschaft für Naturforschung* 1931;**1**:108–11.
Dupret V. The pleurosaurs: anatomy and phylogeny. *Revue de Paléobiologie, Genève* 2004;**9**:61–80.
Edwards DL, Avila LJ, Martinez L *et al.* Environmental correlates of phenotypic evolution in ecologically diverse *Liolaemus* lizards. *Ecology and Evolution* 2022;**12**:e9009. https://doi.org/10.1002/ece3.9009
Evans SE. Caudal autotomy in a Lower Jurassic eosuchian. *Copeia* 1981a;**1981**:883–4. https://doi.org/10.2307/1444191
Evans SE. The postcranial skeleton of the Lower Jurassic eosuchian *Gephyrosaurus bridensis*. *Zoological Journal of the Linnean Society* 1981b;**73**:81–116. https://doi.org/10.1111/j.1096-3642.1981.tb01580.x
Evans SE. The skull of lizards and tuatara. *Biology of Reptilia* 2008;**20**:1–347.
Evans SE, Prasad GVR, Manhas BK. Rhynchocephalians (Diapsida: Lepidosauria) from the Jurassic Kota Formation of India. *Zoological Journal of the Linnean Society* 2001;**133**:309–34. https://doi.org/10.1111/j.1096-3642.2001.tb00629.x
Ezcurra MD. Exploring the effects of weighting against homoplasy in genealogies of palaeontological phylogenetic matrices. *Cladistics* 2024;**40**:242–81. https://doi.org/10.1111/cla.12581
Fabre J. Un squelette de *Pleurosaurus ginsburgi* nov. sp. (Rhynchocephalia) du Portlandien du Petit Plan de Canjuers (Var). *Comptes Rendus Hebdomadaires Des Seances De l'Academie Des Sciences Serie D* 1974;**278**:2417–20.
Fabre J. *Les rhynchocéphales et les ptérosauriens à crête pariétale du Kiméridgien supérieur-Berriasien d'Europe occidentale: le gisement de Canjuers (Var-France) et ses abords*. Paris, France: Éditions de la Fondation Singer-Polignac, 1981.
Feiner N, Jackson IS, Munch KL *et al.* Plasticity and evolutionary convergence in the locomotor skeleton of Greater Antillean *Anolis* lizards. *eLife* 2020;**9**:e57468. https://doi.org/10.7554/eLife.57468
Feiner N, Jackson ISC, Stanley EL *et al.* Evolution of the locomotor skeleton in *Anolis* lizards reflects the interplay between ecological opportunity and phylogenetic inertia. *Nature Communications* 2021;**12**:1525. https://doi.org/10.1038/s41467-021-21757-5
Fontanarrosa G, Abdala V. Bone indicators of grasping hands in lizards. *PeerJ* 2016;**4**:e1978. https://doi.org/10.7717/peerj.1978
Foster KL, Garland T Jr, Schmitz L *et al.* Skink ecomorphology: forelimb and hind limb lengths, but not static stability, correlate with habitat use and demonstrate multiple solutions. *Biological Journal of the Linnean Society* 2018;**125**:673–92. https://doi.org/10.1093/biolinnean/bly146
Fraser NC. The osteology and relationships of *Clevosaurus* (Reptilia: Sphenodontida). *Philosophical Transactions of the Royal Society B: Biological Sciences* 1988;**321**:125–78. https://doi.org/10.1098/rstb.1988.0092
Fraser NC, Walkden GM. The ecology of a Late Triassic reptile assemblage from Gloucestershire, England. *Palaeogeography, Palaeoclimatology, Palaeoecology* 1983;**42**:341–65. https://doi.org/10.1016/0031-0182(83)90031-7
Gentil AR, Agnolin FL, Garcia Marsà JA *et al.* Bridging the gap: sphenodont remains from the Turonian (Upper Cretaceous) of Patagonia. Palaeobiological inferences. *Cretaceous Research* 2019;**98**:72–83. https://doi.org/10.1016/j.cretres.2019.01.016
Goloboff PA, Morales ME. TNT version 1.6, with a graphical interface for MacOS and Linux, including new routines in parallel. *Cladistics* 2023;**39**:144–53. https://doi.org/10.1111/cla.12524
Goodman BA. Nowhere to run: the role of habitat openness and refuge use in defining patterns of morphological and performance evolution in tropical lizards. *Journal of Evolutionary Biology* 2009;**22**:1535–44. https://doi.org/10.1111/j.1420-9101.2009.01766.x
Goodman BA, Miles DB, Schwarzkopf L. Life on the rocks: habitat use drives morphological and performance evolution in lizards. *Ecology* 2008;**89**:3462–71. https://doi.org/10.1890/07-2093.1
Griffin CT, Stocker MR, Colleary C *et al.* Assessing ontogenetic maturity in extinct saurian reptiles. *Biological Reviews* 2021;**96**:470–525. https://doi.org/10.1111/brv.12666
Grinham LR. The ecomorphology of facultative bipedality in Lepidosauria: implications for the evolution of reptilian bipedality. PhD Thesis, University of Cambridge, 2020. https://www.repository.cam.ac.uk/handle/1810/308977
Grizante MB, Navas CA, Garland T Jr *et al.* Morphological evolution in Tropidurinae squamates: an integrated view along a continuum of ecological settings. *Journal of Evolutionary Biology* 2010;**23**:98–111. https://doi.org/10.1111/j.1420-9101.2009.01868.x
Günther A. Contribution to the anatomy of *Hatteria* (*Rhynchocephalus*, Owen). *Philosophical Transactions of the Royal Society of London* 1867;**157**:595–629.
Gutarra S, Stubbs TL, Moon BC *et al.* The locomotor ecomorphology of Mesozoic marine reptiles. *Palaeontology* 2023;**66**:e12645. https://doi.org/10.1111/pala.12645
Haeckel E. *Generelle Morphologie der Organismen. Allgemeine Grundzüge der Organischen Formen-Wissenschaft, Mechanisch Begründet Durch die von C. Darwin Reformirte Descendenz-Theorie, etc* (Vol. **1**). Berlin, Germany: Georg Reimer, 1866.
Hagey TJ, Harte S, Vickers M *et al.* There's more than one way to climb a tree: limb length and microhabitat use in lizards with toe pads. *PLoS One* 2017;**12**:e0184641. https://doi.org/10.1371/journal.pone.0184641
Hammer O, Harper DAT, Ryan PD. PAST: paleontological statistics software package for education and data analysis. *Palaeontologia Electronica* 2001;**4**:9.
Herrel A, Moore JA, Bredeweg EM *et al.* Sexual dimorphism, body size, bite force and male mating success in tuatara. *Biological Journal of the Linnean Society* 2010;**100**:287–92. https://doi.org/10.1111/j.1095-8312.2010.01433.x
Herrera-Flores JA, Stubbs TL, Benton MJ. Macroevolutionary patterns in Rhynchocephalia: is the tuatara (*Sphenodon punctatus*) a living fossil? *Palaeontology* 2017;**60**:319–28. https://doi.org/10.1111/pala.12284
Herrera-Flores JA, Stubbs TL, Elsler A *et al.* Taxonomic reassessment of *Clevosaurus latidens* Fraser, 1993 (Lepidosauria, Rhynchocephalia) and rhynchocephalian phylogeny based on parsimony and Bayesian inference. *Journal of Paleontology* 2018;**92**:734–42. https://doi.org/10.1017/jpa.2017.136
Herrera-Flores JA, Stubbs TL, Benton MJ. Ecomorphological diversification of squamates in the Cretaceous. *Royal Society Open Science* 2021;**8**:201961. https://doi.org/10.1098/rsos.201961
Herrera-Flores JA, Stubbs TL, Sour-Tovar F. Redescription of the type specimens for the Late Jurassic rhynchocephalian *Opisthias rarus* and a new specimen of *Theretairus antiquus* from Quarry 9,

Morrison Formation, Wyoming, USA. *Acta Palaeontologica Polonica* 2022;**67**:623–30. https://doi.org/10.4202/app.00929.2021
Hoffstetter R, Gasc J-P. Vertebrae and ribs of modern reptiles. *Biology of the Reptilia* 1969;**1**:201–310.
Höhna S, Landis MJ, Heath TA *et al.* RevBayes: Bayesian phylogenetic inference using graphical models and an interactive model-specification language. *Systematic Biology* 2016;**65**:726–36. https://doi.org/10.1093/sysbio/syw021
Houssaye A. 'Pachyostosis' in aquatic amniotes: a review. *Integrative Zoology* 2009;**4**:325–40. https://doi.org/10.1111/j.1749-4877.2009.00146.x
Howell BK, Winchell KM, Hagey TJ. Geometric morphometrics reveal shape differences in the toes of urban lizards. *Integrative Organismal Biology (Oxford, England)* 2022;**4**:obac028. https://doi.org/10.1093/iob/obac028
Howes GB, Swinnerton HH. On the development of the skeleton of the tuatara, *Sphenodon punctatus*; with remarks on the egg, on the hatching, and on the hatched young. *The Transactions of the Zoological Society of London* 1901;**16**:1–84. https://doi.org/10.1111/j.1096-3642.1901.tb00026.x
Hsiou AS, Nydam RL, Simões TR *et al.* A new clevosaurid from the Triassic (Carnian) of Brazil and the rise of sphenodontians in Gondwana. *Scientific Reports* 2019;**9**:11821. https://doi.org/10.1038/s41598-019-48297-9
Huie JM, Prates I, Bell RC *et al.* Convergent patterns of adaptive radiation between island and mainland *Anolis* lizards. *Biological Journal of the Linnean Society* 2021;**134**:85–110. https://doi.org/10.1093/biolinnean/blab072
Jones MEH. Skull shape and feeding strategy in *Sphenodon* and other Rhynchocephalia (Diapsida: Lepidosauria). *Journal of Morphology* 2008;**269**:945–66. https://doi.org/10.1002/jmor.10634
Jones MEH. Dentary tooth shape in *Sphenodon* and its fossil relatives (Diapsida: Lepidosauria: Rhynchocephalia). In Koppe T, Meyer G, Alt KW (eds), *Comparative Dental Morphology*, Vol. **13**. Greifswald, Germany: Karger, 2009, 9–15.
Jones MEH, Lappin AK. Bite-force performance of the last rhynchocephalian (Lepidosauria: *Sphenodon*). *Journal of the Royal Society of New Zealand* 2009;**39**:71–83. https://doi.org/10.1080/03014220909510565
Jones MEH, Curtis N, Fagan MJ *et al.* Hard tissue anatomy of the cranial joints in *Sphenodon* (Rhynchocephalia): sutures, kinesis, and skull mechanics. *Palaeontologia Electronica* 2011;**14**:92.
Jones MEH, O'Higgins P, Fagan MJ *et al.* Shearing mechanics and the influence of a flexible symphysis during oral food processing in *Sphenodon* (Lepidosauria: Rhynchocephalia). *The Anatomical Record: Advances in Integrative Anatomy and Evolutionary Biology* 2012;**295**:1075–91. https://doi.org/10.1002/ar.22487
Jones ME, Anderson C, Hipsley CA *et al.* Integration of molecules and new fossils supports a Triassic origin for Lepidosauria (lizards, snakes, and tuatara). *BMC Evolutionary Biology* 2013;**13**:208. https://doi.org/10.1186/1471-2148-13-208
Khakurel B, Grigsby C, Tran TD *et al.* The fundamental role of character coding in Bayesian morphological phylogenetics. *Systematic Biology* 2024;**73**:861–71. https://doi.org/10.1093/sysbio/syae033
Klein N, Scheyer TM. Microanatomy and life history in *Palaeopleurosaurus* (Rhynchocephalia: Pleurosauridae) from the Early Jurassic of Germany. *Die Naturwissenschaften* 2017;**104**:4. https://doi.org/10.1007/s00114-016-1427-3
Klingenberg CP. Size, shape, and form: concepts of allometry in geometric morphometrics. *Development Genes and Evolution* 2016;**226**:113–37. https://doi.org/10.1007/s00427-016-0539-2
Lee MSY, Palci A, Jones MEH *et al.* Aquatic adaptations in the four limbs of the snake-like reptile *Tetrapodophis* from the Lower Cretaceous of Brazil. *Cretaceous Research* 2016;**66**:194–9. https://doi.org/10.1016/j.cretres.2016.06.004
Lewis PO. A likelihood approach to estimating phylogeny from discrete morphological character data. *Systematic Biology* 2001;**50**:913–25. https://doi.org/10.1080/106351501753462876
Martínez RN, Simões TR, Sobral G *et al.* A Triassic stem lepidosaur illuminates the origin of lizard-like reptiles. *Nature* 2021;**597**:235–8. https://doi.org/10.1038/s41586-021-03834-3
Mäuser M. Die laminierten Plattenkalke von Wattendorf in Oberfranken. In: Arratia G, Schultze H-P, Tischlinger H *et al.* (eds), *Solnhofen. Ein Fenster in die Jurazeit*. Munich: Dr. Friedrich Pfeil, 2015, 515–35.
Meiri S. SquamBase—a database of squamate (Reptilia: Squamata) traits. *Global Ecology and Biogeography* 2024;**33**:e13812. https://doi.org/10.1111/geb.13812
Meloro C, Jones MEH. Tooth and cranial disparity in the fossil relatives of *Sphenodon* (Rhynchocephalia) dispute the persistent 'living fossil' label. *Journal of Evolutionary Biology* 2012;**25**:2194–209. https://doi.org/10.1111/j.1420-9101.2012.02595.x
Moazen M, Curtis N, O'Higgins P *et al.* Biomechanical assessment of evolutionary changes in the lepidosaurian skull. *Proceedings of the National Academy of Sciences of the United States of America* 2009;**106**:8273–7. https://doi.org/10.1073/pnas.0813156106
Mosimann JE. Size allometry: size and shape variables with characterizations of the lognormal and generalized gamma distributions. *Journal of the American Statistical Association* 1970;**65**:930–45. https://doi.org/10.2307/2284599
Müller J. Early loss and multiple return of the lower temporal arcade in diapsid reptiles. *Naturwissenschaften* 2003;**90**:473–6. https://doi.org/10.1007/s00114-003-0461-0
Niebuhr B, Pürner T. Lithostratigraphie der Weißjura-Gruppe der Frankenalb (außeralpiner Oberjura) und der mittel- bis oberjurassischen Reliktvorkommen zwischen Straubing und Passau (Bayern): beitrag zur Stratigraphie von Deutschland. *Schriftenreihe der Deutschen Gesellschaft für Geowissenschaften* 2014;**83**:5–72.
O'Brien A, Whiteside DI, Marshall JEA. Anatomical study of two previously undescribed specimens of *Clevosaurus hudsoni* (Lepidosauria: Rhynchocephalia) from Cromhall Quarry, UK, aided by computed tomography, yields additional information on the skeleton and hitherto undescribed bones. *Zoological Journal of the Linnean Society* 2018;**183**:163–95. https://doi.org/10.1093/zoolinnean/zlx087
O'Leary MA, Kaufman SG. 2012. MorphoBank 3.0: Web application for morphological phylogenetics and taxonomy. http://www.morphobank.org (15 April 2025, date last accessed)
Paparella I, Palci A, Nicosia U *et al.* A new fossil marine lizard with soft tissues from the Late Cretaceous of southern Italy. *Royal Society Open Science* 2018;**5**:172411. https://doi.org/10.1098/rsos.172411
Pelegrin N, Mesquita DO, Albinati P *et al.* Extreme specialization to rocky habitats in *Tropidurus* lizards from Brazil: trade-offs between a fitted ecomorph and autoecology in a harsh environment. *Austral Ecology* 2017;**42**:677–89. https://doi.org/10.1111/aec.12486
Rauhut OWM, López-Arbarello A. Zur Taxonomie der Brückenechse aus dem oberen Jura von Schamhaupten. *Archaeopteryx* 2016;**33**:1–11.
Rauhut OWM, Heyng AM, López-Arbarello A *et al.* A new rhynchocephalian from the Late Jurassic of Germany with a dentition that is unique amongst tetrapods. *PLoS One* 2012;**7**:e46839. https://doi.org/10.1371/journal.pone.0046839
Rauhut OWM, López-Arbarello A, Röper M *et al.* Vertebrate fossils from the Kimmeridgian of Brunn: the oldest fauna from the Solnhofen Archipelago (Late Jurassic, Bavaria, Germany). *Zitteliana* 2017;**89**:305–29.
Regnault S, Jones MEH, Pitsillides AA *et al.* Anatomy, morphology and evolution of the patella in squamate lizards and tuatara (*Sphenodon punctatus*). *Journal of Anatomy* 2016;**228**:864–76. https://doi.org/10.1111/joa.12435
Regnault S, Hutchinson JR, Jones MEH. Sesamoid bones in tuatara (*Sphenodon punctatus*) investigated with X-ray microtomography, and implications for sesamoid evolution in Lepidosauria. *Journal of Morphology* 2017;**278**:62–72. https://doi.org/10.1002/jmor.20619
Renesto S, Viohl G. A sphenodontid (Reptilia, Diapsida) from the Late Kimmeridgian of Schamhaupten (Southern Franconian Alb, Bavaria, Germany). *Archaeopteryx* 1997;**15**:27–46.

Reynoso V-H. A 'beaded' sphenodontian (Diapsida: Lepidosauria) from the Early Cretaceous of central Mexico. *Journal of Vertebrate Paleontology* 1997;**17**:52–9. https://doi.org/10.1080/02724634.1997.10010953

Reynoso V-H. An unusual aquatic sphenodontian (Reptilia: Diapsida) from the Tlayua Formation (Albian), Central Mexico. *Journal of Paleontology* 2000;**74**:133–48. https://doi.org/10.1666/0022-3360(2000)074<0133:auasrd>2.0.co;2

Reynoso V-H. Growth patterns and ontogenetic variation of the teeth and jaws of the Middle Jurassic sphenodontian *Cynosphenodon huizachalensis* (Reptilia: Rhynchocephalia). *Canadian Journal of Earth Sciences* 2003;**40**:609–19. https://doi.org/10.1139/e02-097

Reynoso V-H. Possible evidence of a venom apparatus in a Middle Jurassic sphenodontian from the Huizachal red beds of Tamaulipas, México. *Journal of Vertebrate Paleontology* 2005;**25**:646–54. https://doi.org/10.1671/0272-4634(2005)025[0646:peoava]2.0.co;2

Riedel J, Grismer LL, Higham T *et al.* Ecomorphology of the locomotor apparatus in the genus *Cyrtodactylus* (Gekkota, Squamata). *Evolutionary Biology* 2024;**51**:106–23. https://doi.org/10.1007/s11692-023-09622-3

Rieppel O. The skull in a hatchling of *Sphenodon punctatus*. *Journal of Herpetology* 1992;**26**:80–4. https://doi.org/10.2307/1565028

Ríos-Orjuela JC, Camacho-Bastidas JS, Jerez A. Appendicular morphology and locomotor performance of two morphotypes of continental anoles: *Anolis heterodermus* and *Anolis tolimensis*. *Journal of Anatomy* 2020;**236**:252–73. https://doi.org/10.1111/joa.13092

Robinson PL. How *Sphenodon* and *Uromastyx* grow their teeth and use them. *Morphology and Biology of Reptiles* 1976;**3**:43–65.

Romo de Vivar PR, Martinelli AG, Schmaltz Hsiou A *et al.* A new rhynchocephalian from the Late Triassic of Southern Brazil enhances eusphenodontian diversity. *Journal of Systematic Palaeontology* 2020;**18**:1103–26. https://doi.org/10.1080/14772019.2020.1732488

Romo de Vivar Martínez PR, Soares MB. Dentary morphological variation in *Clevosaurus brasiliensis* (Rhynchocephalia, Clevosauridae) from the Upper Triassic of Rio Grande do Sul, Brazil. *PLoS One* 2015;**10**:e0119307. https://doi.org/10.1371/journal.pone.0119307

Romo-de-Vivar-Martínez PR, Martinelli AG, Paes Neto VD *et al.* Evidence of osteomyelitis in the dentary of the late Triassic rhynchocephalian *Clevosaurus brasiliensis* (Lepidosauria: Rhynchocephalia) from southern Brazil and behavioural implications. *Historical Biology* 2017;**29**:320–7. https://doi.org/10.1080/08912963.2016.1158258

Russell AP, Bauer AM. The appendicular locomotor apparatus of *Sphenodon* and normal-limbed squamates. In: Gans C, Gaunt A, Adler K (eds), *Biology of the Reptilia. Vol. 21, Morphology I: The skull and appendicular locomotor apparatus of Lepidosauria*. Society for the Study of Amphibians and Reptiles, Ithaca, New York, USA, 2008, 1–468.

Schaerlaeken V, Herrel A, Aerts P *et al.* The functional significance of the lower temporal bar in *Sphenodon punctatus*. *The Journal of Experimental Biology* 2008;**211**:3908–14. https://doi.org/10.1242/jeb.021345

Schettino LR, Losos JB, Hertz PE *et al.* The Anoles of Soroa: aspects of their ecological relationships. *Breviora* 2010;**520**:1–22. https://doi.org/10.3099/0006-9698-520.1.1

Scheyer TM, Spiekman SNF, Sues H-D *et al. Colobops*: a juvenile rhynchocephalian reptile (Lepidosauromorpha), not a diminutive archosauromorph with an unusually strong bite. *Royal Society Open Science* 2020;**7**:192179. https://doi.org/10.1098/rsos.192179

Schneider CA, Rasband WS, Eliceiri KW. NIH Image to ImageJ: 25 years of image analysis. *Nature Methods* 2012;**9**:671–5. https://doi.org/10.1038/nmeth.2089

Schweigert G. Biostratigraphie der Plattenkalke der südlichen Frankenalb. In: Arratia G, Schultze H.-P., Tischlinger H *et al.* (eds), *Solnhofen. Ein Fenster in die Jurazeit*. Munich: Dr. Friedrich Pfeil, 2015, 63–6.

Seligmann H, Moravec J, Werner YL. Morphological, functional and evolutionary aspects of tail autotomy and regeneration in the 'living fossil' *Sphenodon* (Reptilia: Rhynchocephalia). *Biological Journal of the Linnean Society* 2008;**93**:721–43. https://doi.org/10.1111/j.1095-8312.2008.00975.x

Sherratt E, Del Rosario Castañeda M, Garwood RJ *et al.* Amber fossils demonstrate deep-time stability of Caribbean lizard communities. *Proceedings of the National Academy of Sciences of the United States of America* 2015;**112**:9961–6. https://doi.org/10.1073/pnas.1506516112

Simões TR, Pyron RA. The squamate tree of life. *Bulletin of the Museum of Comparative Zoology* 2021;**163**:47–95. https://doi.org/10.3099/0027-4100-163.2.47

Simões TR, Caldwell MW, Pierce SE. Sphenodontian phylogeny and the impact of model choice in Bayesian morphological clock estimates of divergence times and evolutionary rates. *BMC Biology* 2020;**18**:191. https://doi.org/10.1186/s12915-020-00901-5

Simões TR, Kinney-Broderick G, Pierce SE. An exceptionally preserved *Sphenodon*-like sphenodontian reveals deep time conservation of the tuatara skeleton and ontogeny. *Communications Biology* 2022;**5**:195. https://doi.org/10.1038/s42003-022-03144-y

Smyth RSH, Breithaupt BH, Butler RJ *et al.* Hand and foot morphology maps invasion of terrestrial environments by pterosaurs in the mid-Mesozoic. *Current Biology* 2024;**34**:4894–4907.e3. https://doi.org/10.1016/j.cub.2024.09.014

Sues H-D, Schoch RR. A new early-diverging sphenodontian (Lepidosauria, Rhynchocephalia) from the Upper Triassic of Virginia, U.S.A. *Journal of Paleontology* 2021;**95**:344–50. https://doi.org/10.1017/jpa.2020.87

Sues H, Schoch RR. The oldest known rhynchocephalian reptile from the Middle Triassic (Ladinian) of Germany and its phylogenetic position among Lepidosauromorpha. *The Anatomical Record* 2023;**307**:776–90. https://doi.org/10.1002/ar.25339

Tischlinger H, Rauhut OWM. Schuppenechsen (Lepidosauria). In Arratia G, Schultze HP, Tischlinger H *et al.* (eds), *Solnhofen. Ein Fenster in die Jurazeit*. Munich: Dr. Friedrich Pfeil, 2015, 431–47.

Tischlinger H, Wild R. Den Schwanz verloren–das Leben gerettet. *Fossilien* 2009;**26**:203–9.

Tulli MJ, Cruz FB, Herrel A *et al.* The interplay between claw morphology and microhabitat use in neotropical iguanian lizards. *Zoology (Jena, Germany)* 2009;**112**:379–92. https://doi.org/10.1016/j.zool.2009.02.001

Tulli MJ, Abdala V, Cruz FB. Relationships among morphology, clinging performance and habitat use in Liolaemini lizards. *Journal of Evolutionary Biology* 2011;**24**:843–55. https://doi.org/10.1111/j.1420-9101.2010.02218.x

Vaux F, Morgan-Richards M, Daly EE *et al.* Tuatara and a new morphometric dataset for Rhynchocephalia: comments on Herrera-Flores et al. *Palaeontology* 2019;**62**:321–34.

Velasco JA, Herrel A. Ecomorphology of *Anolis* lizards of the Choco' region in Colombia and comparisons with Greater Antillean ecomorphs. *Biological Journal of the Linnean Society* 2007;**92**:29–39. https://doi.org/10.1111/j.1095-8312.2007.00885.x

Villa A, Montie R, Röper M *et al. Sphenofontis velserae* gen. et sp. nov., a new rhynchocephalian from the Late Jurassic of Brunn (Solnhofen Archipelago, southern Germany). *PeerJ* 2021;**9**:e11363. https://doi.org/10.7717/peerj.11363

Villaseñor-Amador D, Suárez NX, Cruz JA. Bipedalism in Mexican albian lizard (Squamata) and the locomotion type in other Cretaceous lizards. *Journal of South American Earth Sciences* 2021;**109**:103299. https://doi.org/10.1016/j.jsames.2021.103299

Viohl G. Der geologische Rahmen: die südliche Frankenalb und ihre Entwicklung. In: Arratia G, Schultze H-P., Tischlinger H *et al.* (eds), *Solnhofen. Ein Fenster in die Jurazeit*. Munich: Dr. Friedrich Pfeil, 2015, 56–62.

von Meyer, H. *Homoeosaurus maximiliani und Rhamphorhynchus (Pterodactylus) longicaudus: Zwei fossile Reptilien aus dem Kalkschiefer von Solenhofen. S.* Schmerber'schen Buchhandlung, Frankfurt a. M., Germany, 1847.

von Meyer H. *Acrosaurus frischmanni*. *Neues Jahrbuch für Mineralogie, Geologie und Paläontologie*, Stuttgart, Germany, 1854;**22**:47–58.

Watanabe A, Fabre A-C, Felice RN *et al.* Ecomorphological diversification in squamates from conserved pattern of cranial integration. *Proceedings*

*of the National Academy of Sciences of the United States of America* 2019;**116**:14688–97. https://doi.org/10.1073/pnas.1820967116

Whiteside DI. The head skeleton of the Rhaetian sphenodontid *Diphydontosaurus avonis* gen. et sp. nov. and the modernizing of a living fossil. *Philosophical Transactions of the Royal Society of London. B, Biological Sciences* 1986;**312**:379–430. https://doi.org/10.1098/rstb.1986.0014

Yang Z. Maximum likelihood phylogenetic estimation from DNA sequences with variable rates over sites: approximate methods. *Journal of Molecular Evolution* 1994;**39**:306–14. https://doi.org/10.1007/BF00160154

Zaaf A, Van Damme R. Limb proportions in climbing and ground-dwelling geckos (Lepidosauria, Gekkonidae): a phylogenetically informed analysis. *Zoomorphology* 2001;**121**:45–53. https://doi.org/10.1007/s004350100044

Zani PA. The comparative evolution of lizard claw and toe morphology and clinging performance. *Journal of Evolutionary Biology* 2000;**13**:316–25. https://doi.org/10.1046/j.1420-9101.2000.00166.x